A COMPARISON OF RATING AND DATING TECHNIQUES TO ESTIMATE THE THREAT OF SOIL EROSION TO ARCHAEOLOGICAL MONUMENTS UNDER AGRICULTURAL FIELDS

M.A.J. (Maud) van Soest

MSc. Thesis Soil Geography and Landscape

Wageningen University, 2015

A COMPARISON OF RATING AND DATING TECHNIQUES TO ESTIMATE THE THREAT OF SOIL EROSION TO ARCHAEOLOGICAL MONUMENTS UNDER AGRICULTURAL FIELDS

MSc Thesis, 2015

Figure cover page:
Top left, auger head with anthropogenic debris and soil from the study location Meerssen
Down left, overview of the mound of interest Grote Houw
Right, sample pit at the Grote Houw with OSL cores

M.A.J. (Maud) van Soest
91 08 09 784 040
MSc Earth and Environment, specialisation Soil Geography and Landscape
Wageningen University
Supervisors
dr.ir. J.M. (Jeroen) Schoorl
Soil Geography and Landscape, Wageningen UR
dr.ir. D.J. (Hans) Huisman
Rijksdienst voor het Cultureel Erfgoed

ABSTRACT

For the protection of Dutch archaeological sites against degradation, the TOPsites project is investigating the rate, extent and mitigation of the most important processes involved. One of these processes is soil translocation or soil redistribution. For many Dutch archaeological sites the actual extent and rate of soil erosion is not yet known. In this study different techniques for dating and estimating erosion rates have been compared on two archaeological sites on tilled fields with gentle slopes: multi-temporal LiDar, profiles and spatial distribution of ^{137}Cs, anthropogenic Pb, and $^{239+240}Pu$, and moreover OSL. In addition, the added value of the combination of several of these techniques together has been evaluated. The ^{137}Cs surface analysis showed no erosive pattern. All other methods, however, did indicate soil erosion on the two studied locations. Colluvium was found in soil profiles down the slope in Meerssen. In this package were the concentrations of fallout isotopes higher and showed the OSL estimation younger ages. Thereby were the fallout distributions of Cs and Pu upslope obtained in shallower soil depth and were the soil layers directly under the plough zone estimated to be about 200 years older upslope and even 400 years older mid slope than the soil layer at a depth of 40 cm down slope. For the Grote Houw were the results of the different methods a bit varied at the soil pits. The two pits located higher on the mound appeared however erosive, as well as the pit on platform south of the main mound. The pits 4 and 5, located in the lower positions, were mainly indicated as depositional. Erosion rates were calculated (in the range of 0.46 - 1.36 mm/year) with some rough assumptions. More research should been done to the sampling design and statistics of the results in the future to make the combination of the methods used workable.

TABLE OF CONTENTS

LIST OF FIGURES ..... **VI**

LIST OF TABLES ..... **VII**

1. INTRODUCTION **8**

1.1 GENERAL INTRODUCTION 8
1.2 DETERMINATION OF SOIL EROSION 9
1.2.1 behaviour anthropogenic trace elements and soil particles *9*
1.2.2 Anthropogenic fallout isotopes *10*
1.2.4 Anthropogenic Lead *12*
1.2.5 Optically Stimulated Luminescence *12*
1.3 RELEVANCY 13
1.4 RESEARCH OBJECTIVES AND HYPOTHESIS 14

2. METHODS **15**

2.2 FIELD LEVEL 16
2.3 ANTHROPOGENIC FALLOUT 17
2.3.1 Caesium *17*
2.3.2 Plutonium *17*
2.3.3 Lead *17*
2.4 OPTICAL STIMULATED LUMINESCENCE 18

3. MEERSSEN, ONDERSTE HERKENBERG **20**

3.1 STUDY LOCATION 20
3.2 SAMPLING 22
3.3 RESULTS 23
3.3.1 Field work *23*
3.3.2 Anthropogenic tracers *25*
3.3.3 Surface mapping of ^{137}Cs *27*
3.3.4 Performance of the samples to OSL *27*
3.3.4 Age estimation based on OSL *31*
3.4 DISCUSSION 38
3.4.1 Interpretation soil profiles *38*
3.4.2 Interpretation fallout distributions *38*
3.4.3 Interpretation OSL results *39*

4. GROTE HOUW **41**

4.1 STUDY LOCATION 41
4.2 SAMPLING DESIGN 42
4.3 RESULTS 43
4.3.1 field level *43*
4.3.2 Anthropogenic tracers *45*
4.3.3 Surface mapping of ^{137}Cs *46*
4.3.4 Performance of the samples to OSL *46*

4.3.5 Age estimation based on OSL ... *50*
4.4 Discussion Grote Houw ... 57
4.4.1 Interpretation soil profiles and surface processes ... *57*
4.4.2 Interpretation fallout isotopes ... *57*
4.4.3 Interpretation OSL results ... *57*
5. GENERAL DISCUSSION AND CONCLUSION ... **59**
5.1 Determination of soil erosion per soil profile ... 59
5.1.2 The use of anthropogenic Pb ... *61*
5.1.3 The use of OSL ... *61*
5.2 Estimation of erosion rates at field level ... 63
5.2.1 From soil profiles to field level ... *63*
5.2.2 models based on fallout isotopes ... *65*
2.2.3 approximation of soil erosion rates ... *67*
5.3 Recommendations ... 69
6. ACKNOWLEDGEMENT ... **70**
REFERENCES ... **71**
APPENDIX ... **74**
A: Hand-auger descriptions Meerssen ... 74
B: Pit profile descriptions Grote Houw ... 88
C: Surface analysis Medusa ... 90

LIST OF FIGURES

Fig.2: Location of the used archaeological locations in this study
Fig.3: Schematic outline of the process of radiometric sedimentology
Fig.4: Principle of Luminescence dating
Fig.5: Slope-normal and slope-parallel directions and a sketch of the commonly recognized chaotic flow path of soil particles from A to B.
Fig.6: Time periods that can be covered per method since deposition of soil material
Fig.7: Graphical presentation of the equivalent dose determination using the SAR procedure
Fig.8: Meerssen in 1831, 1850 and 1921 AD
Fig.9: DEM with sampling design hand-auger transects and soil collecting cores
Fig.10: Cross sections made from the hand-auger transects
Fig.11: Derivatives from the 5m resolution DEM
Fig.12: Concentration distributions of ^{137}CS, $^{239+240}$Pu and anthropogenic Pb
Fig.13: Correlation of measured Pb concentrations with K2O and Rb
Fig.14: Thermal transfer test result
Fig.15: Dose response
Fig.16: Light sum curve of sample NCL-9314113
Fig.17: FMM sample 113 (0.40 m) and 114 (0.70 m)
Fig.18: FMM sample 115 (1.00 m) and 116 (1.40 m)
Fig.19: FMM sample 117 (1.60 m) and 118 (1.90 m)
Fig.20: FMM sample 119 (2.10 m)
Fig.21: FMM sample 120 (0.23 m) and sample 121 (0.24 m)
Fig.22: The Grote Houw and surroundings
Fig.23: Locations of hand auger transects and soil pits
Fig.24: Cross sections based on hand-auger descriptions
Fig.25: Derivatives from the 5 m resolution DEM
Fig.16: Concentration distributions of ^{137}Cs, $^{239+240}$Pu and anthropogenic Pb in the different soil pits
Fig.27: Correlation of measured Pb concentrations with K20 and Rb
Fig.28: Thermal transfer result
Fig.29: Dose response
Fig.30: CAM pit 1
Fig.31: CAM pit 2
Fig.32: CAM pit 3
Fig.33: CAM pit 4
Fig.34: CAM pit 5
Fig.35: Cs distribution over the Netherlands due to the Chernobyl accident (Stoutjesdijk 1986)
Fig.36: FMM components of sequential samples are related indicating more or less the same age
Fig.37: Concentration profiles of fallout isotopes with age estimate of the youngest component and radial plot of the FMM components
Fig.38:concentration profiles of fallout isotopes with age estimate of the CAM
Fig.39: fallout isotope erosion models (Adopted from Walling 2011)
Fig.40: percentage concentration difference of ^{137}Cs and $^{239+240}$Pu based on the highest concentration and erosion rates in mm/year

LIST OF TABLES

Table 1: Details of the SAR protocol used for each sample
Table 2: Puck analysis with dose rate calculations
Table 3: FMM results C_28
Table 4: FMM results C_29 and C_30
Table 5: Soil ages based on the youngest component of the FMM
Table 6: Puck analysis with dose rate calculation
Table 7: FMM results Grote Houw
Table 8: Soil ages based on the CAM
Table 9: Total isotope concentrations per profile
Table 10: Excel spreadsheet of the erosion rate calculations

1. INTRODUCTION

1.1 GENERAL INTRODUCTION

This study was a contribution to the TOPsites project from the Dutch Ministry of Education, Culture and Science (NL: OCW, Onderwijs, Cultuur en Wetenschap) executed by the RCE, State Agency for Cultural Heritage (NL: Rijksdienst voor het Cultureel Erfgoed). Cultural heritage in the Netherlands is divided in four categories; (1) monuments in de form of buildings with a historical value, (2) archaeological traces and remains of human presence from 300,000 years ago in soil, on the land and in the water, (3) the Dutch landscape which is formed almost entirely by human use, and (4) movable heritage in the form of art and science collections. The goal of the TOPsites project was to protect archaeological monuments, belonging to the second category, *in-situ* from so-called creeping degradation. More than 90% of all archaeological findings in soils were located at a depth of less than 1 m under the surface level (van Os and Kosian 2011). Three locations were selected for this thesis with a highly probable threat to soil erosion and topographical levelling (Fig.2). The first study site was the Roman villa complex Meerssen- Onderste Herkenberg in Southern Limburg. The second site was the Grote Houw Oost in the northern province of Groningen. The field of interest is a mound (NL: wierde or terp), made by early Dutch settlers to protect themselves and their possessions to the sea. The third site was situated in the Limburg as well. This area is called Kelmond and has remains of a Neolithic settlement. Measurements done on this location are however not further described in this thesis.

Fig. 2: Location of the used archaeological locations in this Study

1.2 DETERMINATION OF SOIL EROSION

Soil erosion is defined as the detachment, entrainment and transport of soil particles under influence of natural or anthropogenic forces. The main effects of erosion are in general the loss of soil fertility, increased degradation of vegetation cover and a change in the water holding capacity of the soil (Martin-Fernandez & Martinez-Nunez, 2011). Soil erosion is also known as a selective process in which a relatively high amount of essential nutrients and other elements disappear due to two mean reasons. The first is that most of these nutrients are located in the topsoil and the second that a relatively large amount of organic matter and smaller soil particles, the carriers, are lighter and easier to be moved. Due to the translocation of soil from certain positions on the hillslopes it is assumed that the protective function of the soil to the archaeological monuments declined over time. The main focus of this thesis was to monitor the possible amount of the detachment and loss of soil particles by water and tillage. Tillage forms a possible threat due to mechanical mixing in the plough zone and the redistribution of usually the top 20-30 cm of the soil sequence to a uniform horizon. Soil particles can be displaced via ploughing both horizontal and vertical (Diez-Martín, 2010)**.** Horizontal displacement moves soil particles and objects in the plough zone along the soil surface and vertical displacement accumulates the biggest and heaviest soil particles and objects on the surface, while smaller particles move deeper into the soil sequence. Spatial patterns of interest for archaeologists are likely to be disrupted by this mixing process. In addition archaeological objects in the topsoil are also vulnerable to be physically damaged by the plough.

Soil erosion may be determined in several ways. Erosion can be directly measured on the field with, for example, rainfall simulators to calculate overland flow. One relatively new method is the measurement of soil erosion or soil redistribution directly from the field by tracking the development in changing elevation heights through time. For example, the Digital Elevation Models (DEMs) available for different years of the Meerssen area have been compared (Heeres 2014). Another method often used is to measure colluvial and alluvial sediment bodies produced by erosion. The thickness of the sediment bodies at several locations on a slope can be compared. Location of buried soil layers in the soil profile and a possible age of these bodies may indicate whether the deposition of sediment is still going on or not. The path of the sediment transport is often modelled as well to estimate the amount of and risk for sediment deposition at a certain location (Rompaey et al., 2001). Furthermore, the stability of a certain surface can be modelled with the aid of landscape evolution models e.g. LAPSUS. Several factors are combined in these LEM to predict the vulnerability for erosion at the locations of interest.

1.2.1 BEHAVIOUR ANTHROPOGENIC TRACE ELEMENTS AND SOIL PARTICLES

Anthropogenic trace elements (ATEs) were deposited on the soil surface and accumulated there. The accumulation may have led not directly to changes in the functional properties of the soil. What actually happened with the elements is dependent on various factors. In first instance, the buffer capacity of the soil played a role. This is the capacity of soils to store elements related to the presence of reactive soil components, the environmental conditions in the soil and the specific element properties. Once in the soil, ATEs substances can be absorbed by organisms, decayed to other forms of that element, or even be leached out to end up in the ground water. Bindings of elements can also be formed with metal hydroxides under influence of important element properties such as the charge, polarity and size. Important soil properties needed for these bindings are the clay content, content of Fe- and Al-(hydro) oxides, and the organic matter content. The moisture content,

oxidation and reduction state, pH, salinity, chemical and mineralogical composition including the possible presence of other anthropogenic deposits are known to have an influence on the probability of bindings to soil particles. Finally is also found that foreign soil material can get into the soil in the form of concretions. Transport of ATEs substances from the surface to deeper soil layers and groundwater was regulated as well by their chemical properties and by the displacement of their carrier substance. Clay particles and soil organic matter are proved to act as main carrier for many trace elements in the top soil layer (Tegen & Dörr, 1996). Transport of ATEs in soil can occurs in the form of i) convection or mass transport and ii) diffusion. In the first mechanism, the ATEs elements move along with the carrying element. The other transport mechanism, diffusion, occurs under influence of concentration differences in the soil. In this case, the carrier does not have to be moved as well. The different speeds of the ATEs element transport causes strong spatial variability in the distribution patterns, formed as a result of small local differences in composition of the soil.

Element tracing is often used in radiometric sedimentology by characterizing the various sediment components using the concentration of natural, gamma-ray emitting radionuclides (Fig.3) (van Wijngaarden et al., 2002). Analysis of the γ-ray spectrum is based on the determination of gamma photons emitted by radioactive isotopes. Every radioactive isotope emits specific gamma photons with a specific energy forming typical peaks for certain isotopes. The integral of the peak area(s) is used as a measure of the relative concentration of the isotope. The main radionuclides in a natural environment ^{238}U, ^{232}Th and ^{40}K are generally used as they have a long half-life. These radionuclides would have responded different to a treatment with for example high temperature or x-ray. But also the concentration of non-natural materials can been measured with the same purpose. By using radioactive standards with known concentrations the relative concentrations can be translated to absolute concentrations.

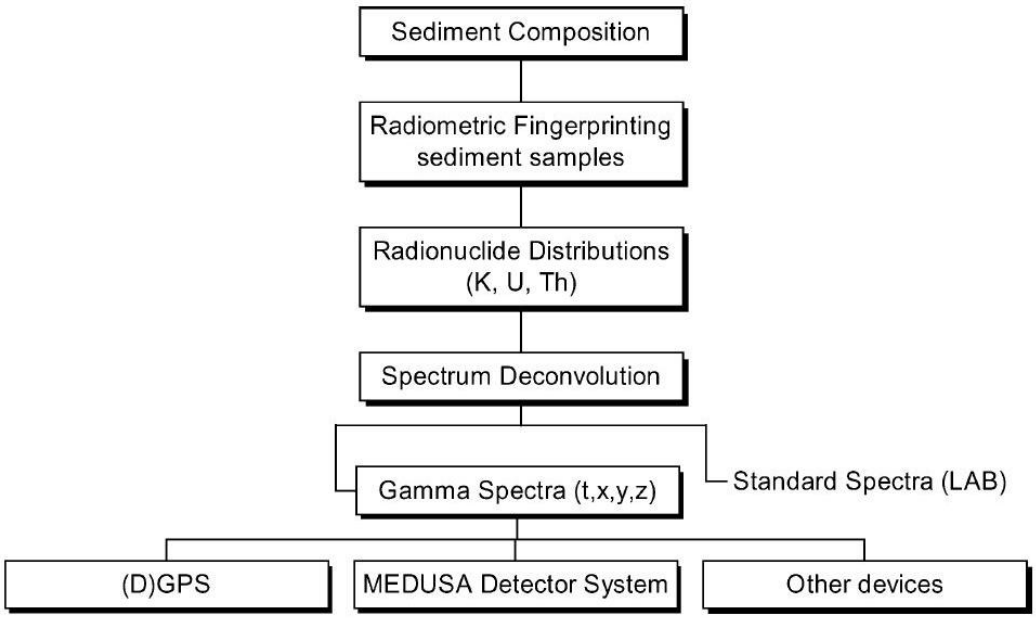

Fig. 3: Schematic outline of the process of radiometric sedimentology (Wijngaarden et al. 2002)

1.2.2 ANTHROPOGENIC FALLOUT ISOTOPES

Atmospheric radioactive isotopes were deposited during several events and periods and have been taken up by soil particles. These fallout isotopes from an anthropogenic source can be used to assess

soil erosion, because the total concentration of the isotopes is assumed to be less in the eroded soils and to increase in the colluvial or alluvial deposits. Two commonly used fallout isotopes are ^{137}Cs and $^{239+240}$Pu. In Europe, they originate both from two major fallout periods. The first peak visible in the ^{137}Cs deposition was around 1963, when the nuclear weapon testing peaked during the Cold War. After this peak, a Limited Test Ban Treaty was signed by the USA, the former Soviet Union and the UK. The latest peak in the fallout resulted from the Chernobyl accident in 1986 (An et al., 2014) and (Olson et al., 2013). The half-life of ^{137}Cs is 30.07 years (Ketterer et al., 2012). This means that a substantial part of the initial concentration after the first fallout period has already disappeared from the soil. The behaviour of ^{137}Cs in soils is largely controlled by sorption processes on the surface of fine particles and the migration on these particles due to soil erosion (Olson et al., 2013). If the distribution of the fallout can be assumed locally uniform, the concentration of the element can be used to estimate this translocation of soil (Schoorl et al., 2004). On local catchment scale is assumed that ^{137}Cs is spilled over the soil surface as a uniform blanket. ^{137}Cs is known to bind mainly with organic matter and clay particles. Tegen and Dörr (1996) published in their article about the mobilization of ^{137}Cs in organic rich soils. They found that it was possible that the transport velocity of ^{137}Cs in undisturbed soils decreased with time as it binds to aged organic material which is less easily decomposable than fresh organic material.

$^{239+240}$Pu originated as well as ^{137}Cs from the atmospheric nuclear weapon tests. The fallout of $^{239+240}$Pu during the Chernobyl accident was confined much more regionally and unlikely to be a significant contributor to the total $^{239+240}$Pu activity deposited in the Netherlands (Alewell et al., 2014). According to Alewell plutonium has a more homogenous spatial deposition than ^{137}Cs. This because $^{239+240}$Pu was deposited throughout the year and not connected to specific fallout events of one major bomb test or an accident as Chernobyl, during which external factors such as the soil cover could have had influenced the uptake. Ibrahim and Morris (1997) suggested that $^{239+240}$Pu is associated primarily with the hydrous oxide coatings of the soil and organic matter. But they found also that the association with the soluble and exchangeable components of the soil is relatively small. The remainder of the $^{239+240}$Pu content is tightly bound to silicates due to which relatively little Pu is available for physicochemical mobilization. $^{239+240}$Pu in a natural form is extremely rare. $^{239+240}$Pu is one of the transuranic elements produced through successive neutron capture processes that began with a Uranium isotope as starting material (Ketterer & Szechenyi, 2008). The half-life of ^{239}Pu is 24,110 years the half-life of ^{240}Pu is 6,561 years (Ketterer et al., 2012). Similar to ^{137}Cs, there was a maximum in the total Pu deposition in 1963. Ketterer and Szechenyi (2008) concluded in their study that activity measurements of $^{239+240}$Pu had the potential to supplement or replace ^{137}Cs as a tracer for soil erosion, deposition and sedimentation. Partly because of the longer half-life time of Pu and partly because of the more even distribution over the soil surface. A ratio of 0.180±0.014$^{239/240}$Pu was determined for Northern Hemisphere fallout. Deviations from this $^{239/240}$Pu range implies the presence of additional $^{239+240}$Pu sources and are used as an indication of post-1950 sediments (Ketterer et al., 2004).

The concentration differences over slope of both fallout isotopes are often analysed and compared as a tracer for soil erosion. In continuous sedimentation sequences, concentration peaks are expected to be related to the depositional peaks in 1963 and 1986. In untilled undisturbed soil profiles, where the deposited isotopes were not buried but rather only slightly mixed with underlying soil layers by bioturbation, it is assumed that the radioactivity decreased exponentially with soil

depth. Tillage mixed the topsoil, and produced a homogeneous distribution of ^{137}Cs and $^{239+240}$Pu isotopes within the tilled layer with an abrupt transition to underlying deposits with no accumulated ^{137}Cs and $^{239+240}$Pu. However, a distinction between the total amount of these components in the soil profile and the concentration visible in the topsoil should have been made when studying erosion processes. Erosion resulted in loss of thickness in the A-horizon. Due to ploughing, the original isotope concentrations were diluted with "clean soil". In depositional locations, the concentration of isotopes at the surface would have been similar to that of the source area of the sediment. However, the thicker A-horizons or stacked sediment layers contained more of these isotopes when summed over the whole profile.

1.2.4 Anthropogenic Lead

Many soils are contaminated with anthropogenic lead in the densely populated Netherland. The composition of natural Pb is different than the isotope composition of anthropogenic Pb. This makes anthropogenic Pb traceable like the fallout isotopes. The deposition in nature areas is particularly derived from atmospheric deposition, while fertilizers containing Pb were added to agricultural fields on top of the atmospheric deposition. Moreover, variety in the total amount of anthropogenic Pb distribution occurred due to the association with organic matter content of soils and the distance to places with higher population- traffic and industrial density (Walraven 2014). Pollution of the environment with Pb started already during the Roman times and increased rapidly during the industrial revolution. The start of the deposition period of Pb from leaded gasoline was approximately around the start of the 20th century (Walling & Fang, 2003). Steps were taken in the 70s to reduce the use and emissions of anthropogenic Pb and improve the health situation. The changes in the deposition of Pb from fuel gasses were for example clearly visible in sediment layers of two lakes near Utrecht (Walraven 2014). The use of Pb and therefore also the anthropogenic deposition is however an ongoing process. Our main interest for this research was the determination of the soil depth at which there might be a peak in the Pb content referring to 1970-1980 AD when the usage of leaded gasoline was the highest.

1.2.5 Optically Stimulated Luminescence

Another dating technique that can be used to estimate soil erosion is optically stimulated luminescence dating, OSL. OSL is based on determining the time elapsed since crystalline materials, for this purpose the quartz grains in the soil, were last exposed to sunlight (Fig. 4).

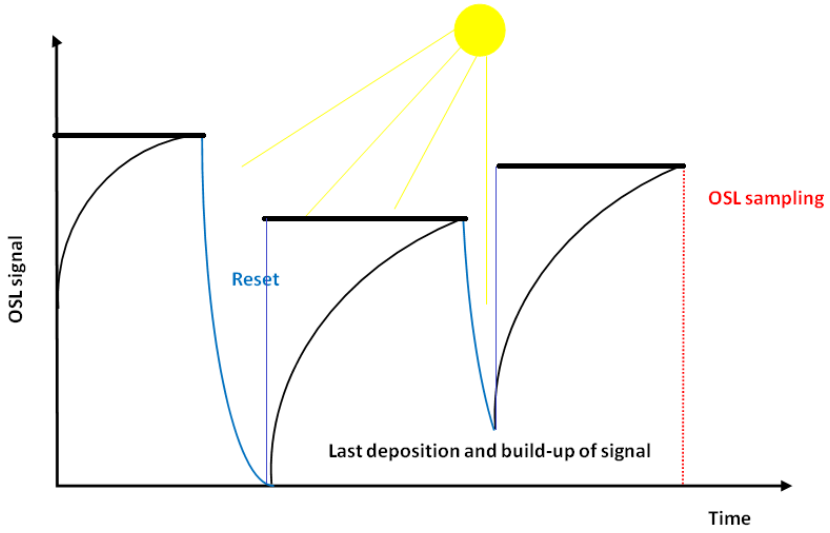

Fig. 4: Principle of Luminescence dating

It is assumed that this was during transport prior to deposition or the movement of grains in the soils due to bioturbation or tillage (Heimsath & Jungers, 2013)**.** Heimsath and Jungers (2013) stated that OSL can only be used to assess the slope-normal velocity of a grain transported downhill. Downhill movement of soil grains resolve, however, into slope-normal and slope-parallel components (Fig. 5).

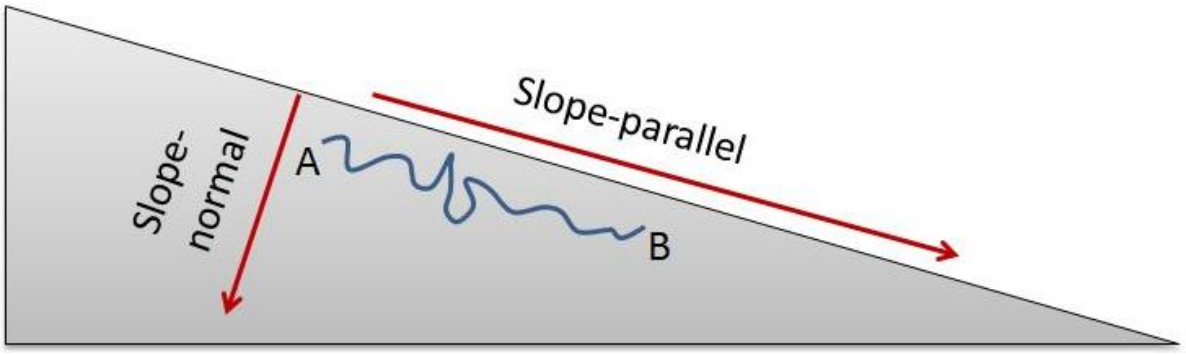

Fig. 5: Slope-normal and slope-parallel directions and a sketch of the commonly recognized chaotic flow path of soil particles from A to B.

In OSL it is assumed that the luminescence signal was completely reset at the time of burial. The luminescence signal increased after burial due to exposure of the mineral grain to ionizing radiation from natural occurring radioactivity in its direct environment and a small amount of cosmogenic rays. OSL on hillslope deposits has some major limitations (Fuchs & Lang, 2009; Preusser et al., 2008). One is the incomplete bleaching of the grains during the process of soil erosion. Considering small catchment sizes and short slopes and thus a short potential transport distance and time, the light exposure is expected to be relatively short. The signal may not have been completely reset because only a small fraction of the sediment was exposed to daylight, during which the luminescence signal can be set to zero. Another potential problem is the formation of agglomerates of individual grains. In that case only the outsides of the aggregates will be sufficiently bleached. Single aliquot methodologies were developed (Murray & Wintle, 2000) to improve the precision and reliability of OSL on young and poorly bleached sediments that were exposed only partially to light prior to deposition. The main aspect of this method is that all measurements were carried out on a single portion or aliquot of the same grains. Results are tested and corrected for sensitivity changes that may occurred during the measurement procedure (Murray & Wintle, 2000). Statistical analysis of the single aliquot distribution proved to give a reliable age estimate per sample (e.g. Reimann et al., 2012). Two other processes that are known to influence the dating of hillslope sediments are the repeatedly reworking of the sediments by tillage or bioturbation. Both processes ensure that mineral grains were frequently exposed to daylight before the sediment grains were eroded and transported. Bioturbation and ploughing continues however after the sediment is deposited, which increase the probability of daylight exposure after deposition. Mixing exposes younger grains with the original older colluvium. The mixing of younger grains with the original older soil layer influences the OSL result. After a period of time it becomes more difficult to determine the initial age of the colluvium, since more and more grains contain new information regarding the last exposure to light.

1.3 Relevancy

The major part of the TOPsites project budget is dedicated to physical measurements to protect the archaeological monuments against degradation. The selected archaeological locations are currently in use as agricultural fields. Levelling and soil erosion are considered common problems on sloping

agricultural fields. However, bare ground stimulates water driven erosion, while ploughing causes small soil translocations and favours the levelling of relief in the long term. As long as the monuments are buried in the soil they are considered to be protected. Measures are taken to prevent the degradation of the protective layer by soil erosion. A problem in protecting the monuments is however that the rate of the degradation and its impact on the monuments is often unknown. Since farmers are limited in their actions on these fields, it is essential to understand whether and how soil erosion takes place on the selected locations in order to estimate the severity of the situation and the urgency of intervention.

1.4 RESEARCH OBJECTIVES AND HYPOTHESIS

The aim of this research was to compare the different methods mentioned, involving sediment tracing and dating of burial ages, to measure the soil erosion rates at archaeological monuments under agricultural fields in order to determine whether action is needed or not to protect these monuments further for degradation. A couple of objectives were formulated. **The first objective was to estimate the rate of erosion. The second objective was to determine the differences and accuracy of the different used methods. The third objective was to model the erosion on the archaeological sites.**

The outline of this report is formed by two chapters on the materials, methods and results per location. Because the aim of the research was the same for both locations but the way of measuring differed at some points. In the end a general synthesis of all different parts will come together in a joint discussion (chapter five) and conclusion (chapter six).

2. METHODS

We focused on measuring the age of soil material at certain depths in a profile. Dating of colluvium is essential for the quantification of surface development and another used method to model soil erosion. A full spectrum of dating methods are developed covering the Earth's history (Lair et al., 2009). The use of the radioactive fallout isotopes ^{137}Cs, $^{239+240}Pu$ and anthropogenic Pb in environmental science is not new. Lair et al. (2009) combined ^{137}Cs and Optically Stimulated Luminescence (OSL) in a chronofunction and connected in this way millennial or centennial time scales (OSL) with decadal time scales (^{137}Cs). The combination of the four methods has not been done to my knowledge. By doing so, different periods of time will be covered (fig. 6).

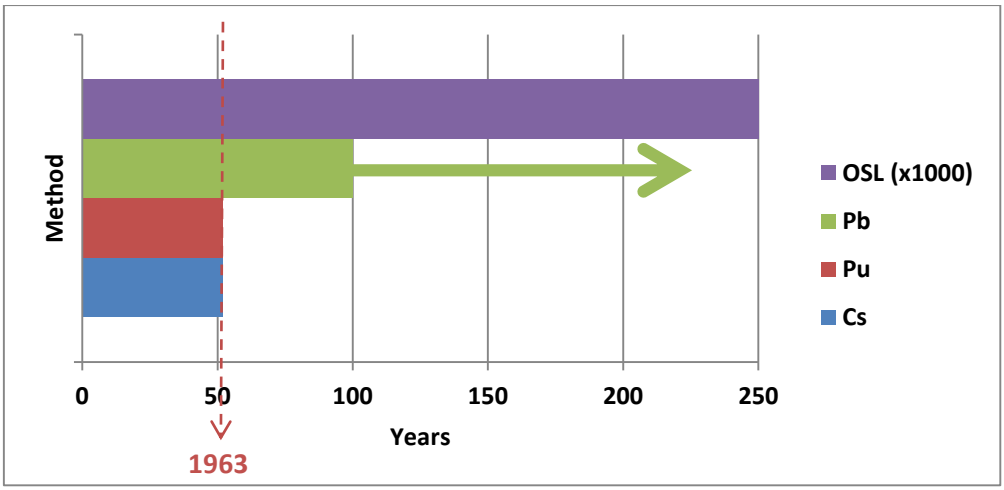

Fig. 6: Time periods that can be covered per method since deposition of soil material

The methods used will be discussed in general, because most operations were the same for all locations. Differences in sampling design and in the treatment of the obtained samples will be handled per location in the next chapters.

Two study locations are situated in the southern part of the province of Limburg on an incised plateau with heights up to 320m.a.s.l. This landscape was formed by active and recent uplifting associated to the Ardennen Massif and incision of the uplifted area by the river Meuse. River terraces formed under the influence of climate fluctuations and the changing flow patterns of the Meuse. River terraces were defined as relatively flat areas of land with a small height difference separated by a steep edge. A loess package was deposited on this undulating landscape during the Weichsel ice age. The thickness of the package at the time ranged from a few centimetres up to 20 meters (Jongmans et. al., 2012). Slope angles are relatively low and only 2% of the current agricultural areas is situated on slopes of more than 18% (Winteraeken & Spaan, 2010). The soils developed on the fertile loess are however vulnerable to surface runoff and soil erosion. Erosion rates and changing agricultural land use seemed to be strongly related. Pasture is, in general, less susceptible to soil erosion than arable soil. Several management projects have been launched since the mid-1970s when soil erosion and muddy floods were recognised as a problem by the local authorities. The Erosion Ordinance (EO) was presented in 1990 for the first time and later improved several times (Spaan et al. 2010). The EO was part of the EU Common Agricultural Policy (CAP) and farmers working according to these regulations relied on EU-subsidies. Non-inversion tillage was the most important part of the new regulation.

The northern part of the Netherlands, where the mounds (introduced in the general introduction) are situated, is for the eye quite flat compared to South Limburg. During the Pleistocene, a surface was formed under influence of formation and retreat of the ice sheets. Parts of this area developed into bays during the Holocene and became permanent elements in the coastal relief development. A salt marsh landscape originated with salt marshes and intermediate marsh basins. Silt on the higher areas alternated with clay in the basins. The first human settlers build mounds in several phases in pace with the accretion of the salt marsh (Jongmans et. al., 2012). These mounds were raised with sods of clay, manure and organic waste. Later, end 19th begin 20th century, this fertile soil had been excavated and sold by the time that living on mounds was no longer necessary because of the dikes. Instead of layers there were whole pieces removed from several places of the mounds. So this form of levelling was not a smooth process. These mounds have not only become lower by the aforementioned excavations, also erosion of centuries of ploughing had to be considered. Currently, 52.7% of the agricultural fields in Groningen is in use for the cultivation of crops. Over the years there was a slight shift towards grassland going on (Landbouwagenda 2012-2015 Provincie Groningen).

2.2 FIELD LEVEL

Digital elevation models, AHN2, from Meerssen and the Grote Houw are used to visualize the different slopes. Two other derivatives from the DEM are the multiple flow map and the modelled tillage erosion map. The multiple flow map simulated the accumulation of water at certain points in the field following a multiple flow algorithm. Flow out of a cell is divided over all lower grid cells. With the factor P more water can be directed to the cell with the highest altitude difference (the lowest), as compared to the other surrounding cells. This multiple flow simulation gives a better representation of the divergent and convergent properties of convex slopes (Schoorl 2004 part II). The tillage map was based on an erosion simulation calculated in LAPSUS with a diffusion-type equation:

$S_{till} = C_{till} * H * \Lambda$

A linear relation between the soil flux (S_{till}; m^2 a^{-1}) and the slope is assumed where C_{till} (m a^{-1}) is a tillage transport coefficient and H (m) is the ploughing depth (Baartman et al., 2012; Schoorl et al., 2004).The multiple flow directions of the soil particles were used in the tillage simulation as well to allow for better representation of the diverging and converging properties of the topography. The use of multiple flow directions in both models implemented causes longer paths of transport, decreasing tangents and decreasing effective erosion. The spatial impact of water erosion appeared however to be different from the spatial effect of tillage erosion (Schoorl 2004). Converging water flows enhanced erosion down slope and into the main transporting channels. Tillage erosion occurred in convex areas over the whole slope while net accumulation took place in concave areas down slope. These different erosive patterns were compared and used to explain the main factor causing soil erosion on the study location.

Transects were plotted for hand augering to describe the soil profiles. Special attention was paid in the auger description to the thickness of the plough layer, typical soil horizons such as the Bt (argic) and the depth at which natural lime was found (from the unweathered, not leached Loess parent material). Finally the presence of colluvium was established. The auger descriptions are included in the Appendix A and B.

2.3 ANTHROPOGENIC FALLOUT

2.3.1 CAESIUM

Spatial measurements on the ^{137}Cs activity concentration were done by the Dutch company MEDUSA Explorations BV. The variation in ^{137}Cs concentration at the soil surface was measured with a MS-4000 gamma spectrometer. This device was mounted on a quad and coupled to a RTK-GPS. To generate a high spatial density of measurement points a transect pattern with a distance of 2 meters was used. The quad drove with a speed of 5 km/h in combination with a log speed of 2 Hz. This resulted in a collection of data for every half a second (Appendix C). Based on previous research, a second device was used for the location in Meerssen to detect possible disruption in the pattern due to objects in the topsoil. With the 300 MHz ZOND radar antenna was searched, for among others, anthropogenic debris. Soil was collected as well in 300 ml trays for radiometric measurements from the aforementioned cores at exact the same depth as where the soil for OSL was taken from. Analysis were done with a NaI detector after which the total activity of the nuclides was determined with a Full Spectrum Analysis on the measured signal. The NaI-detector measured the ^{137}Cs concentration with a crystal that established the γ-ray that was emitted by the ^{137}Cs in the soil. Next to the amount of radiation, was the division of the energy or the spectra of the radiation estimated. The position of the peak in the energy spectrum specific for the ^{137}Cs spectrum was extracted. This was divided by the mass of the soil sample and the percentage dry matter. The radioactivity measurements were performed conform NVN 6595; norm sample preparation soil, sediment and sewage sludge. More information on the methods and materials used during the caesium fieldwork can be found in the Medusa report (van Egmond, 2014).

2.3.2 PLUTONIUM

Soil samples for the plutonium measurement were taken at the same depth as the samples for OSL and ^{137}Cs. The moisture and organic matter was removed overnight in an ashing oven with a constant temperature of 550°C for 3 hours. On average 6 gram of every sample was grinded for further analyses, which was carried out in Denver. The chemical procedures were adapted from those reported in Ketterer et al. (2004). Analysis is performed using a Thermo X Series II quadruple ICP-MS located at Northern Arizona University. The ICP-MS (Inductively Coupled Plasma Mass Spectrometer) worked with an argon plasma that was heated. The soil sample was ejected in the cooler central hole of the plasma and formed atomic ions under influence of the temperature. Emitted ions were than analysed with the mass spectrometer. The whole principle of the ICP-MS is explained by Houk (1994). Quality control samples were used obtained from different sources. Ketterer, who did the analysis, used several aliquots of Pu-devoid Triassic sandstone, Moenkopi material that had been spiked with small quantities of Rocky Flats Soil No.2 and several additional in-house check samples. Signals were collected for ^{238}U, ^{239}Pu, ^{240}Pu and ^{242}Pu. Ratios of $^{240/239}$Pu, $^{239/242}$Pu and $^{240/242}$Pu were calculated and corrected for mass discrimination based upon the $^{238/236}$U determined for a natural U solution. Specific information on the materials used for analysis was found in the report made by Ketterer (2015).

2.3.3 LEAD

X-ray fluorescence (XRF) is widely used to the investigation of metals. Ionization typical to the anthropogenic lead metal occurred after exposure to radiation with an energy greater than its ionization potential. The amount of released photons indicated the concentration of the specific metal of interest. In this research a handheld XRF, Thermo Scientific Niton XL3t Goldd+, was used to

determine the Pb concentration in the soil. A first scan was done directly under moist conditions. A more precise description can been given from dry soil. Small amounts of in general 10g soil were sampled from the 3 cores in Meerssen. These were measured on Pb concentration with the XRF after drying overnight at 105 °C and grinding. In both cases the measurement time was 110 seconds. The sampled core depth locations were based on the soil profile descriptions and on expert knowledge. Metal bins from 50:15:10 cm were beaten in the soil profile at the Grote Houw, with the purpose to do a second analysis in the lab. The profile was scanned over a line with a distance of 2 cm and an elapsing time of 110 seconds per measuring. A scaffold was used to stabilize the XRF during the measurements.

2.4 Optical Stimulated Luminescence

The sampled soil for the OSL was kept in the dark in order not to disturb the signal by exposure with daylight. Part of the samples were prepared for the equivalent dose (D_e) measurements and the other part for dose rate measurements. The part for the D_e was wet sieved to obtain a fraction of grains. For the analysis of the study location Meerssen the fraction of 212-250 µm was used and for the Grote Houw 125-180 µm. The fractions were treated with 10% HCl for 40 minutes and overnight with 10% H_2O_2. Quartz was separated from feldspar with LST p=2.58 overnight and sieved with a Whatmann 54 filter. LST is a solution of sodium heteropolytungstates in water and used for density separation. To remove the alpha-irradiated outer rim of the grains and to remove feldspar contaminations the fraction was treated with HF. 10% HF was used to catch on the first reaction and settle for 15 minutes. In addition the sample was etched with 40% HF for 30 minutes. Thereafter, the fraction was wet sieved again to obtain a purified quartz fraction. The other sieved (but not chemically treated) fractions were kept in the dark. The prepared fractions of the samples NCL-9214100 and NCL-9214101 got lost during a next step. So these samples were sieved again to obtain the fraction 90-125 µm. Then this fraction was also chemically treated.

Subsequently, several steps were followed to determine the preferable conditions for the dose equivalent measurements, which were all done on a Risø TL/OSL-DA-20 reader for Meerssen and a Risø TL/OSL-DA-15 reader for the Grote Houw. The Single Aliquot Regenerative (SAR) dose procedure (Murray and Wintle, 2000) was followed to determine the equivalent dose. Within this procedure the natural luminescence signal was first measured and compared to laboratory induced luminescence signals to find the radiation dose needed to obtain an equally bright signal. Luminescence sensitivity changes were monitored during a thermal transfer test, preheat plateau test and dose response test. Further steps were if necessary corrected to the changes by changing the temperature or amount of given radiation. The SAR procedure comprised seven cycles and was run six times per measurement (Table 1). In each cycle a regenerative dose was given and the ratio of regeneration (Lx) to test dose (Tx) OSL response was plotted on a dose response curve. The equivalent dose was then obtained by interpolation through projecting the Lx/Tx ratio on the dose response curve. Each of these aliquots consists of a sample disc containing ~30 grains on a 1-mm diameter sample. Several wheels per sample were made to obtain a batch of at least 20 approved D_e results. Acceptance criteria were a recycling ratio limit of 10 %, maximum test dose error of 10 % and signals that were more than 3 sigma above back ground. The most light-sensitive OSL-signal of quartz grains was selected using the "Early Background' approach (Cunningham & Wallinga, 2010). Integration time intervals were set at 0-0.5 seconds signal and 0.5-1.76 seconds as background. The records that fall in these intervals were represented in decay curves (Fig. 7).

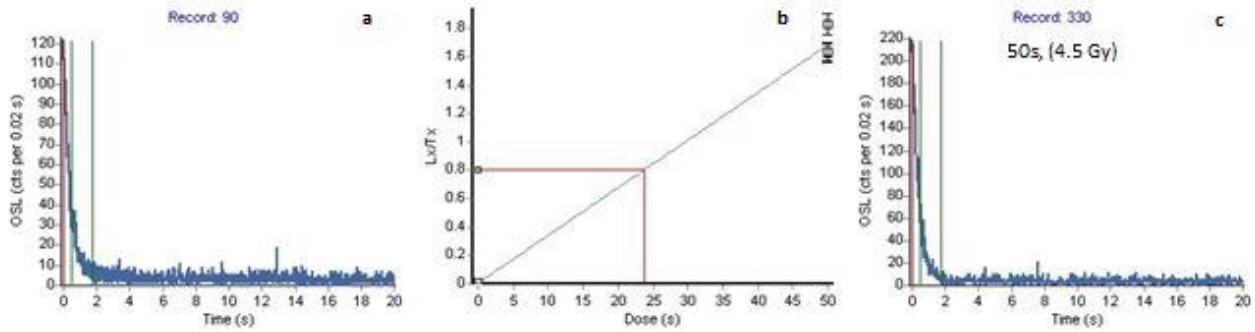

Fig. 7: Graphical presentation of the equivalent dose determination using the SAR procedure. One disc of sample NCL-9314117 gave **a.** natural luminescence decay curve, **b.** dose response curve and **c.** regenerative decay curve with a given dose of 4.5 (Gy) over 50 s. Integration time intervals are set at 0-0.5 seconds signal and 0.5-1.76 seconds as background.

Table 1: Details of the SAR protocol used for each sample. The sequence consist out of six runs comprising one on the natural signal and repeated tests of the regenerative β dose.

Step	Treatment	Meerssen	Grote Houw
1	Regenerative β dose	N, 4.5, 0, 4.5, 4.5, 45 Gy	N, 6.4, 0, 6.4, 6.4, 64 Gy
2	Preheat	200˚C for 10s	200˚C for 10s
3	IR exposure		For sample 100 and 101
4	Blue simulation	125˚C for 20s	125˚C for 20s
5	Fixed β test dose	2.7 Gy	3.9 Gy
6	Cutheat	180˚C	180˚C
7	IR exposure		
8	Blue stimulation	125˚C for 20s	125˚C for 20s
9	Blue bleaching at elevated temperature	210˚C for 20s	210˚C for 20s
10	Repeat step 1-9 for number of regenerative doses		
Extra 1	Additional IR measurement prior to step 4	30˚C for 40s	30˚C for 40s
Extra 2	LM-OSL to inspect dominance of the fast component	125˚C for 20s	125˚C for 20s

The part of the sample for the dose rate measurement was firstly dried overnight in the oven at 105°C to determine the water content. Secondly, the samples were placed in the ashing oven (500°C overnight) to remove and determine the organic matter content. The ashed sediment was grinded before making the pucks consisting out preferably a mixture of 70% sediment and wax. The wax served to provide a pre-determined geometry and to retain radon in the sample. The mixture was melted at 90°C. Pucks of 2 cm thickness and a diameter of 9cm were made when possible. If not, pucks of 1 cm were used. After two weeks of settling, the pucks were measured with a Canberra broad energy HPGe gamma spectrometer. The activity of isotopes within the U and Th decay chain and ^{40}K was measured and converted into dose rate using the conversion factors described in Guérin et al., (2011). These were corrected for moisture content and soft component attenuation of the effective dose rate ((Aitken, 1985; Madsen et al., 2005). The cosmic dose rate was thereafter calculated based on the geographic location of the sampling site (Prescott & Hutton, 1994) and information on the burial history.

3. MEERSSEN, ONDERSTE HERKENBERG

3.1 STUDY LOCATION

The first studied location was the Roman villa complex Meerssen- Onderste Herkenberg in Southern Limburg and selected as a monuments of high archaeological value. The villa was part of a concentration of villas north of the river Geul between Meerssen and Valkenburg that have been investigated in the late 19th and early 20th century. Some parts of this site were already described by Habets in 1871 (cited by De Kort 2013). Thanks to these detailed descriptions by Habets, the location in Meerssen has been subject of several studies ((De Groot, 2005; De Kort et al., 2013; Heeres 2014). Trenches were dug in 2003 to locate and estimate the value of other archaeological remains and soil profile descriptions were made as well (De Groot, 2005). Heeres conducted a research in 2014 to estimate the soil redistribution with AHN's, terrestrial LiDAR and a Landscape Evolution Model named LAPSUS, but concluded that further research was needed for a reliable result.
This Roman villa was build, probably in the first or second century AD, on the south facing slope of the Herkenberg. Habets assumed that the villa was destroyed in the year 176/177 AD. This he based largely on historical sources, archaeological remains and several traces of fire. In general it appeared that most villas in the Limburg loess have been abandoned around the late 2nd or early 3rd century AD. They belong to the type *villa rustica*, which was a farmhouse with land, barns, accommodation for the staff and stables for the livestock. Servants who worked for the owner permanently resided in the villa.

A road is dividing the nearly 1km long slope in an upper part and a lower less steep part on which the villa was found. The road is already visible on the map of 1831 (Fig. 8). So the flow connectivity of the catchment is disrupted for more than 150 years at least. In the southwest corner of the site was a water buffer made in which archaeological remains were found as well. The surface of the protected monument is 68.460m^2 and that became the extent of the research area. The generally fertile loess was in the past centuries used for both grassland and arable land. The lower part of the area had been used as an orchard, visible on the map of 1850 (Fig. 8). The railway was already present by that time and was thus constructed between 1832 and 1850. From the article by Habets it was also known that a plough competition took place in the 19th century within the area. The first houses built to the north of the border of the study location were drawn on the map of 1921. At this time the entire location seemed to be in use for the same land use type. All these events could be considered as influencing factors on the results of soil redistribution.

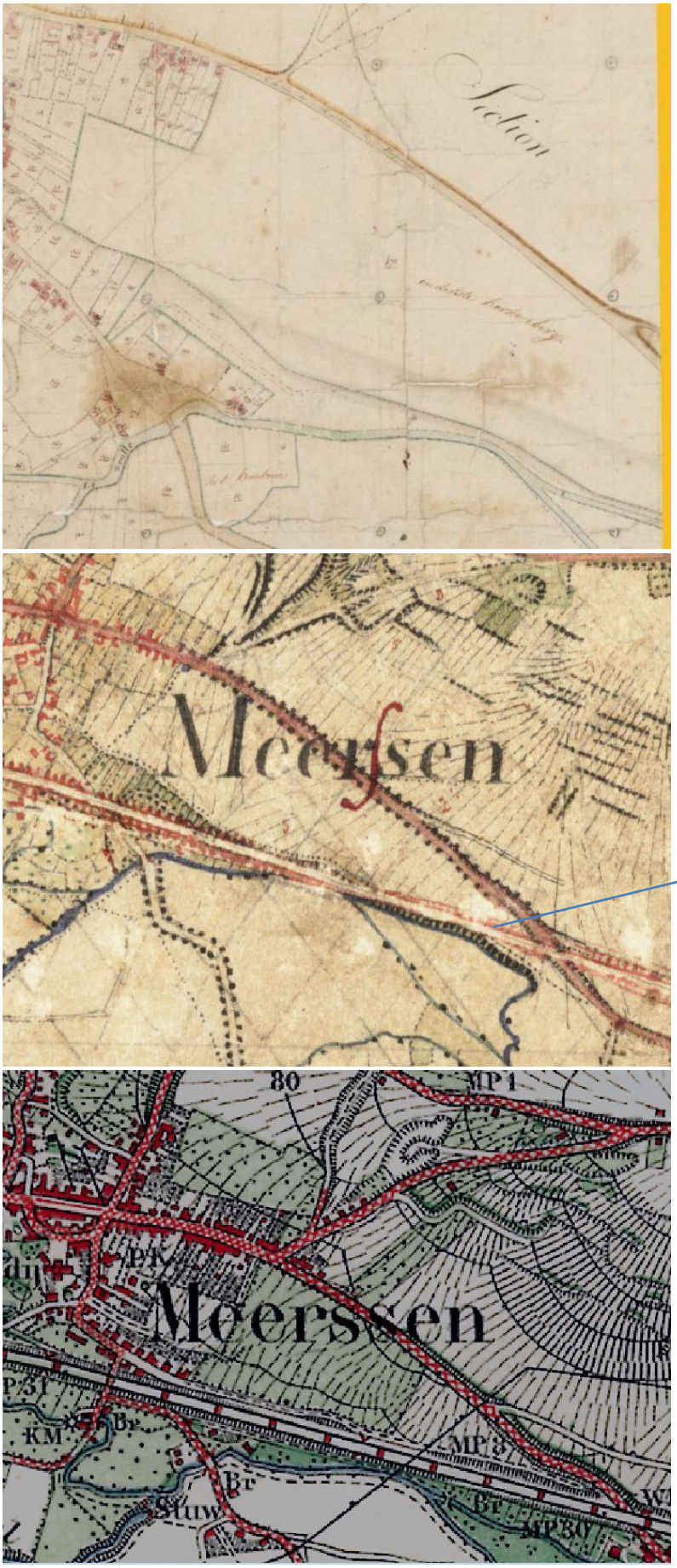

Fig. 8: Meerssen in 1831, 1850 and 1921 AD

3.2 SAMPLING

3 transects were hand-augered parallel to the slope to describe the soil profiles. Special attention was paid to the depth of possible colluvial layers. The transects were oriented roughly in a north-south direction and had a length of 250 m. Hand augerings were taken every 25 m which resulted in a pattern of 30 auger points (Fig. 9). The distance between the three transects was 100 m. The exact locations of the auger points were determined with a GPS. The augered soil was described conform NEN-5104 and the Standard Archaeological Auger description (NL; ASB). To collect soil for the OSL and other analyses, cores of 1 m and 10 cm in diameter were drilled into the soil at 3 locations close to the first transect. Some overlap was created between the cores to reach a depth of 3 meter at the location downslope where colluvium was expected. The cores were drilled by Thyssen drilling company and opened at the laboratory of TNO in Utrecht. One half of each core was taken to a lighted area for a horizon description. Soil was sampled for OSL based on this description from the other half of the core that remained in the dark.

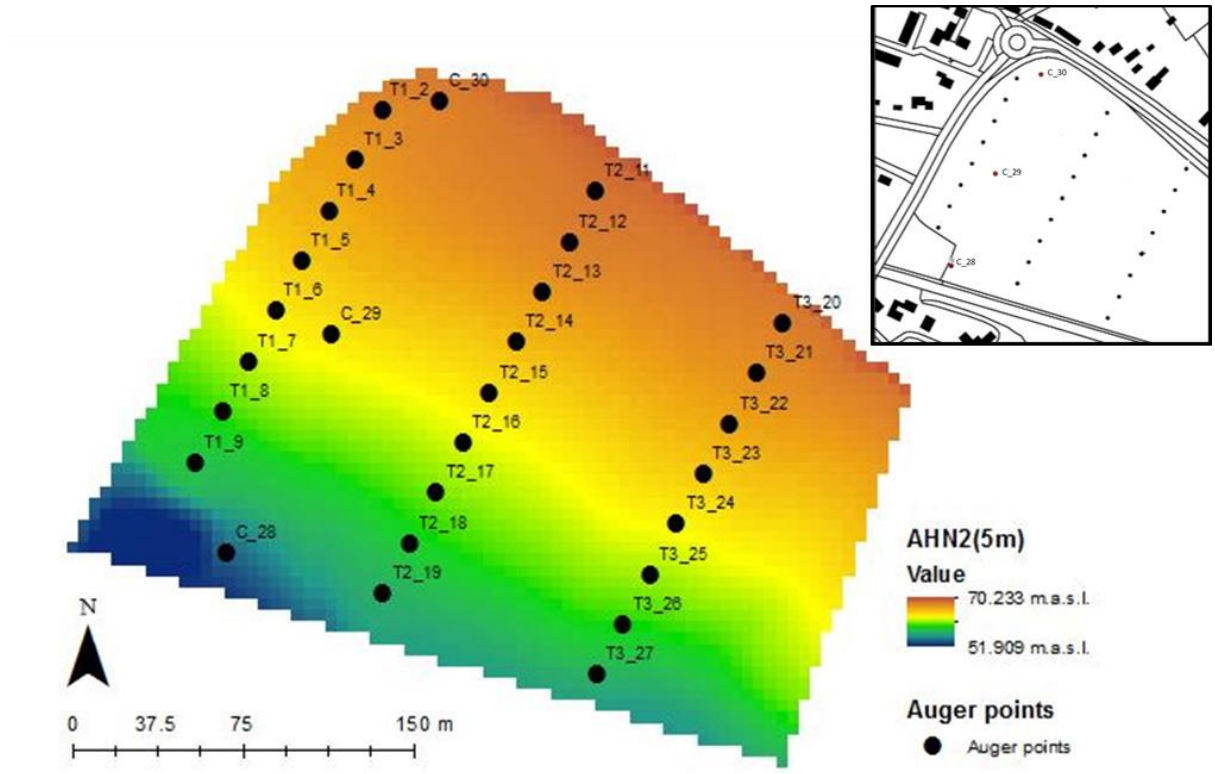

Fig. 9: DEM with sampling design hand-auger transects (T) and soil collecting cores (C)

3.3 RESULTS

3.3.1 FIELD WORK

Difference in height of the field level is respectively 12.61m, 10.68m and 10.15m between the first and the last point in the transects over a distance of 200m. The steepness of slopes of the three transects are therefore 6.31%, 5.35% and 5.08%. Out of the cross sections made from the data obtained by the hand-auger investigation, it became clear that the build-up of the soil layers in Meerssen is quite divers (Fig 10). Especially transect 1 and 3 are different at deeper soil depth. The plough layer was consistently found to have a thickness of c. 30 cm for the whole field. Calcareous loess can be found in both transect, but in transect 3 lime also occurred in the form of concretions whereas in transect 1 and 2 the lime was dissolved. Colluvium was only found at the foot of the slope in transect 1 (T1_9, T1_10 and C_28). Two palaeosols were buried by the deposition of the colluvium. In the northern part of the field, a horizon with solid clay was found in transect 3. Thereafter is the Bt horizon thinner and even absent at several locations mid- and downslope. T2 seems to have a deeper decalcified C horizon over the total length of the slope. On the other hand there is a decline in the thickness of the various C horizons visible in T3.

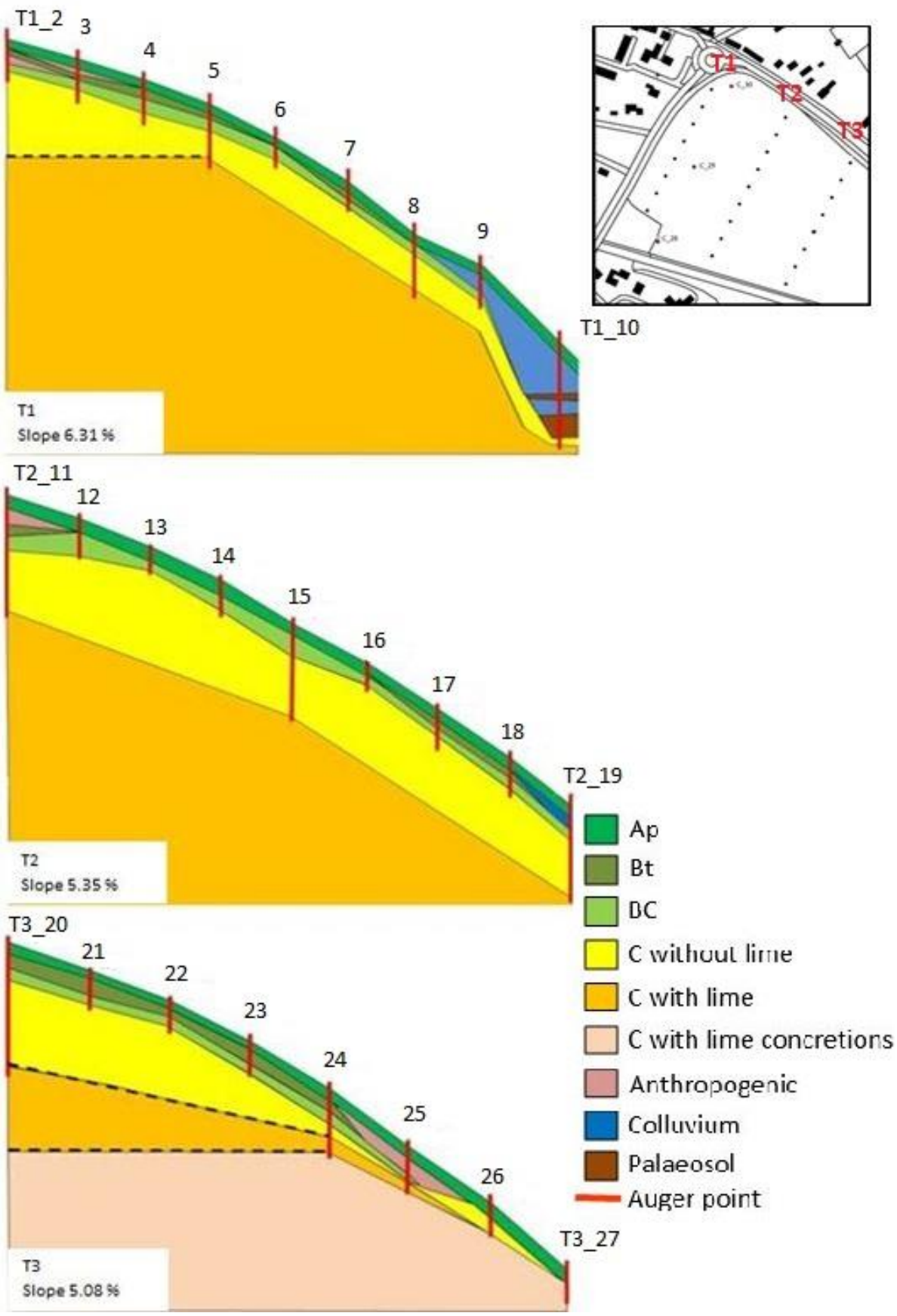

Fig.10: Cross sections made from the hand-auger transects

The slope derivative from the 5 m DEM resulted in an increasing slope profile more downslope. This same DEM is used to draw the water flow accumulation and tillage erosion estimation (Fig. 11). Some erosive lines became visible along the slope.

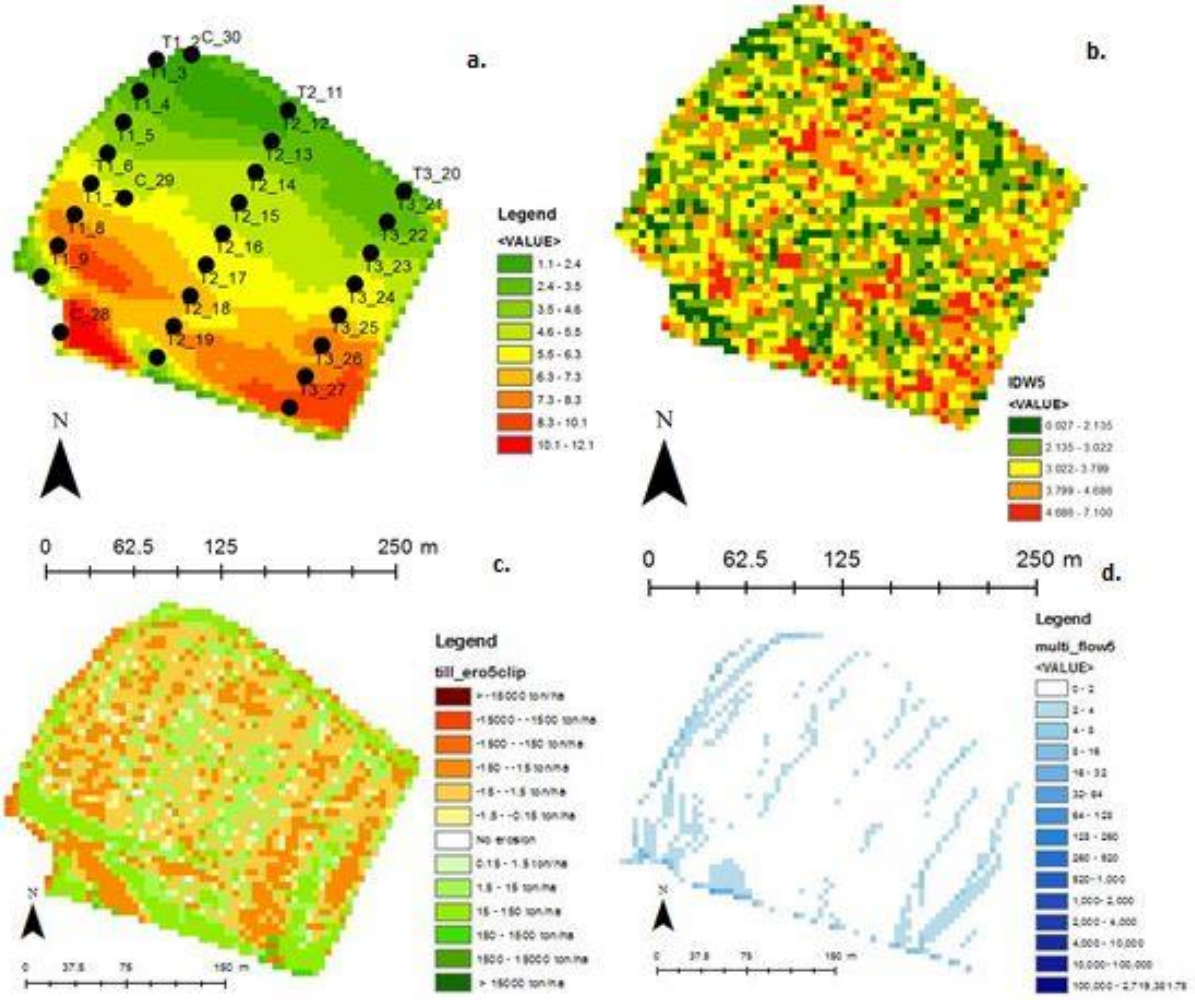

Fig. 11: Derivatives from the 5m resolution DEM, a. Slope in %, b. ^{137}Cs distribution, c. simulation of tillage erosion and d. simulation of water flow accumulation.

3.3.2 ANTHROPOGENIC TRACERS

The concentrations of caesium, plutonium and lead were measured as well at several depths in the soil profiles. Concentration differences were visible in the results for all elements of interest. The topsoil of the three cores contained more ^{137}Cs, Pu and Pb then the layers deeper in the soil (Fig. 12). The total amount of Plutonium was relatively low. $^{239+240}$Pu activities were measured between 0.010 ± 0.001 bq/kg and 0.156 ± 0.007 bq/kg. In 7 of the 12 samples, the Pu was even undetectable. $^{240/239}$Pu activity ratio of 0.189±0.028 indicated that the Pu was consistent with stratospheric fallout material from the 1958-1962 high-altitude H-bomb tests. Apparently, detectable amounts of Chernobyl-derived materials (with a ratio of c. 0.4) were present as well. The average atom ratio of $^{240/239}$Pu was 0.180±0.014, resulting from several tests for the 31-70° N latitude band (Ketterer et al., 2012).

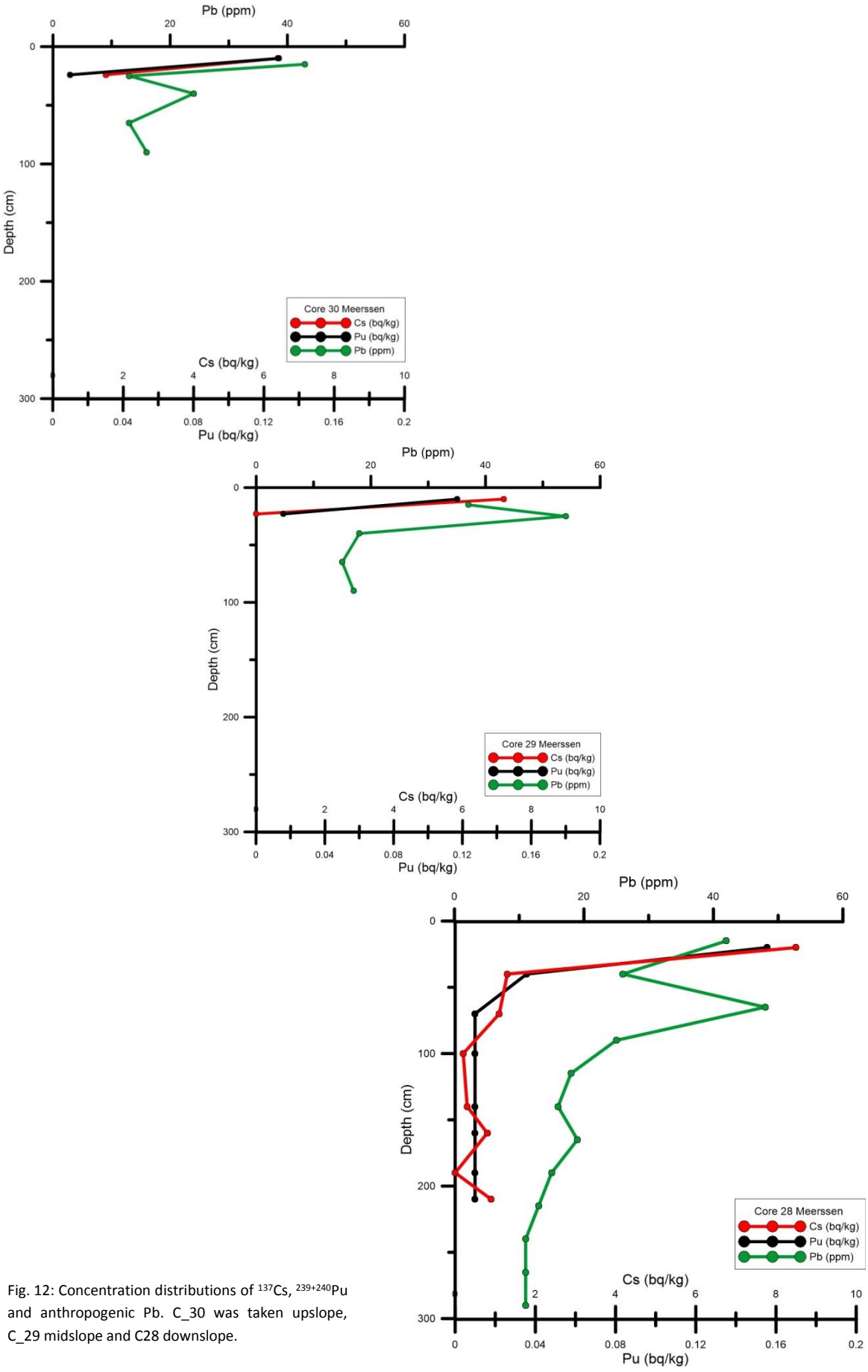

Fig. 12: Concentration distributions of ^{137}Cs, $^{239+240}Pu$ and anthropogenic Pb. C_30 was taken upslope, C_29 midslope and C28 downslope.

Concentrations measured in the same layer at several slope positions were different. Both $^{239+240}$Pu and ^{137}Cs are found at relatively high concentrations in the soil profile down slope. At a depth of 20 cm these concentrations were 0.156 ± 0.007 bq/kg $^{239+240}$Pu and 8.5 ± 0.5 bq/kg ^{137}Cs where the concentrations of these elements at this depth in the upper two cores had been reduced to almost zero. $^{239+240}$Pu and ^{137}Cs were in the lowest core still measurable at a depth of 40cm under field level. On top of the slope were the concentrations in the upper part of the topsoil higher than mid slope. The correlation of the measured Pb concentrations with the amounts of rubidium (Rb) and potassium Oxide (K_2O) was determined to trace the origin of the Pb. No clear relationship can been drawn from the scatter plots (Fig. 13). The patterns would have shown a linear correlation in the case of natural Pb instead of the point clouds that are visible now. The R^2 for all correlations was very low and ranges between 0.007-0.529. This indicate that there was in fact anthropogenic lead measured and no significant influence of natural isotope concentrations.

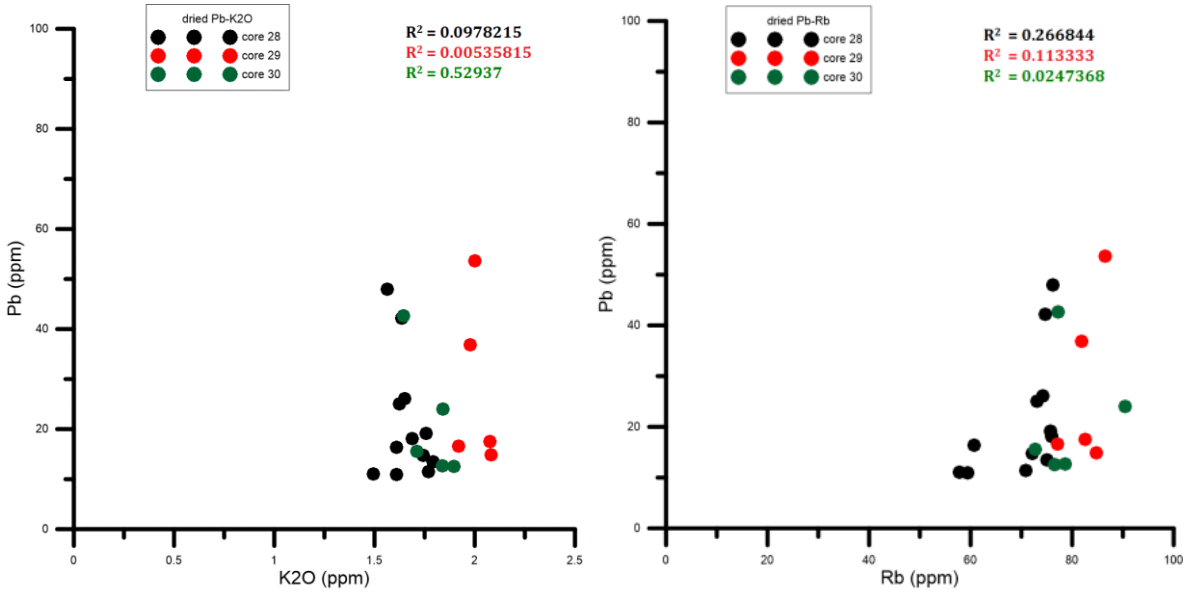

Fig. 13: Correlation of measured Pb concentartions with K2O and Rb

3.3.3 Surface mapping of ^{137}Cs

The surface ^{137}Cs investigation by Medusa resulted in a scattered pattern without clear relations in the pattern over the slope (Fig. 11b). The ^{137}Cs concentration in the topsoil varied from 0-7 Bq/kg. The green colour range, indicating a concentration of 2.5-3.5 Bq/kg, was the most abundant. Medusa concluded that less clay was present in the middle of the northern half of the parcel on the basis of time slices (van Egmond, 2014). This corresponded to the location of the Roman Vila. Influence of a lower clay content also applied to the lower part of the plot, but here the water content seemed to be higher.

3.3.4 Performance of the samples to OSL

Discussed concentration differences of the ATEs can indicate mainly potential erosion in the past 100 years. The depositional ages of the several soil layers per core were estimated by measuring the OSL signals. Special attention was paid to layers that were described as colluviums. For the selection of the most appropriate equivalent dose (D_e) measurements an IR test, preheat temperature test, thermal transfer test and dose recovery test were done according to the SAR protocol. The IR test was done to check if the samples were clean of feldspar. Quartz did in contrast to feldspar not

respond to IR stimulation (Duller, 2003). No strong reactions with feldspar were observed. Therefore, it was not necessary to clean the samples again. Besides, an IR bleaching was built at the end of each following sequence to determine the possible influence of feldspar on aliquots. These aliquots were then rejected for further analysis. Thermal transfer is a phenomenon that has a major effect on the natural sample and not on subsequent regenerative dose measurements. Young sediments are particularly susceptible. In this test the luminescence signal was measured after erasing the latent luminescence. If the equivalent dose was significantly > 0 Gy this was due to a transfer of charge from hard-to-bleach to easy-to-bleach traps. Thermal transfer was observed at temperatures above 220 °C (Fig. 14).

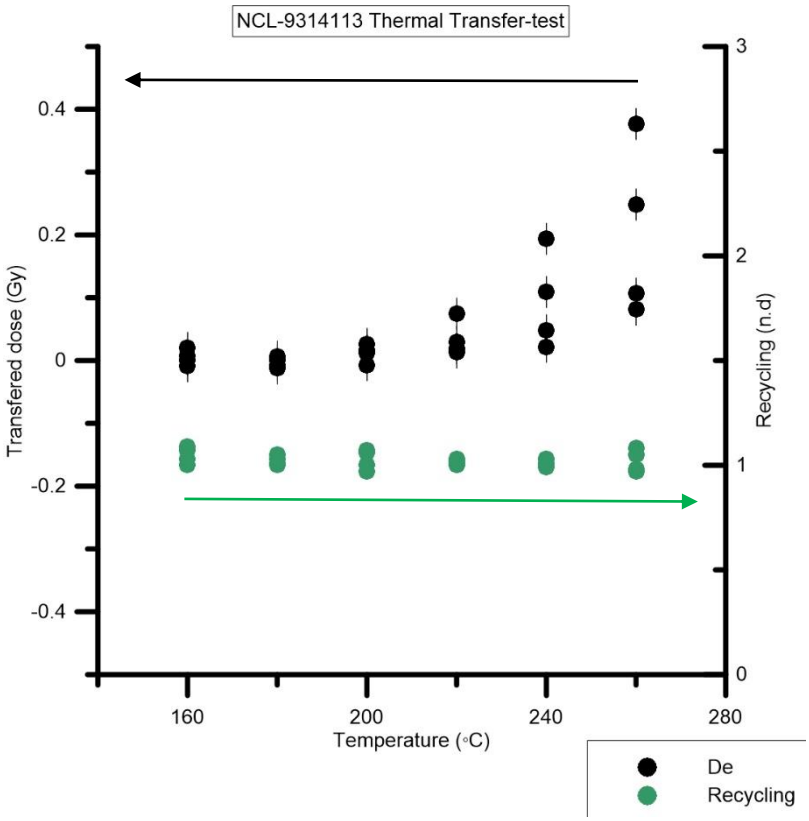

Fig. 14: Thermal transfer visible at a temperature of 220°C at sample 113

Another temperature related test is the preheat plateau test to check whether the applied preheating procedure of the sample is sufficient to remove unstable signal components. To prevent both thermal transfer as an unstable charge tested with the preheat plateau test was chosen for a preheat and cutheat of 200°C and 180°C, respectively. To prove the suitability of these choices was a dose recovery test conducted in which the natural signal was erased first. Instead, a known dose was treated as the natural signal. Four discs with a diameter of 5 mm were measured per sample. The ratio of measured/given dose should have been equal to unity. The dose recovery ratio for all samples is given in figure 15. Seven of the thirty-six points deviated more than 2 sigma from one (1.00 ± 0.02). A large part of the deviation was derived from ample 119, which has an average dose recovery ratio of 1.07 ± 0.03, n=4. The average dose recovery ratio of all samples indicate however that the SAR protocol could be used to accurately determine a laboratory dose. CAM gave an average dose recovery ratio of 1.03 ± 0.01, n=36. During the SAR protocol, the samples were measured on discs of 1 mm in the order to ensure that there was actually a single aliquot measurement preformed.

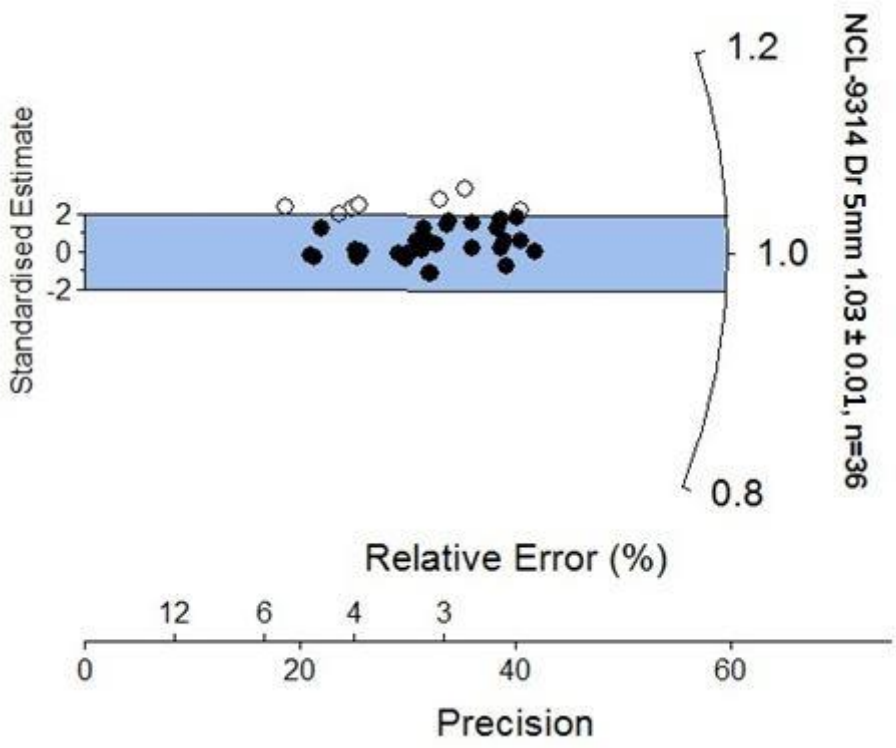

Fig. 15: Dose response of all samples

Dose rates of the different samples are in line with expectations (Table 2). Water content and organic matter content were used for calculation of the environmental dose rate. The water content was on average 22.3 ± 1.3 % and the organic matter content 1.8 ± 0.04 %. For calculation of the cosmic dose rate it is assumed that the samples were gradually covered by younger sediments since deposition. Attenuation by the water column is taken into account, because the attenuation of ionising radiation is much greater if the pores in sediments are filled with water rather than air. The average dose rate was rather constant during time as there are no big differences per sample. Results ranged from 2.57 Gy/ka tot 3.42 Gy/ka.

Table 2: Puck analysis with dose rate calculations

	113	114	115	116	117	118	119	120	121
K-40 (Bq/g)	0.626 ± 0.013	0.630 ± 0.012	0.611 ± 0.012	0.518 ± 0.010	0.634 ± 0.012	0.541 ± 0.011	0.536 ± 0.011	0.539 ± 0.011	0.686 ± 0.013
Pb-210 (Bq/g)	0.055 ± 0.003	0.060 ± 0.003	0.061 ± 0.003	0.043 ± 0.002	0.058 ± 0.003	0.046 ± 0.003	0.042 ± 0.002	0.037 ± 0.002	0.055 ± 0.003
Pb-212 (Bq/g)	0.041 ± 0.003	0.043 ± 0.003	0.044 ± 0.003	0.039 ± 0.003	0.042 ± 0.003	0.038 ± 0.003	0.039 ± 0.003	0.037 ± 0.003	0.044 ± 0.003
Bi-212 (Bq/g)	0.052 ± 0.003	0.051 ± 0.002	0.051 ± 0.003	0.040 ± 0.002	0.046 ± 0.003	0.043 ± 0.003	0.044 ± 0.002	0.043 ± 0.002	0.052 ± 0.002
Pb-214 (Bq/g)	0.052 ± 0.001	0.055 ± 0.001	0.051 ± 0.001	0.042 ± 0.001	0.052 ± 0.001	0.043 ± 0.001	0.047 ± 0.001	0.044 ± 0.001	0.054 ± 0.001
Bi-214 (Bq/g)	0.052 ± 0.001	0.052 ± 0.001	0.050 ± 0.001	0.044 ± 0.001	0.051 ± 0.001	0.044 ± 0.001	0.047 ± 0.001	0.045 ± 0.001	0.052 ± 0.001
Ac-228 (Bq/g)	0.049 ± 0.001	0.050 ± 0.001	0.049 ± 0.001	0.042 ± 0.001	0.047 ± 0.001	0.042 ± 0.001	0.045 ± 0.001	0.044 ± 0.001	0.051 ± 0.001
Th-234 (Bq/g)	0.052 ± 0.002	0.051 ± 0.002	0.045 ± 0.002	0.039 ± 0.002	0.048 ± 0.002	0.041 ± 0.002	0.040 ± 0.002	0.041 ± 0.002	0.047 ± 0.002
Water content (%)	20.51 ± 1.052	24.42 ± 1.492	25.48 ± 1.623	25.40 ± 1.613	22.28 ± 1.241	20.99 ± 1.102	21.82 ± 1.189	20.19 ± 1.020	19.55 ± 0.956
LOI (%)	2.140 ± 0.004	2.850 ± 0.008	1.930 ± 0.004	1.920 ± 0.004	1.490 ± 0.002	1.170 ± 0.001	1.040 ± 0.001	2.290 ± 0.005	1.760 ± 0.317
Attenuation %	22.65 ± 1.113	27.27 ± 1.636	27.41 ±1.645	27.31 ± 1.639	23.78 ± 1.427	22.16 ± 1.108	22.86 ± 1.143	22.48 ± 1.124	21.31 ± 1.066
Dose rate (Gy/ka)	3.240 ± 0.421	3.190 ± 0.140	3.120 ± 0.140	2.570 ± 0.120	3.190 ± 0.140	2.770 ± 0.120	2.740 ± 0.120	2.700 ± 0.110	3.420 ± 0.140

3.3.4 AGE ESTIMATION BASED ON OSL

The D_e distributions obtained from the single aliquots measured per sample were more scattered than expected for this kind of deposit. It was assumed that this scatter was mainly caused by post-depositional mixing due to bioturbation or ploughing. We made use of the Finite Mixture Model (FMM) to provide an age estimate for the primary deposition and the termination of the mixing process. A first estimation was made based on the average D_e with standard deviation divided by the square root of the total amount of aliquots. Outliers were removed by fitting the results of the samples in a Gaussian by the lowest peak in the distribution. A second Gaussian was fitted to the remaining data to aid the fitting procedure. Both a Central Age Model (CAM) and a Minimum Age Model (MAM) were run over the single aliquots per sample. Those models estimate, as appears from the name, the central and minimum age of the sample. Whereas the FMM can be used to identify several populations within a dose distribution (Roberts et al., 2000; Reimann et al., 2012). The model calculates the number of components or populations that give the best fit to the D_e distribution of the single aliquots. To estimate the best number of components the lowest BIC (Bayesian Information Criterion) score was used. The finite mixture model was considered to be dangerous to apply to D_e estimates other than single grain (Arnold & Roberts, 2009). Even to aliquots with a few grains, because they could contain luminescent grains from more than one parent population. Reimann et al. (2012) proved that it is appropriate to use the FMM if the small aliquot measurements are a good proxy for single grain measurements. To check this the light sum curve was measured on quartz single grains (Fig. 16). On average more than 75% of the luminescence intensity in response to a known dose is emitted by 5% brightest grains. Because there are approximately 30 grains on one disc this corresponds to a response from a single grain.

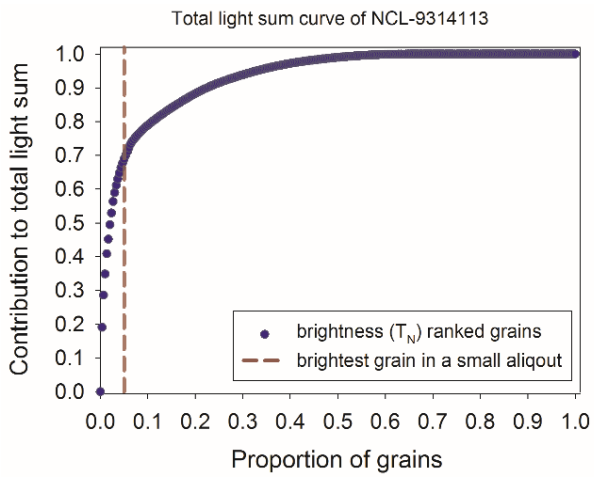

Fig.16: Light sum curve of sample NCL-9314113. The proportion of light that is emitted by the brightest quartz grain in a small aliquot is indicated by the dashed line.

Rstudio is used to calculate the FMM for all samples:

calc_FiniteMixture(DE121,sigmab=0.2,n.components=c(2:4),plot=TRUE)

In which “sigmab” is the expected overdispersion in the data should the sample be mainly un-mixed or un-disturbed (Cunningham & Wallinga, 2012) and “n.components” the range of possible number of components to be fitted. A sigma b value of 0.2 is used and the maximal number of components is set to 4. The probability gives the percentage of aliquots from the total amount that fits to the

certain component of the FMM for that sample (Table 3). Radial plots are made to display the results visually. The main component of sample 113 is the second with a probability of 88%, referring to an age of 0.33 ka. This is more or less the same age giving to the second component of sample 114 (Fig. 17). The main component of sample 114 is however younger with an age estimate of 0.16 ka.

Table 3: FMM results C_28

ID	n	Age (ka) per component based on De distribution							
		1st	P (%)	2nd	P (%)	3rd	P (%)	4th	P (%)
113	28	0.11 ± 0.02	12	0.33 ± 0.02	88				
114	28	0.16 ± 0.03	59	0.34 ± 0.06	38	4.73 ± 1.08	4		
115	32	0.33 ± 0.02	89	0.95 ± 0.26	7	6.19 ± 1.27	3		
116	22	0.64 ± 0.04	68	13.4 ± 2.95	28				
117	26	0.77 ± 0.05	61	1.36 ± 0.15	27	3.27 ± 0.45	11		
118	29	0.78 ± 0.12	19	2.07 ± 0.16	47	7.64 ± 0.80	20	14.1 ± 1.69	15
119	18	3.04 ± 0.34	27	11.5 ± 0.74	73				

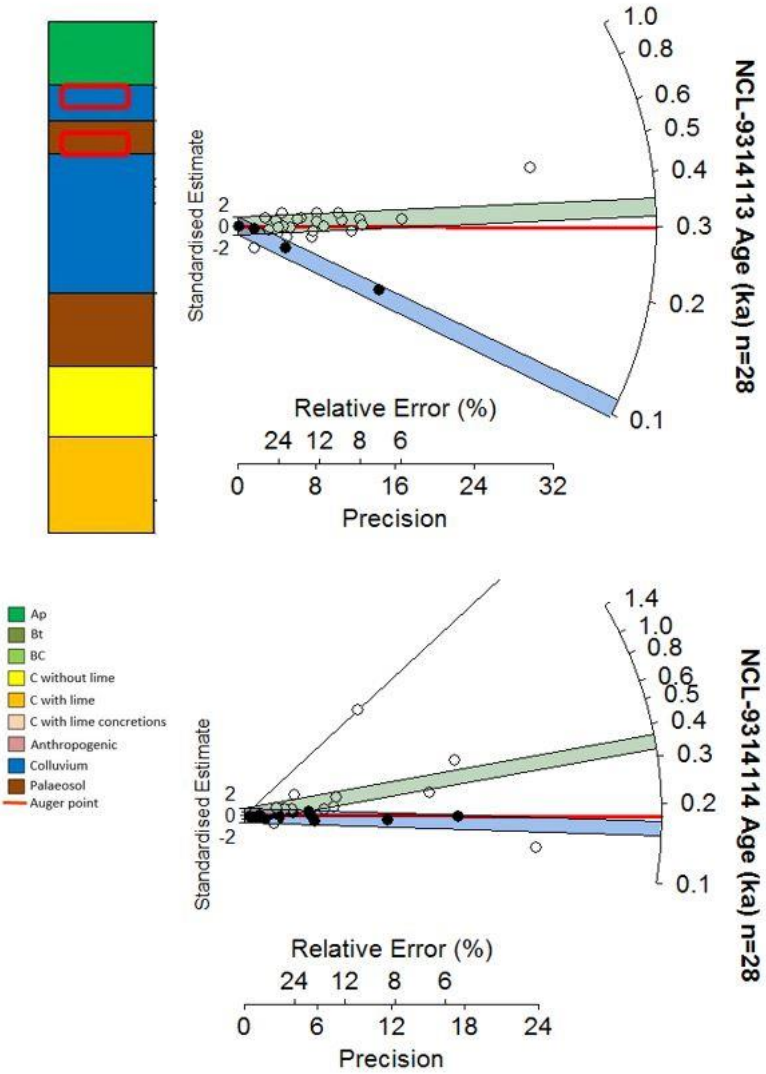

Fig.17: FMM sample 113 (0.40m) and sample 114 (0.70m). The red line shows the average Age (ka).

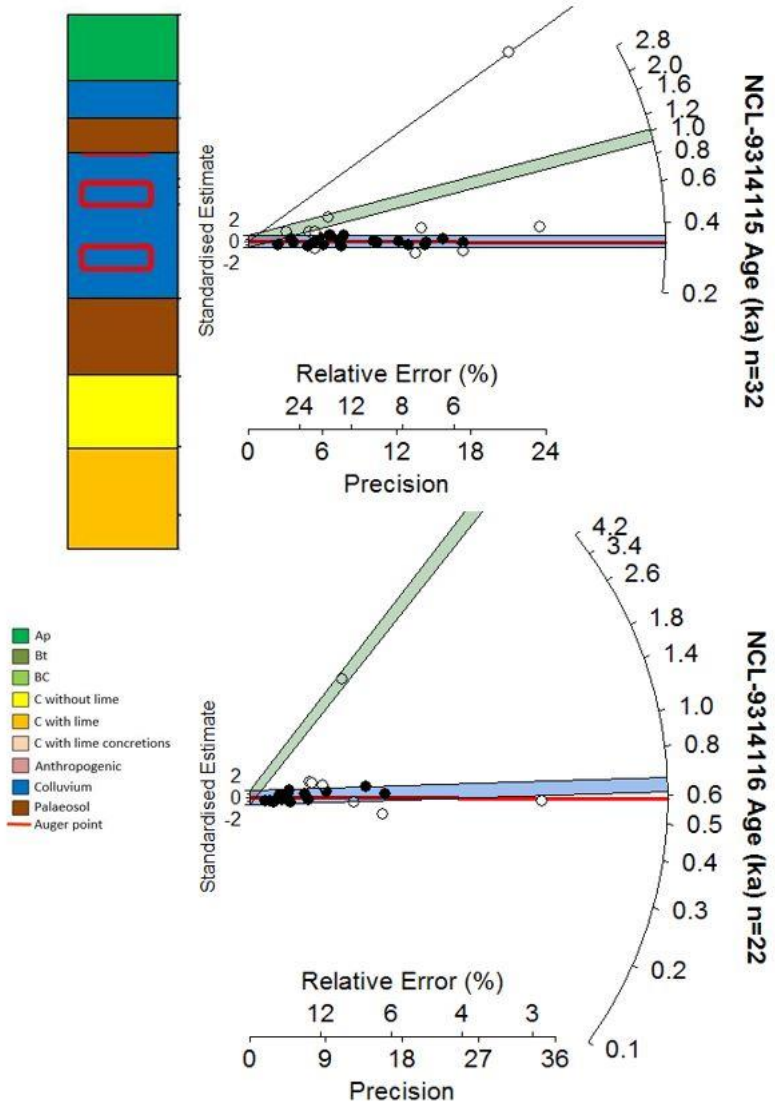

Fig.18: FMM sample 115 (1.00m) and sample 116 (1.40m). The red line shows the average Age (ka).

Sample 115 was taken from the first colluvial layer. The average age of the largest component is again 0.33 ka, which is the same as the average age of the largest component of the first sample in this profile. Sample 116 was taken from the same colluvial layer, but a bit deeper where the soil properties were slightly different. The main component of this sample refers to an age of 0.64 ka.

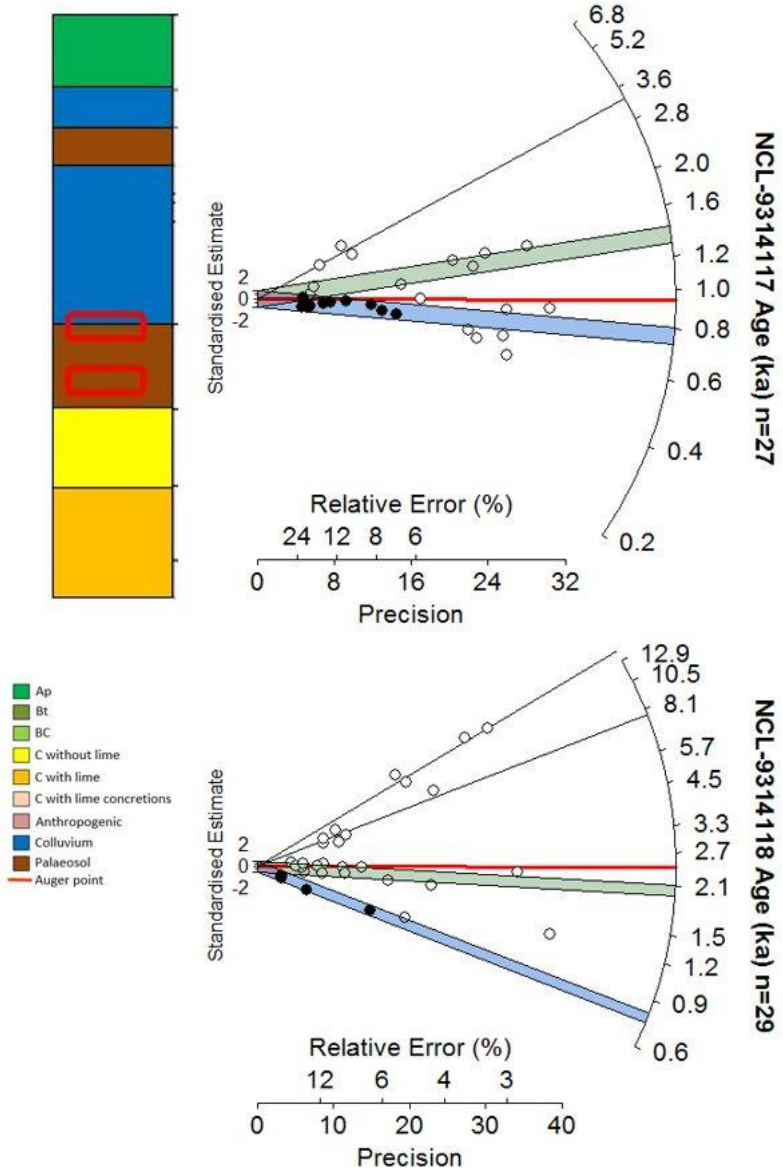

Fig.19: FMM sample 117 (1.60m) and sample 118 (1.90m). The red line shows the average Age (ka).

Sample 117 (Fig. 19) was taken in a palaeosol as well as sample 114. The youngest, main, component has the same average age, 0.77 ka, as the main component of 116 from the colluvial layer on top of this palaeosols. The second component is just a little bit younger than the main component of sample 118 (Fig. 19). This is a mixture of four components from which the second is the largest with an average of 2.07 ka. The two oldest components refer to the deposition or reworking of the loess. Sample 119 (Fig. 20) was taken from the decalcified C horizon, which is considered to be the original depositional loess. A smaller first component is indicating some mixing with younger aliquots.

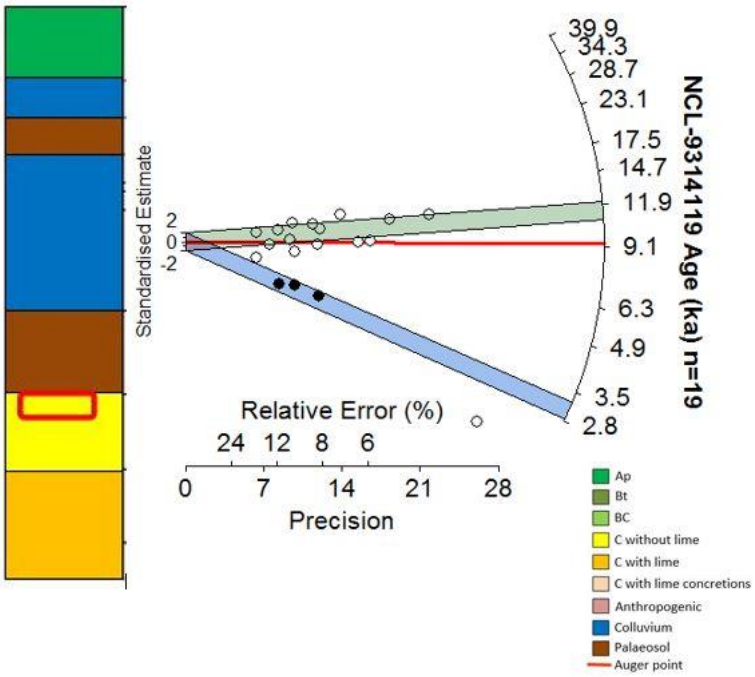

Fig.20: FMM sample 119 (2.10m). The red line shows the average Age (ka).

Sample 120 is taken from core 29 on the mid slope position. The FMM gives a mixture of four components at a depth of 0.23m, just below or partially in the plough zone of the soil (Fig. 21). The average age of the total mixture is 1.90 ka (Table 4). The difference between the first and last component is 7.48 ka. The youngest sample is with a probability of only 4% by far the smallest. Sample 121 (Fig. 21) is taken from more or less the same depth, but from core 30 at the top of the slope. This sample is as well a mixture of four components and in this sample is the youngest component again the smallest. Both samples are taken in horizons indicated as illuviation layers. The main components refer to the period in which loess was deposited.

Table 4: FMM results C_29 and C_30

ID	**n**	**Age (ka) per component**							
		1st	P (%)	2nd	P (%)	3rd	P (%)	4th	P(%)
120	26	0.15	4	0.59	28	1.57	33	7.63	35
121	25	0.55	5	1.70	39	4.81	31	10.18	25

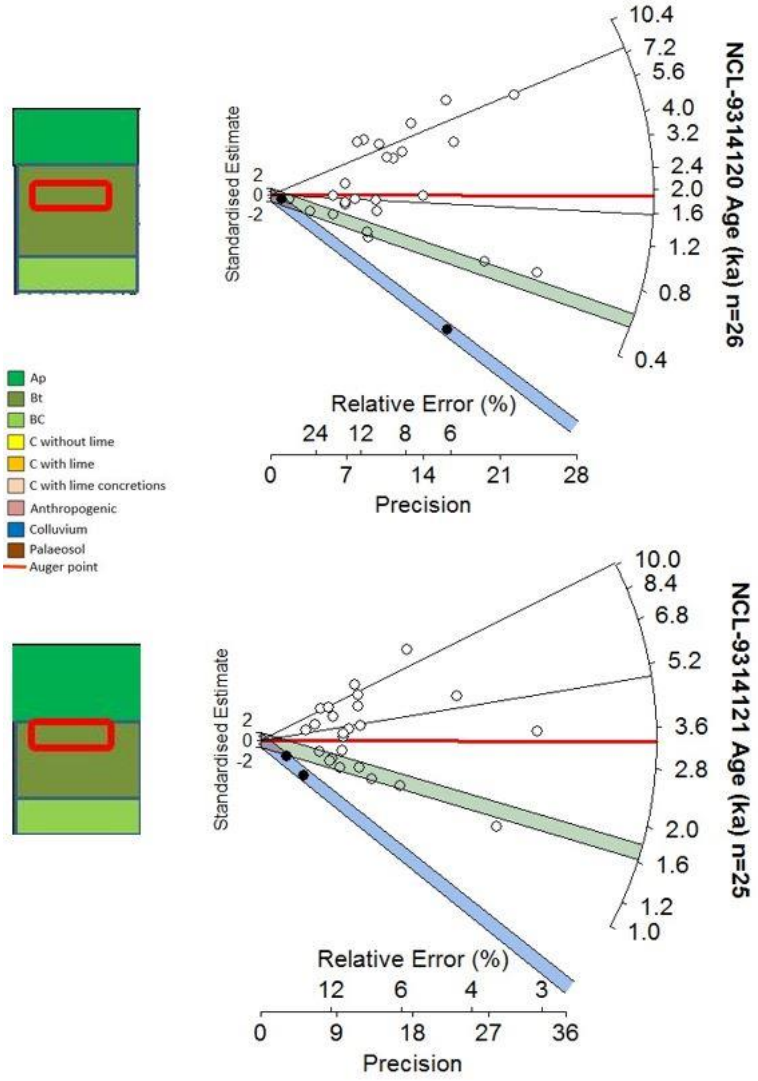

Fig.21: FMM sample 120 (0.23m) and sample 121 (0.24m). The red line shows the average Age (ka).

The OSL burial ages for all samples are estimated by dividing the equivalent dose of the primary component by the dose rate. Results are shown in table 5.

Table 5: Soil ages based on the youngest component of the FMM

ID	Depth (m)	Equivalent dose (Gy)	Dose rate (Gy/ka)	Age (ka)	Age (AD)
113	0.40	0.34 ± 0.06	3.24 ± 0.13	0.11 ± 0.02	1910 ± 19
114	0.70	0.51 ± 0.08	3.19 ± 0.14	0.16 ± 0.03	1855 ± 26
115	1.00	1.04 ± 0.05	3.12 ± 0.14	0.33 ± 0.02	1682 ± 22
116	1.40	1.64 ± 0.09	2.57 ± 0.12	0.64 ± 0.05	1376 ± 46
117	1.60	2.46 ± 0.16	3.19 ± 0.14	0.77 ± 0.06	1244 ± 60
118	1.90	2.16 ± 0.32	2.77 ± 0.12	0.78 ± 0.12	1236 ± 120
119	2.10	8.33 ± 0.93	2.74 ± 0.12	3.03 ± 0.36	- 1015 ± 360
120	0.23	0.40 ± 0.08	2.70 ± 0.11	0.15 ± 0.03	1876 ± 30
121	0.24	1.88 ± 0.53	3.42 ± 0.14	0.55 ± 0.16	1466 ± 156

3.4 DISCUSSION

3.4.1 INTERPRETATION SOIL PROFILES

The soil profiles were studied to determine the depth of the plough layer, differences in texture and to detect the presence of colluvium deposits. Bt horizons were detected locally along the slope. This meant translocation of clay particles to deeper soil depth and should be the normal situation in soil formation on Loess. The absence of the Bt at some locations indicated erosion or at least disturbance of the soil. The depth of the top of the C-horizon was also not constant over the slope. Less soil depth upslope is an indication of soil erosion.

Colluvium was found down slope transect T1 and as well in the mechanical core, C_28, drilled between T1 and T2. A thinner layer of colluvium was found in T2, but no colluvium was detected in T3.

From the DEM was evident that the difference in height was in the first transect the largest. The bottom part was also defined as the lowest point of the whole field. It could be that the various forms of soil erosion have worked against each other. In that case, it may be that soil at a certain place eroded under the influence of ploughing and was deposited by water erosion.

A scattered surface distribution of ^{137}Cs was obtained by Medusa. Radiation from below 18 cm soil depth had a minor influence on the measured surface activity (Schaub et al., 2010). This could cause a part of the scatter. Transported soil contained ^{137}Cs mixed with clean soil and had therefor a lower concentration in the top soil. The total concentration in the depositional locations was expected to be higher instead. The old situation should be kept in mind in the description of the development of the study location to its current state, as this had an influence. Houses and the paved road above the study location were constructed during at least the last 150 years. Before this, the catchment of the total slope was longer than only the Onderste Herkenberg. The amount of soil on top of the archaeological remains indicated how much soil was at least deposited since the destruction of the villa in 176/177 AD. Habets described the depth of the basement very accurately, but this part of the villa was probably situated under field level and therefore, in itself, not a good reference for this study. The depth of the basement is not known. It can be however a reference for the estimation of soil replacement after the excavation in 1860. The remains of the walls found at a depth of 40 cm elsewhere in the field can indicate several heights, because it was not known which part of the wall is still standing. More information is needed to make this a reliable reference.

3.4.2 INTERPRETATION FALLOUT DISTRIBUTIONS

Anthropogenic Pb concentration seemed to be related with the translocation of the clay particles. Pb was found throughout the whole soil profiles. The peaks in the Pb distribution corresponded with the depth of the palaeosols in C_28. But the Pb concentration in the other two cores was also quite high related to the estimated age of the soil layers. This can be explained by the use of anthropogenic Pb since centuries.

At a depth of already 25 cm in C_30 and C_29, directly under the plough layer, was nearly no ^{137}Cs and $^{239+240}$Pu measured. This indicated that all Cs and Pu is situated in the plough layer. On an undisturbed soil profile was over 70% (Schaub et al., 2010) and even over 80% according to Yamamoto et al., (1980) of the ^{137}Cs located in the first 10 cm of the soil. They proved as well a high relationship between the concentration and soil particle size. The higher plutonium concentrations deeper in some of the profiles could have been caused by percolation through the soil or outflowing

loss of the fine particle fraction absorbing higher amounts of radionuclides. The same had likely happened to ^{137}Cs.

Probably the same principle was true for ^{137}Cs. The concentration was assumed to decrease exponentially to a maximal depth of 30-40 cm in undisturbed soils. The ^{137}Cs concentrations deeper than plough zone were below the detection limit of the atmospheric deposition at the time of the fallout. Vertical migration values of 0.03 cm and 1.30 cm per year were however estimated (Schaub et al., 2010). ^{137}Cs fluxes were found to be correlated with soil dissolved organic carbon fluxes with a correlation coefficient of r=0.63 (Tegen & Dörr, 1996). Due to these bindings the ^{137}Cs could have been displaced by seepage water into deeper soil layers.

Remarkable is the Pu pattern visible in the core on the mid slope (C_29). The Pu concentration is lower at 10cm depth as at a depth of 24cm. The difference in the behaviour of plutonium and caesium at those locations is therefore not yet explained. A part can be explained by differences in mobility's of the isotopes. ^{137}Cs was specified once absorbed on the soil particles very hard to remove from the soil, whereas fall-out plutonium could easily be extracted from the soil by using nitric acid. Both isotopes acted on the other hand as nutrients when bound to organic matter. We cannot rule out the possibility that the two samples were swapped accidentally. ^{137}Cs shows a distribution pattern as it was expected, and as mentioned before, the distribution patterns of the two isotopes normally correspond.

3.4.3 Interpretation OSL results

The OSL samples from the two cores on the top- and mid-slope were dated much older than the first OSL sample taken at even a deeper soil depth down slope. Scatter in these samples could have been explained by the mixing of older soil layers with the top soil by ploughing. And therefor, these OSL results are clear signals of an eroding soil where instead of younger grains older grains are incorporated. In C_30 indicated the youngest component to the late Middle Ages, the second to roman times and the third to the deposition of loess. C_29 was a bit younger overall and located at a transport zone of soil. Particles from upslope positions influenced these data before they were detached again and transported further downslope.

The palaeosols down slope (C_28) were clearly visible in the obtained OSL results. Scatterings differed per sample depending on location to A-horizon. This was the soil layer where most of the anthropogenic activity and bioturbation occurred. Finite mixture models showed that these samples consisted of the most components. Dating of the first buried A-horizon corresponded quite well to the construction of the railway between 1830 and 1850 AD. During the investigation of the Roman villa by Habets was the site open for a long time. This would have had an impact on land use at the time. It is unlikely that the field at the time of the investigation was overgrown with crops and bare soil is more susceptible to erosion. In addition, there may also have been soil displacement as an effect of excavation work. The plough contest as described by Habets did not influence the situation on the field. They would not have ploughed deeper than 25 cm. It is, however, possible that a very loose topsoil was the result of the contest, which was more susceptible to soil erosion. The second palaeosol was according to the OSL results buried during the late Middle Ages. Forest slowly returned after the cultivated Romans had given way to the early medieval peasants. Around the year 1000, however, the demand for land increased and there was a lot of deforestation (Stoepker, 2005). Due to this the flooding and threat of soil erosion increased as well. This package of colluvium could thus been built up over a longer period of time.

The oldest component in sample 119 seems to be more or less 10.000 years old. This sample was taken from the layer defined as parent material and was thus not formed by soil forming processes.
Most age distributions show different exposure events due to bioturbation, ploughing and mixing. This resulted in relatively high overdispersion of the age estimates. An overdispersion of more or less 20% would have been normal were some samples had an over dispersion of more than 60%. Overdispersion was formulated as the statistical term for the presence of greater variability in a data set than would have been expected based on a given statistical model.

4. GROTE HOUW

4.1 STUDY LOCATION

As stated in the introduction the second studied location was the Grote Houw Oost in the northern province of Groningen. This is part of the Houw, which is a double mound cut into the eastern Kleine Houw and the western Grote Houw (Fig. 22). Presumably, the structure of the double mound results from originally smaller mounds. Based on the geology in the marsh landscape, the origin of the mound is estimated to 600 AD, the third generation mounds. Lots of archaeological materials were found. Previous research has shown that the steep sides of these mounds, often in use as agricultural fields, are prone to erosion (Nicolay, 2010; de Langen & Hommes, 1998; de Langen, 2007a)**.** Only at the end of summer and the beginning of the spring the location is crop free. At the end of the sixties, the mound has been levelled by excavation of the top part with 0.5m and spreading the vacant soil over the lower parts (van der Heiden etal., 2014). After levelling, the land use had changed from grassland into arable land. In a field audit in 1971 is found that on the northeast side of the road part of the mound was excavated. Findings were gathered in 1994 to learn more about the ancient residents of the mound. Erosion gullies have been recorded during this field survey as well. However, during an auger investigation it was not possible to determine colluviums (van der Heiden et al., 2014) it was too difficult to distinguish colluvium from the layers out of which the mound was build. The total surface of the location is 58500m^2.

Fig. 22: The Grote Houw and surroundings (van der Heiden, 2014. The red square indicates the total area of the Grote Houw, but the part left of the hatched part belongs not to the study area.

4.2 SAMPLING DESIGN

Based on the results of earlier studies on the land use, the ground level heights, the findings from the topsoil and an auger investigation, a number of locations are chosen on the Grote Houw to dig tiny profile pits of 2:1 m and a depth of about 0.6 m (Fig. 23). The pits are primarily constructed to be able to view the profiles described during the auger investigation over a wider surface area. In this way, several layers of the mound became better visible. Soil samples are collected for the Cs, Pu, Pb and OSL analyses from all layers up to and including the first undisturbed level.

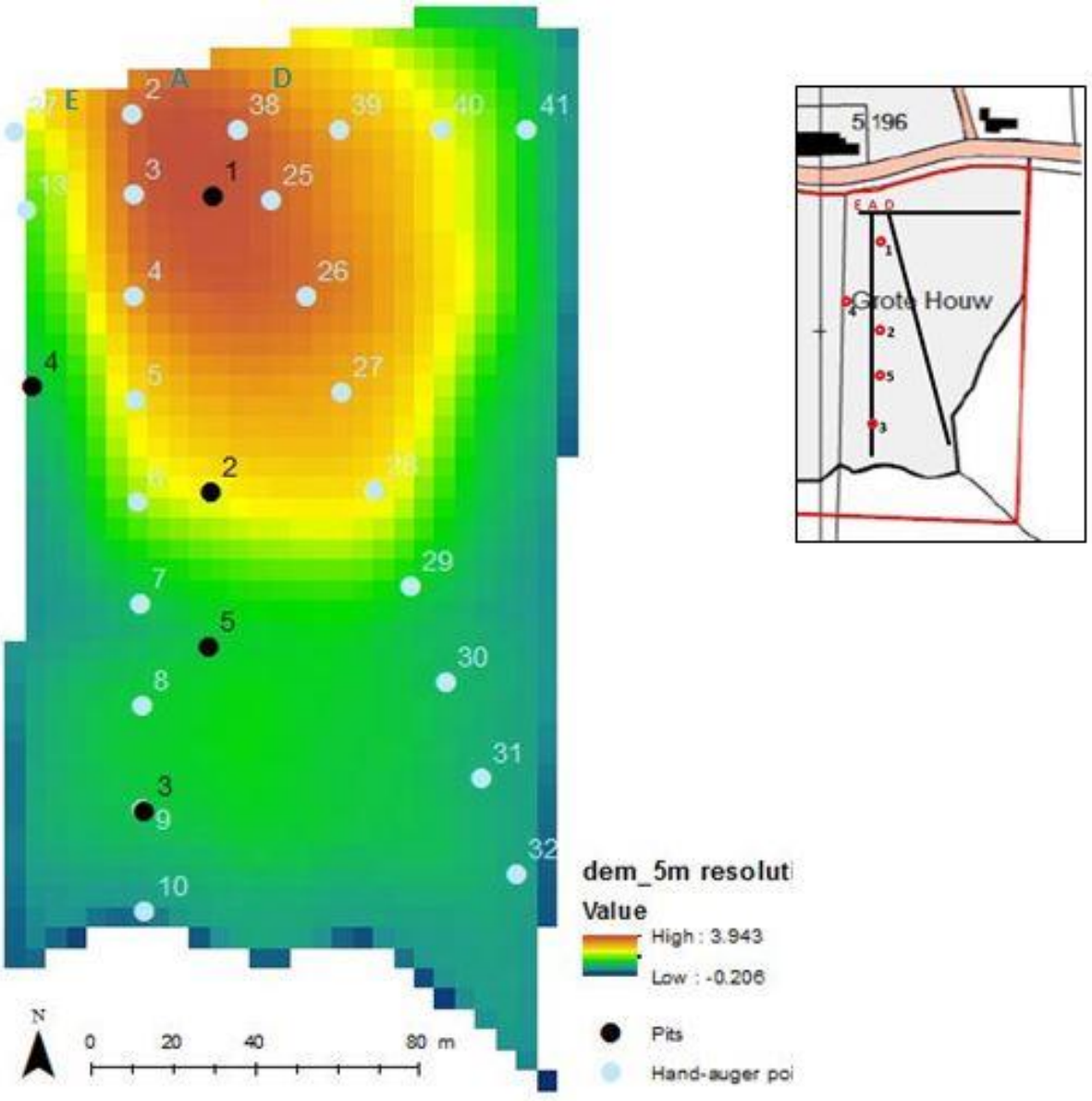

Fig. 23: Locations of hand auger transects and soil pits

4.3 RESULTS

4.3.1 FIELD LEVEL

Cross sections of the mound (Fig. 24) were made by van der Heiden (2014) based on the hand-auger transects. As they already concluded was it difficult to define colluvial or anthropogenic mound layers. The cross sections, however, did indicate that the soil layers of the mound are highly variable in texture. Especially the lower parts are identified as sandy, while at higher elevations of the mound more clay is found. The thickness of the plough zone varied between 20 and 40 cm.

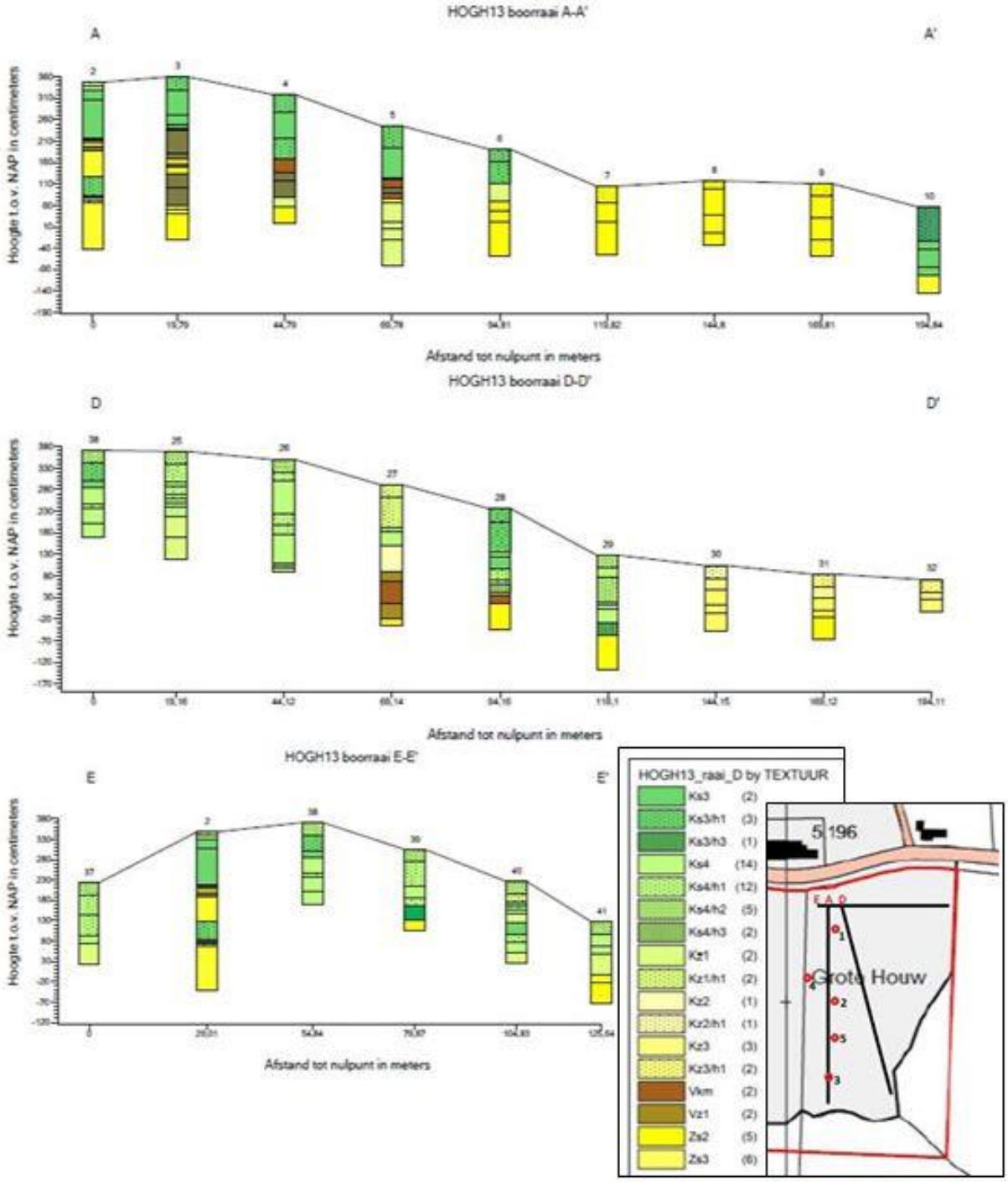

Fig. 24: Cross sections based on hand-auger descriptions (van der Heiden, 2014). K=clay, S=silt, Z=sand, V=Peat, h=humus. The number in the letter code indicated the amount of the second type in the mixture, increasing from 1 to 4 in strength.

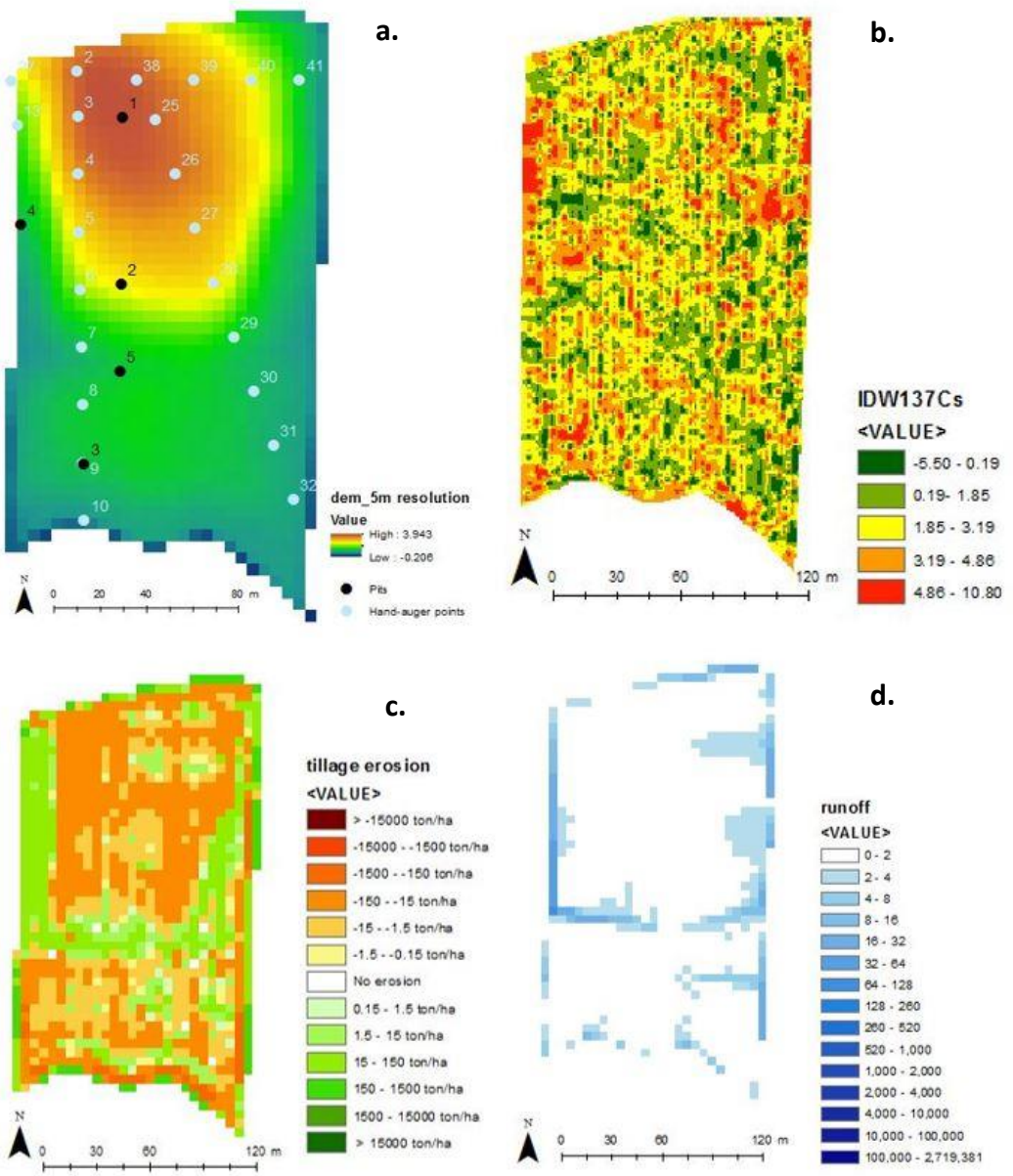

Fig. 25: Derivatives from the 5m resolution DEM, a. AHN2 b. ^{137}Cs distribution, c. simulation of tillage erosion and d. simulation of water flow accumulation.

What emerged most clear from the DEM derivatives was the little gully between pit 3 and 5 (Fig. 25). Water seemed to accumulate on the borders, and lower parts, of the mound. This was in contrast to the pattern obtained from the tillage erosion simulation. Not surprisingly, under influence of ploughing the soil was deposited at the edges of the field.

4.3.2 ANTHROPOGENIC TRACERS

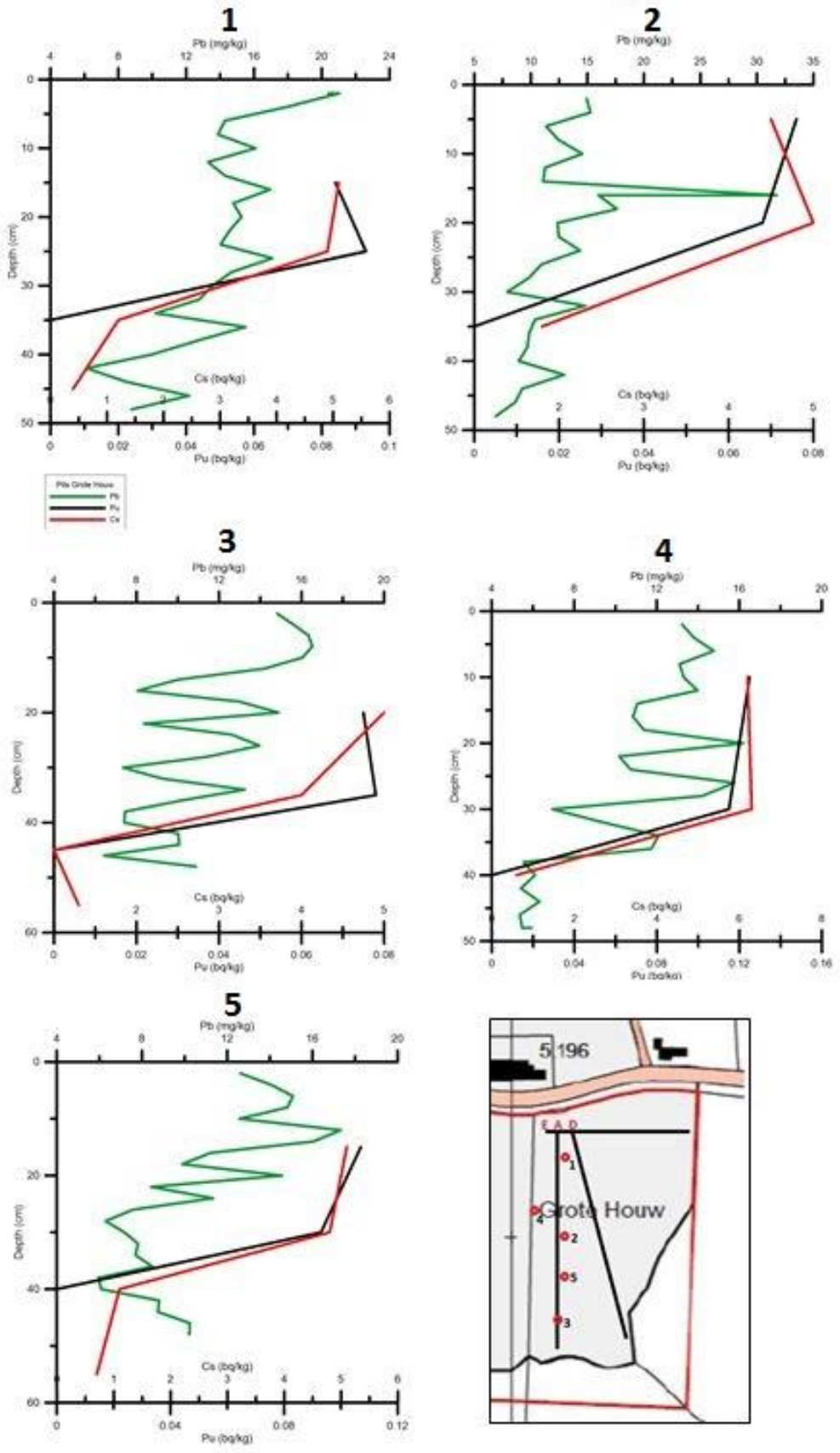

Fig. 26: Concentration distributions of ^{137}Cs, $^{239+240}Pu$ and anthropogenic Pb in the different soil pits.

The concentrations of caesium, plutonium and lead were measured as well at several depths in the soil profiles. Concentration differences were visible in the results for all elements of interest (Fig. 26). The total amount of $^{239+240}$Pu was relatively low. $^{239+240}$Pu activities were measured between 0.010 ± 0.001 bq/kg and 0.125 ± 0.004 bq/kg. In 8 of the 18 samples, the Pu was even undetectable. $^{240/239}$Pu activity ratio ranged from 0.166 ± 0.010 and 0.210 ± 0.006 and therefor indicated that the Pu was consistent with stratospheric fallout material from the 1958-1962 high-altitude H-bomb tests. Apparently, detectable amounts of Chernobyl-derived materials (with a ratio of c. 0.4) was present. The average atom ratio of $^{240/239}$Pu was 0.180±0.014, resulting from several tests for the 31-70° N latitude band (Ketterer et al., 2012). Concentrations measured in the same layer at several slope positions were different. Both $^{239+240}$Pu and ^{137}Cs are found at relatively high concentrations in the soil profile down slope (pit 5) and on the side of the mound (pit 4). Pb showed in general a declining concentration trend. There was only a strong Pb peak visible in pit 2.

The correlation of the measured Pb concentrations with the amounts of rubidium (Rb) and potassium Oxide (K_2O) was determined to trace the origin of the Pb. No clear relationship can been drawn from the scatter plots (Fig. 27). The patterns would have shown a linear correlation in the case of natural Pb instead of the point clouds that are visible now. Out of the statistics resulted as well a very low R^2 ranging between 0.022-0.254 for K2O and 0.009-0.251 for Rb.

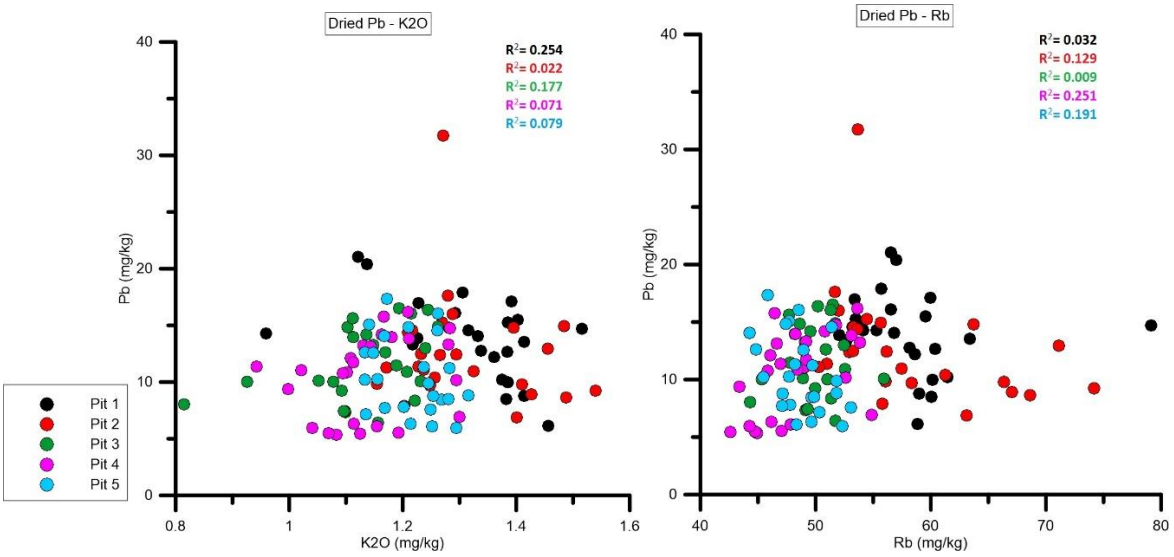

Fig. 27: Correlation of measured Pb concentartions with K2O and Rb

4.3.3 Surface mapping of ^{137}Cs

The surface ^{137}Cs investigation by Medusa resulted in a scattered pattern (Fig 25b). Ridges made for growing potatoes did came forward in the pattern obtained. In addition, the measured concentration in the ditch was slightly higher and on top of the mound lower. Compared to Meerssen the total amount was less on this location with an average amount of 2.6 bq/kg where it was 3.3 bq/kg in Meerssen.

4.3.4 Performance of the samples to OSL

For the selection of the most appropriate dose equivalent (D_e) measurements an IR test, preheat temperature test, thermal transfer test and dose recovery test were done according to the SAR protocol. No strong signals of feldspar to IR were observed. Therefore, it was not necessary to clean the samples again. Thermal transfer was observed at a temperature of 260 °C (Fig. 28).

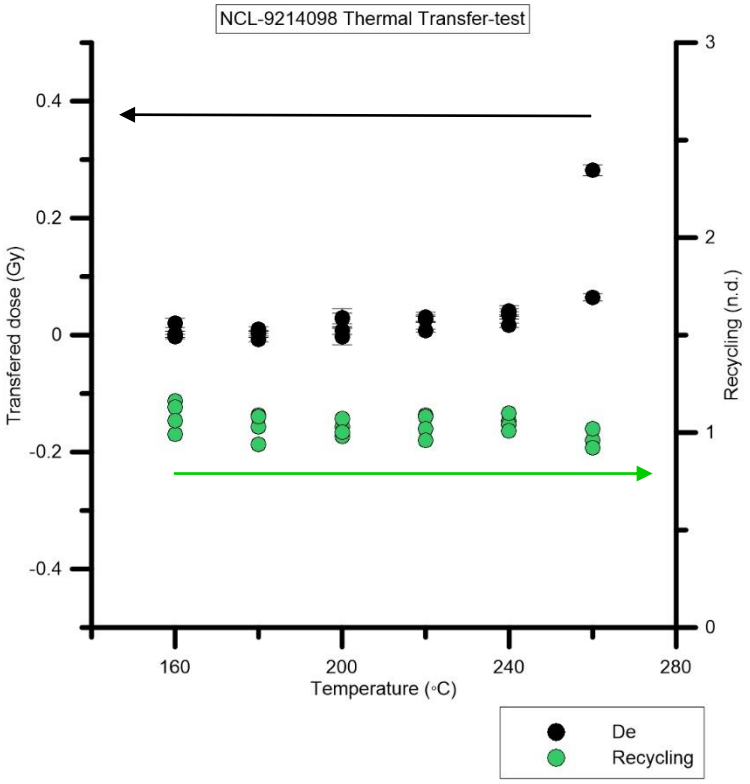

Fig. 28: Thermal transfer visible at a temperature of 260°C at sample 098

To prevent both thermal transfer as unstable charge is chosen again for a preheat and cutheat of respectively 200°C and 180°C. To prove the suitability of these choices is a dose recovery test conducted in which the natural signal was erased first. Instead, a known dose is treated as the natural signal. The ratio of measured/given dose should be unity. The average dose recovery ratio was 0.98 ± 0.01 (Fig. 29). An extra dose recovery test was performed on the samples 100 and 101, because these were measured over a smaller fraction (90-120 µm). This fraction showed comparable results to the dose recovery of the rest of the samples with an average ratio of 0.95 ± 0.04, but seemed to react strongly with IR. Therefore an IR wash was included at the beginning of the D_e measurements to filter the reaction of feldspar from the luminescence signal.

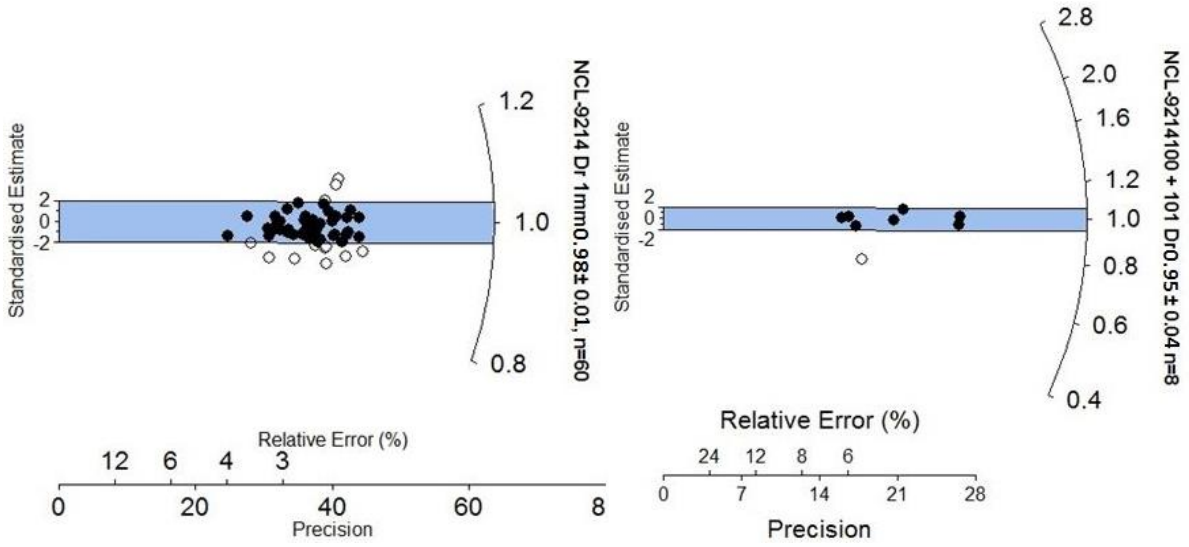

Fig. 29: Dose response of all samples of NCL-9214 and the extra measurements on NCL-9214100 + 101

Gamma spectrometry done to obtain the background radiation dose rates of the different samples showed no remarkably results (Table 6). There are however some differences obtained per soil pit. Some of the upper layers appeared to have lower dose rate radiation than deeper soil layers. Results ranged from 2.28 Gy/ka tot 3.24 Gy/ka. Water content and organic matter content were used for calculation of the environmental dose rate. The water content was on average 19.3 ± 1.2 % and the organic matter content 2.2 ± 0.002 %. For calculation of the cosmic dose rate is assumed that the samples were gradually covered by younger sediments since deposition. Attenuation by the water column is taken into account, because the attenuation of ionising radiation is much greater if the pores in sediments are filled with water rather than air.

Table 6: Puck analysis with dose rate calculations

	98	99	100	101	102	103	104	105	106	107	108	109	110	111	112
K-40 (Bq/g)	0.479 ± 0.010	0.514 ± 0.010	0.611 ± 0.012	0.518 ± 0.010	0.634 ± 0.012	0.541 ± 0.011	0.536 ± 0.011	0.626 ± 0.013	0.630 ± 0.012	0.611 ± 0.012	0.518 ± 0.010	0.634 ± 0.012	0.541 ± 0.011	0.536 ± 0.011	0.536 ± 0.011
Pb-210 (Bq/g)	0.031 ± 0.002	0.025 ± 0.002	0.061 ± 0.003	0.043 ± 0.002	0.057 ±0.003	0.046 ± 0.003	0.042 ± 0.002	0.055 ± 0.003	0.060 ± 0.003	0.061 ± 0.003	0.043 ± 0.002	0.058 ± 0.003	0.046 ± 0.003	0.042 ± 0.002	0.042 ± 0.002
Pb-212 (Bq/g)	0.023 ± 0.003	0.028 ± 0.003	0.044 ± 0.003	0.039 ± 0.003	0.042 ± 0.003	0.038 ± 0.003	0.039 ± 0.003	0.042 ± 0.003	0.043 ± 0.003	0.044 ± 0.003	0.039 ± 0.003	0.042 ± 0.003	0.038 ± 0.003	0.039 ± 0.003	0.039 ± 0.003
Bi-212 (Bq/g)	0.025 ± 0.002	0.034 ± 0.002	0.051 ± 0.003	0.040 ± 0.002	0.046 ± 0.003	0.043 ± 0.003	0.044 ± 0.002	0.052 ± 0.003	0.051 ±0.002	0.051 ± 0.003	0.040 ± 0.002	0.046 ± 0.003	0.043 ± 0.003	0.044 ± 0.002	0.044 ± 0.002
Pb-214 (Bq/g)	0.030 ± 0.000	0.028 ± 0.000	0.051 ± 0.001	0.042 ± 0.001	0.052 ± 0.001	0.043 ± 0.001	0.047 ± 0.001	0.052 ± 0.001	0.055 ± 0.001	0.051 ± 0.001	0.042 ± 0.001	0.052 ± 0.001	0.043 ± 0.001	0.047 ± 0.001	0.047 ± 0.001
Bi-214 (Bq/g)	0.030 ± 0.001	0.029 ± 0.001	0.050 ± 0.001	0.044 ± 0.001	0.051 ± 0.001	0.044 ± 0.001	0.047 ± 0.001	0.052 ± 0.001	0.052 ± 0.001	0.050 ± 0.001	0.044± 0.001	0.051 ± 0.001	0.044 ± 0.001	0.047 ± 0.001	0.047 ± 0.001
Ac-228 (Bq/g)	0.031 ± 0.001	0.033 ± 0.001	0.049 ± 0.001	0.042 ± 0.001	0.047 ± 0.001	0.042 ± 0.001	0.045 ± 0.001	0.049 ± 0.001	0.050 ± 0.001	0.049 ± 0.001	0.042 ± 0.001	0.047 ± 0.001	0.042 ± 0.001	0.045 ± 0.001	0.045 ± 0.001
Th-234 (Bq/g)	0.026 ± 0.002	0.028 ± 0.002	0.045 ± 0.002	0.039 ± 0.002	0.048 ± 0.002	0.041 ± 0.002	0.040 ± 0.002	0.052 ± 0.002	0.051 ± 0.002	0.045 ± 0.002	0.039 ± 0.002	0.048 ± 0.002	0.041 ± 0.002	0.040 ± 0.002	0.040 ± 0.002
Water content	20.33 ± 0.010	22.39 ± 0.013	25.48 ± 1.623	25.40 ± 1.613	22.28 ± 1.241	20.99 ± 1.102	21.82 ± 1.189	20.51 ± 1.052	24.42 ± 1.492	25.48 ± 1.623	25.40 ± 1.613	22.28 ± 1.241	20.99 ± 1.102	21.82 ± 1.189	21.82 ± 1.189
LOI	2.845 ± 0.000	2.974 ± 0.000	1.930 ± 0.004	1.920 ± 0.004	1.490 ± 0.002	1.170 ± 0.001	1.040 ± 0.001	2.140 ± 0.004	2.850 ± 0.008	1.930 ± 0.004	1.920 ± 0.004	1.490 ± 0.002	1.170 ± 0.001	1.040 ± 0.001	1.040 ± 0.001
Attenuation %	23.17 ± 0.012	25.36 ± 0.014	27.41 ± 1.645	27.31 ± 1.639	23.78 ± 1.427	22.16 ± 1.108	22.86 ± 1.143	22.65 ± 1.133	27.27 ± 1.636	27.41 ± 1.645	27.31 ± 1.639	23.78 ± 1.427	22.16 ± 1.108	22.86 ± 1.143	22.86 ± 1.143
Dose rate (Gy/ka)	2.280 ± 0.060	2.310 ± 0.070	3.120 ± 0.140	2.570 ± 0.120	3.190 ± 0.140	2.770 ± 0.120	2.740 ± 0.120	3.240 ± 0.130	3.190 ± 0.140	3.120 ± 0.140	2.570 ± 0.120	3.190 ± 0.140	2.770 ± 0.120	2.740 ± 0.120	2.740 ± 0.120

4.3.5 AGE ESTIMATION BASED ON OSL

To keep the methods applied to both study locations more or less the same is the FMM used for the Grote Houw as well as for Meerssen. Most of the samples had the smallest BIC score for a mixture of two components (Table 7). In sample 100 and 108 had the two components the same age, but with a different error of prediction.

Table 7: Results finite mixture model Grote Houw

ID	**n**	**Age (ka) per component**					
		1st	P (%)	2nd	P (%)	3rd	P (%)
98	29	0.34	54	2.47	46		
99	32	2.80	32	4.87	68		
100	23	6.97	58	6.97	42		
101	25	3.27	35	5.19	65		
102	26	0.49	26	0.52	74		
103	30	0.42	66	1.49	34		
104	23	2.13	86	5.12	14		
105	25	2.02	14	3.48	86		
106	18	0.33	78	2.83	22		
107	24	0.39	69	0.41	31		
108	17	6.84	41	6.84	59		
109	26	0.42	83	1.67	17		
110	14	0.70	54	1.26	46		
111	17	1.31	48	3.71	46	33.88	6
112	18	7.60	54	7.60	46		

The unexpected scatter in the D_e distribution is smaller than for the samples from Meerssen and in fact likely represent a single age estimation. The Central Age Model was considered to represent the development of the soil profiles the best. Kernel density (*KDE*) plots were made for the samples that contained negative D_e values and these cannot be displayed in a radial plot. Which should not been confused with each other was that the peak in the *KDE* represented not the same as the D_e obtained from the CAM. The other D_e distributions were here nonetheless represented in radial plots based on the CAM, because these are statistically more valid than *KDE* plots.

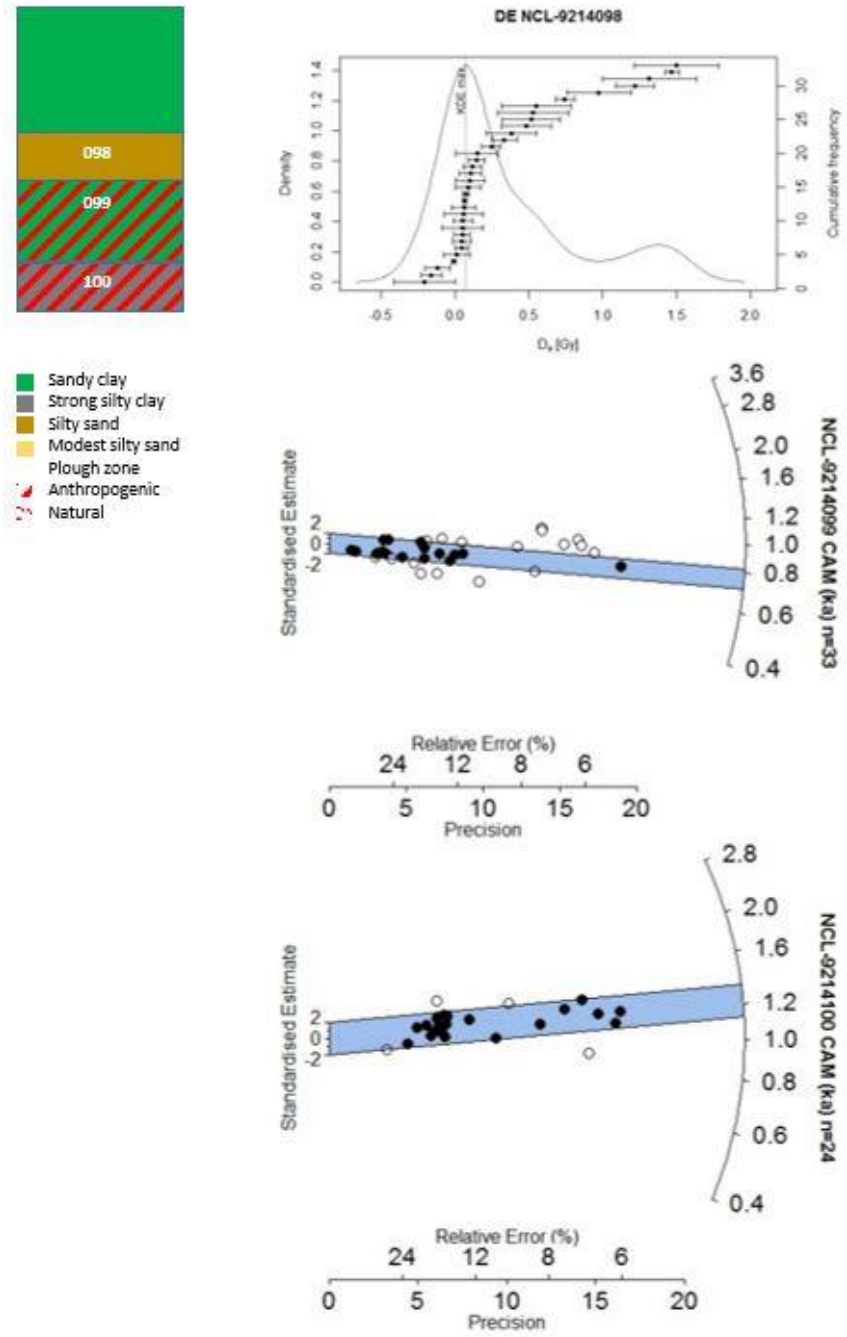

Fig. 30: Age estimate pit 1; CAM samples 098 (0.25 m), 099 (0.35 m) and 100 (0.45 m).

In the top sample of pit 1 were the *De* estimations the most scattered (Fig. 30). Under this layer, the age increased and was the assay more precisely because there was less scatter in the results.

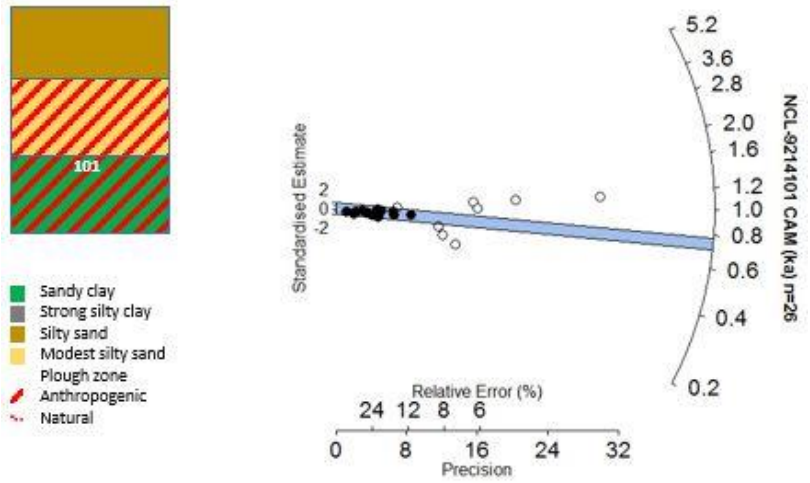

Fig. 31: Age estimate pit 2; CAM sample 101 (0.35 m).

Only one OSL sample was taken in pit 2 located on the mid slope of the mound. The *De* distribution at this location (Fig. 31) was comparable to the second sample of pit 1, but these two samples were collected from more or less the same soil depth. Pit 3 (Fig. 32) was located at a small jump in the south of the study location. The total soil profile was more sandy here than on the other locations. The central ages derived from the CAM were also younger. Two samples were taken from the ploughlayer and resulted in negative *De* values. Circumstances in pit 4 were very different from those in the other pits. Pit 4 was located at the side of the mound were the soil was more moist and even a bit grey. The De estimations in the top soil were less spread than in the other pits and the average age of the soil layers were older (Fig. 34). In pit 5, located at the bottem of the mound, were the middle two samples the most widespread (Fig. 35).

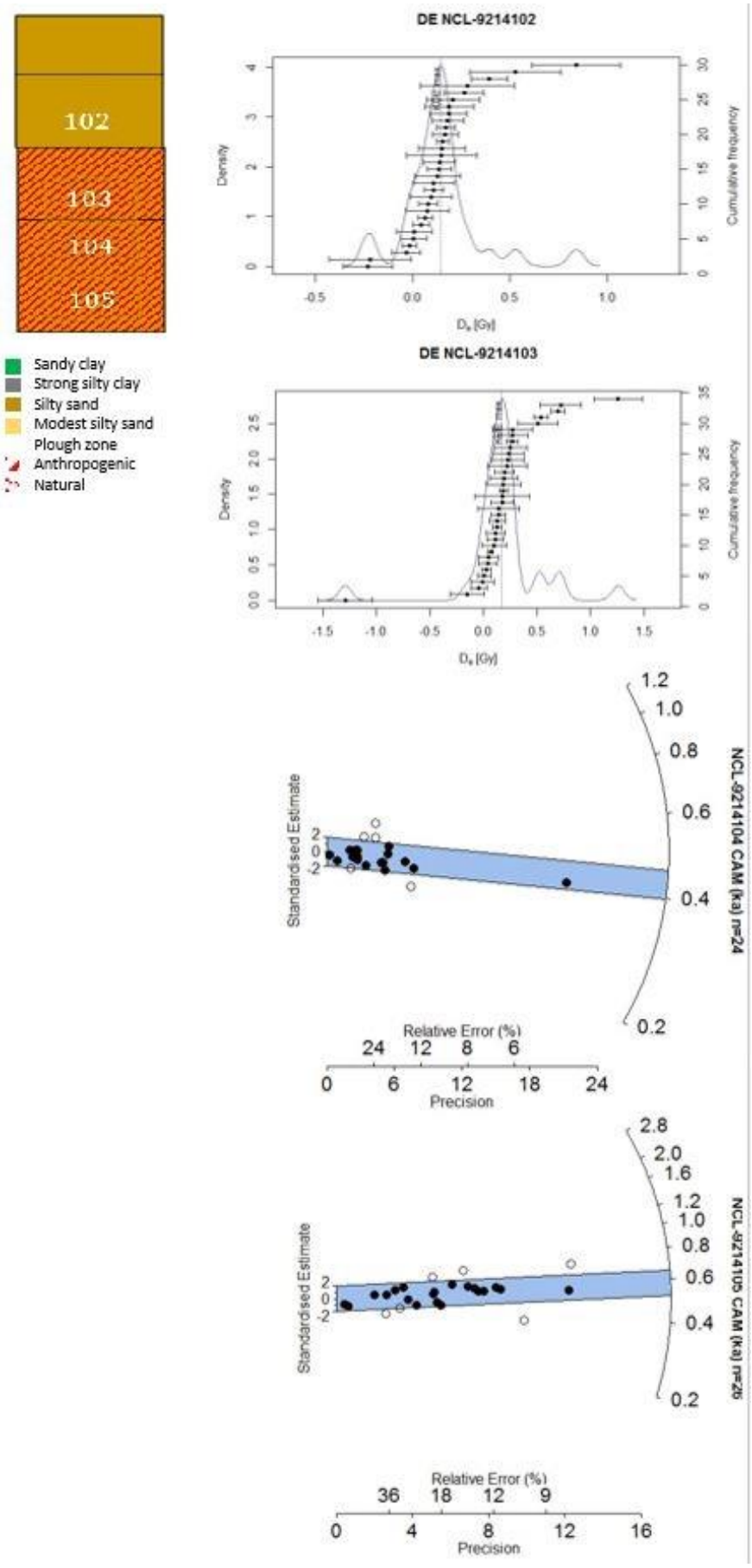

Fig. 32: Age estimate pit 3; CAM samples 102 (0.20 m), 103 (0.35 m), 104 (0.45 m) and 105 (0.55 m).

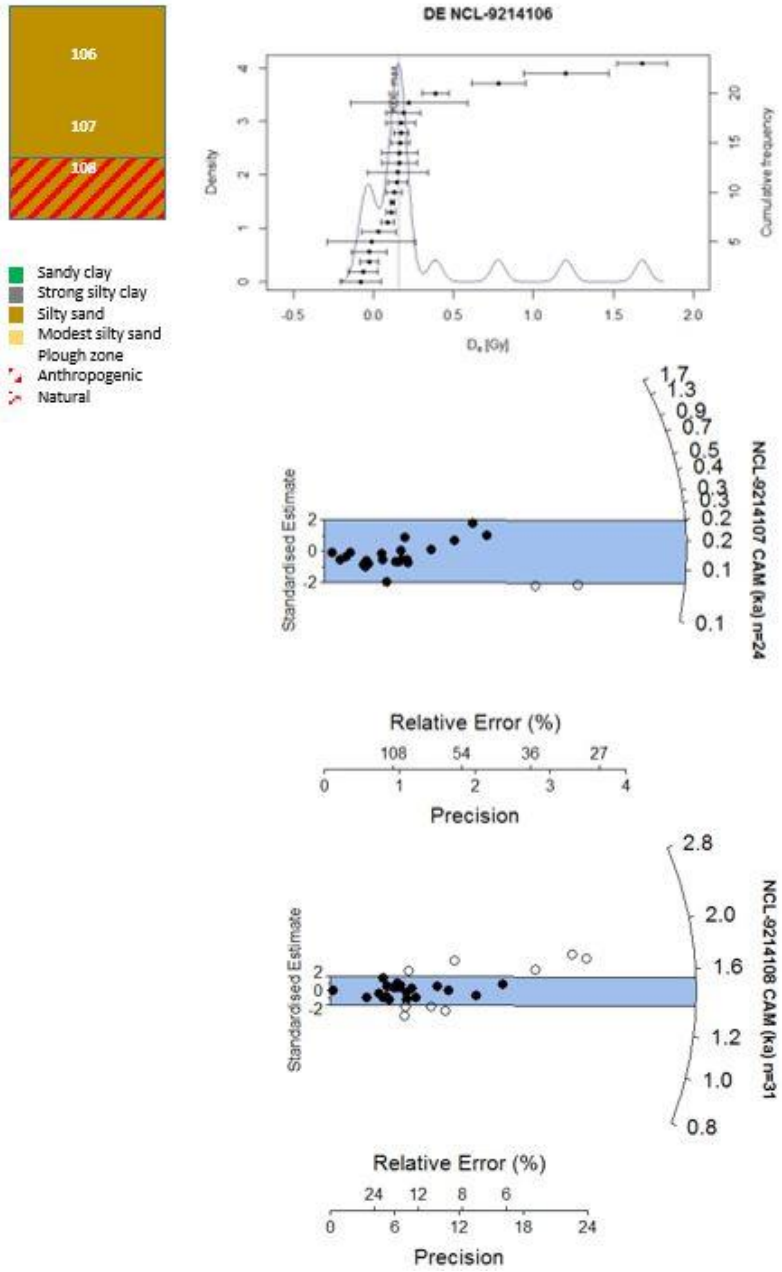

Fig. 33: Age estimate pit 4; CAM samples 106 (0.10 m), 107 (0.30 m) and 108 (0.40 m).

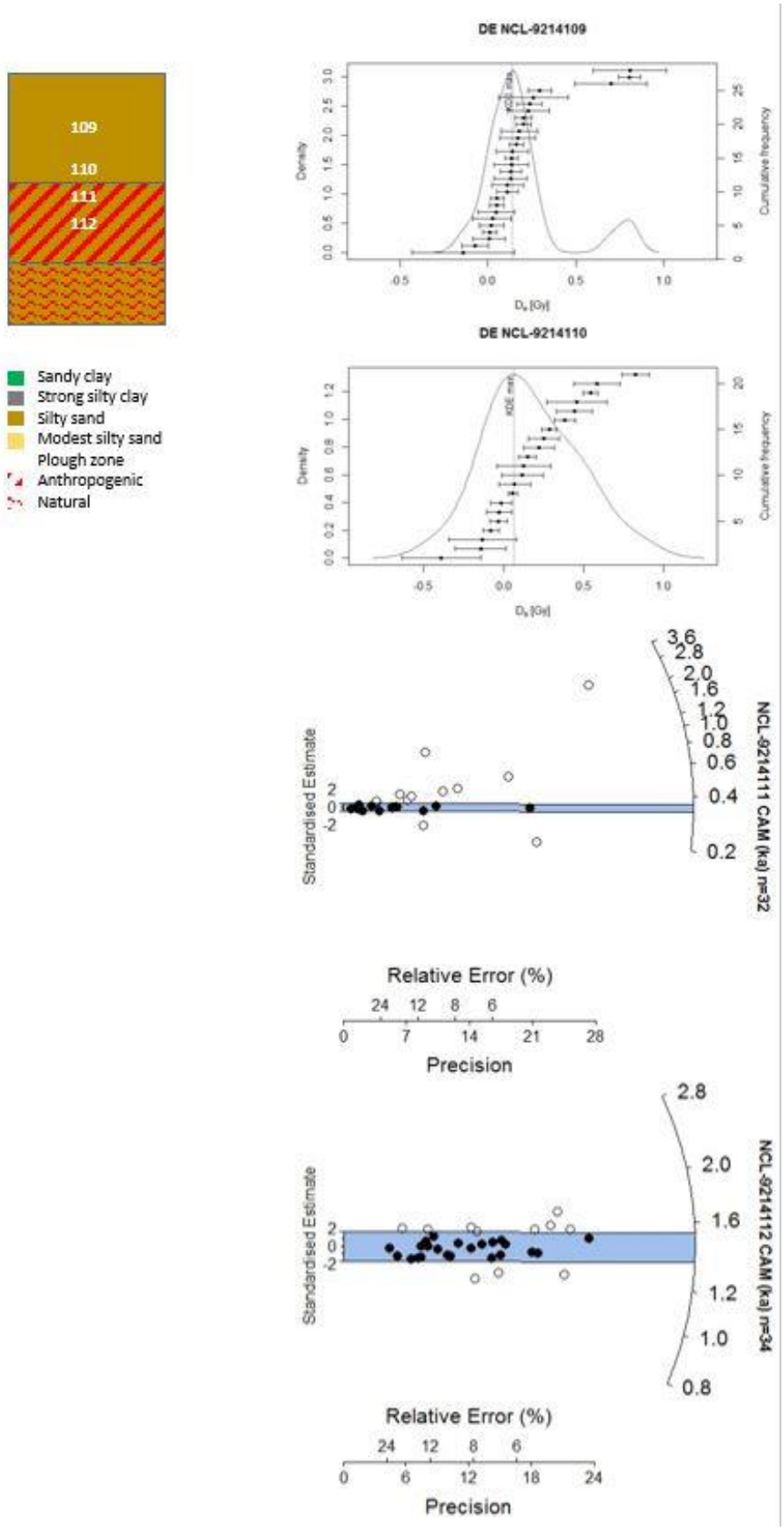

Fig. 34: Age estimate pit 5; CAM samples 109 (0.15 m), 110 (0.30 m), 111 (0.40 m) and 112 (0.55 m).

Although the difference in depth between the sampled soil layers in some pits was quite small, the results clearly traced back to different periods in time. The radial plots indicate that there is only little dispersion in the results of the single aliquots. However, there are differences visible in the ages of soil layers from the same depth at other positions on the mound (Table 8).

Table 8: OSL estimation of soil sample ages based on the CAM

ID	Depth (m)	Equivalent dose (Gy)	Dose rate (Gy/ka)	Age (ka)	Age (AD)
98-1	0.25	0.62 ± 0.11	2.28 ± 0.06	0.27 ± 0.05	1743 ± 49
99-1	0.35	1.77 ± 0.12	2.31 ± 0.07	0.77 ± 0.06	1249 ± 56
100-1	0.45	2.89 ± 0.11	2.37 ± 0.07	1.22 ± 0.06	791 ± 57
101-2	0.35	1.83 ± 0.14	2.46 ± 0.07	0.74 ± 0.06	1271 ± 62
102-3	0.20	0.26 ± 0.02	2.34 ± 0.07	0.11 ± 0.03	1904 ± 26
103-3	0.35	0.29 ± 0.15	2.31 ± 0.06	0.12 ± 0.07	1891 ± 67
104-3	0.45	1.01 ± 0.08	2.37 ± 0.07	0.43 ± 0.04	1589 ± 37
105-3	0.55	1.37 ± 0.09	2.35 ± 0.07	0.58 ± 0.04	1435 ± 40
106-4	0.10	0.51 ± 0.18	2.19 ± 0.06	0.23 ± 0.08	1782 ± 82
107-4	0.30	0.29 ± 0.06	2.29 ± 0.06	0.13 ± 0.03	1888 ± 26
108-4	0.40	3.30 ± 0.13	2.25 ± 0.06	1.46 ± 0.07	550 ± 71
109-5	0.15	0.52 ± 0.16	2.23 ± 0.06	0.23 ± 0.07	1783 ± 72
110-5	0.30	0.39 ± 0.07	2.25 ± 0.06	0.18 ± 0.03	1839 ± 31
111-5	0.40	0.80 ± 0.09	2.26 ± 0.06	0.35 ± 0.04	1663 ± 42
112-5	0.55	3.30 ± 0.09	2.29 ± 0.06	1.45 ± 0.06	570 ± 57

4.4 Discussion Grote Houw

4.4.1 Interpretation soil profiles and surface processes

The first interpretation of the soil profiles was done by van der Heiden et al. (2014). He concluded that it was difficult to make a distinction between anthropogenic layers and colluvium. What became clear from the hand-auger descriptions was that the mound was quite divers in soil horizons. At some positions was the texture sandier where on other positions dense clay was found in the upper soil layers.

Tillage erosion was visible from the simulation on the higher parts of the mound and even on the little jump in the south of the study location. While the height differences on this jump were not that big was the amount of the simulated erosion on the jump more or less the same as on the mound. One explanation may have been the differences in texture of the top soil. Possible is also that the farmer drove in a different direction at this part of the field. If this is not the case, the gully had to be dug every time after ploughing.

4.4.2 Interpretation fallout isotopes

The concentration profiles of ^{137}Cs and $^{239+240}Pu$ appeared in all pits contradictory, while it was expected that they would show both the same decreasing pattern. Concentrations of all fallout isotopes decreased however to almost zero directly under the plough zone. Pb showed a decreasing concentration pattern, but the differences with depth were not that big. Probably was the measured depth of maximal 60 cm too much exposed to soil and leaching processes of the Pb and was there less deposition in the first place. Ridges observed on the field could have had an influence on the spread of the Anthropogenic fallout material in the form of small local differences. In addition, these ridges were also a reason for the various thicknesses of the plough zone and the depth to which the material of interest was mixed with clean soil. However, it was not known whether these ridges were continuous present on the field during the last 50 years since 1963.

4.4.3 Interpretation OSL results

Some negative values were obtained for the equivalent doses of the top soil samples. These were the samples represented in *KDE* plots. Negative values were results from a statistical effect. If the left part of the distribution would be cut off, the average *De* would become biased towards the larger values. In the end, this would have caused an age overestimation of the very young samples. The overdispersion of the CAM were not surprisingly high and ranged around 30%. From the dissemination of the equivalent doses also showed that the samples were properly bleached. This made it possible to describe the samples with the aid of the CAM.

When the OSL ages obtained were analysed, the anthropogenic structure of the mound had to be taken into account. Ages of soil layers at comparable depths spread over the mound belonged to different depositional periods. Although only one sample was taken in pit 2, there was an apparent agreement with pit 1 higher on the slope. For a soil depth of 35 cm were ages obtained of more or less 750 years from now. The start of the construction of the mound was estimated around 600 AD. This year came back nicely in the lower measured samples. Younger ages were obtained for the little jump in the south of the field. Probably had this piece of the study location undergone many changes around land consolidation and was the ground raised here at the beginning of the 20th century. The depth of the plough zone varied across the mound surface, but also in the samples below this layer were variations in ages visible.

Sample tubes in which soil was collected from the Grote Houw for OSL were not packaged properly. At least one of the two sides was covered with white painters tape. In this part of the tube, the soil was dehydrated. On the other hand were the samples that were packed with a cap so tight that they had to be cut open with a saw. Rough handling of a relatively dry sample may have caused mixing with the grains that were exposed to daylight during collection.
During the sampling process were the samples 100 and 101 lost, so that they had to be sampled again over a smaller fraction. By introduction of an IR wash could the samples further been treated the same as the other samples. They gave similar reactions and results to the statistical tests.

5. GENERAL DISCUSSION AND CONCLUSION

The aim of this thesis was to measure soil erosion rates at archaeological monuments under agricultural fields. Different methods were used to trace erosion, involving sediment tracing and dating of burial ages. This was in the order to determine whether action is needed or not to protect these monuments and to find a good method that the RCE can use in other studies. Three objectives were formulated: (1) estimate the rate of erosion, (2) determine the differences and accuracy of the different used methods and (3) model the erosion on the archaeological sites. First was defined what soil erosion is and how the possible presence was determined on the selected study locations.

5.1 DETERMINATION OF SOIL EROSION PER SOIL PROFILE

Colluvium found in the down slope corner of the study location in Meerssen was one of the first indications of soil erosion. The analysis of the anthropogenic fallout isotopes and the OSL results confirmed this observation.

5.1.1 *THE USE OF ^{137}CS AND $^{239+240}$PU*

Concentrations of anthropogenic fallout isotopes measured on the two locations are low (Table 9) compared to studies in other European countries. Concentrations of $^{239+240}$Pu were only detectable in 16 of the 30 samples. A nationwide study is done to the deposition of radioactive substances in the Netherlands after the Chernobyl accident (Stoutjesdijk 1986). The average additional ^{137}Cs deposition was 1.8 kBq/m^2, where the concentration after the bomb testing was estimated at 4.6 kBq/m^2. Additional ^{239}Pu due to Chernobyl was only measured at one location and covered and amount of only 1x10^{-6} kBq/m^2. The deposition of ^{239}Pu as a consequence of Chernobyl is therefore questionable. The concentration after the bomb testing of ^{239}Pu was estimated at 0.035 kBq/m^2. The measured $^{239+240}$Pu concentrations correspond to the ^{239}Pu values estimated by Stoutjesdijk (1986).

Table 9: Total isotope concentrations per profile

	Measured ^{137}Cs (kBq/m^2)	Measured $^{239+240}$Pu (kBq/m^2)
Meerssen - 30	3.1	0.06
29	2.7	0.05
28	6.1	0.10
Grote Houw - 1	4.1	0.07
2	4.8	0.06
3	4.7	0.07
4	6.7	0.13
5	5.7	0.11

Possible causes could have been low initial depositions or the long period since deposition due to which the initial amount of ^{137}Cs had decreased through radioactive decay. A portion of the ^{137}Cs had been taken up by crops immediately in the year of deposition and the subsequent years as both fields were under cultivation. Crops were in contrast to natural non disturbed soils harvested, having a direct reduction in the quantity of ^{137}Cs on the plot as a result. The concentrations of ^{137}Cs and $^{239+240}$Pu were overall lower at the Grote Houw then in Meerssen. For ^{137}Cs is known that it was distributed unequally over the Netherlands after the Chernobyl accident (Fig. 35). The deposition was strongly influenced by rainfall. On the small field level scale of this study, however, this had no impact on the results. Besides, the values indicated by the RIVM are lower than the measured

concentrations at the Grote Houw and in Meerssen (Table 9). The difference between the values is a combination of radioactive decay of the ^{137}Cs and soil erosion since the bomb testing period.

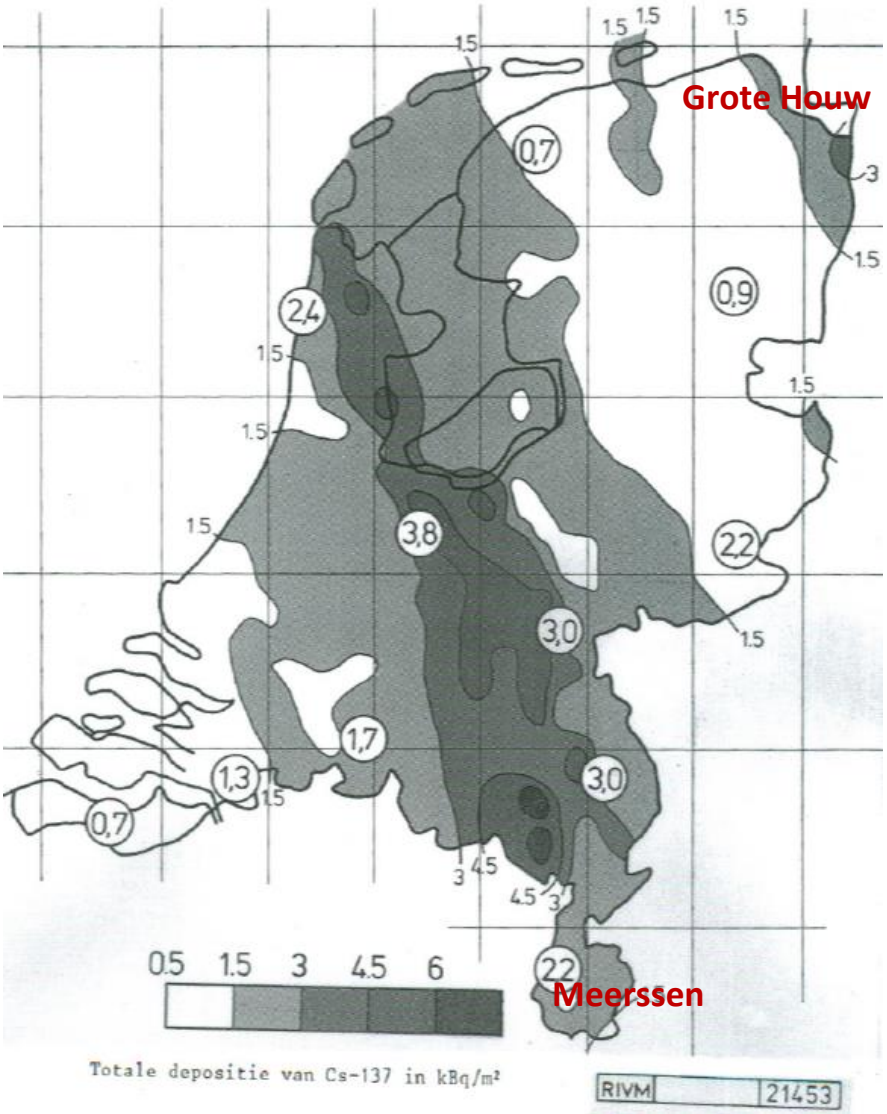

Fig. 35: Cs distribution over the Netherlands due to the Chernobyl accident (Stoutjesdijk 1986)

For the visualization of the ^{137}Cs and $^{239+240}Pu$ distribution would it have been better to sample the soil at smaller differences of for example only 2 cm. Although the pattern was probably still disturbed by the soil cultivation there was possibly more apparent in the distribution of the concentration than it was previously the case. The decrease in the concentration under the plough zone was visible now, but could be perhaps determined more precisely with a denser sampling design. The concentrations of the fallout isotopes ^{137}Cs and $^{239+240}Pu$ were measured moreover with different devices. For the estimation of the ^{137}Cs concentration the decay of the isotopes was established with the NaI-detector and for the estimation of the Pu concentration were the atoms counted it selves with the ICP-MS. According to (Ketterer & Szechenyi, 2008) was one method preferred above the other depending on the isotope of interest: "If the isotope produces countable decays that can be counted faster than the atom count rates achieved in mass spectrometry, then decay counting is usually more sensitive and is the preferred approach. On the other hand, if the decay process produces counted events relatively slowly compared to the rate at which the atoms themselves can be counted, then mass spectrometry prevails. These generalizations are compiled by considerations of background signals

and the efficiencies with which the decays or atoms can actually be counted." Since the purpose of this investigation was to compare the different methods with each other had it been better to perform the methods in a similar manner.

5.1.2 The use of anthropogenic Pb

Differences in anthropogenic Pb content between the two study locations are explained on the basis of the distance to population density and industrial and traffic. Differences in concentration per soil profile corresponded to the patterns shown by ^{137}Cs and $^{239+240}Pu$. Concentration significantly decreased immediately after the plough zone, but were measureable till a deeper soil depth. This is certified by the longer time period over which anthropogenic Pb is used. In addition, it is assumed that Pb has a certain mobility in the soil. This mobility is related to e.g. the pH of the soil and the redox potential. In this study, however, too little attention was paid to the behaviour of Pb in the soil to draw conclusions on the in depth profile concentrations. The differences in total concentrations for each profile are, though, used as a confirmation of the conclusions based on post depositional distribution of the fallout isotopes.

5.1.3 The use of OSL

OSL is used in this study to date the different soil layers described. In particular down slope in Meerssen, there has been found a strong correlation between human activity and soil forming processes. Soil layers, colluvium and the loess deposit contained a different rate of mixing. This post depositional mixing occurred due to bioturbation and ploughing and was higher in the top soil and palaeosols than in the colluvium and more stable soil layers. Several components obtained in the FMM relate one component of a sample to another component of the next sample in the soil layer sequence (Fig. 36). Heimsath et al. (2002) concluded in a study to the determination of soil creep that repeated grain displacements lead to mixing through the entire soil column as the soil moves downhill. They used OSL for this and counted the number of grains belonging to components obtained with the FMM. The number of bleached grains was for them an indication of the bioturbation effect. Such an application of the OSL could been considered in other researches to the estimation of soil creep at archaeological monuments as well.

The appearance depth of zero and negative D_e values varied for the different pits at the Grote Houw. This cannot be simply explained by ploughing. A difficulty in the estimation of soil erosion on the Grote Houw was that the mound was built by humans. However, it appeared from the results that the samples, and therefore the layers, did not consist essentially of a blend of material of different ages. The obtained D_e estimates were therefore too constant.

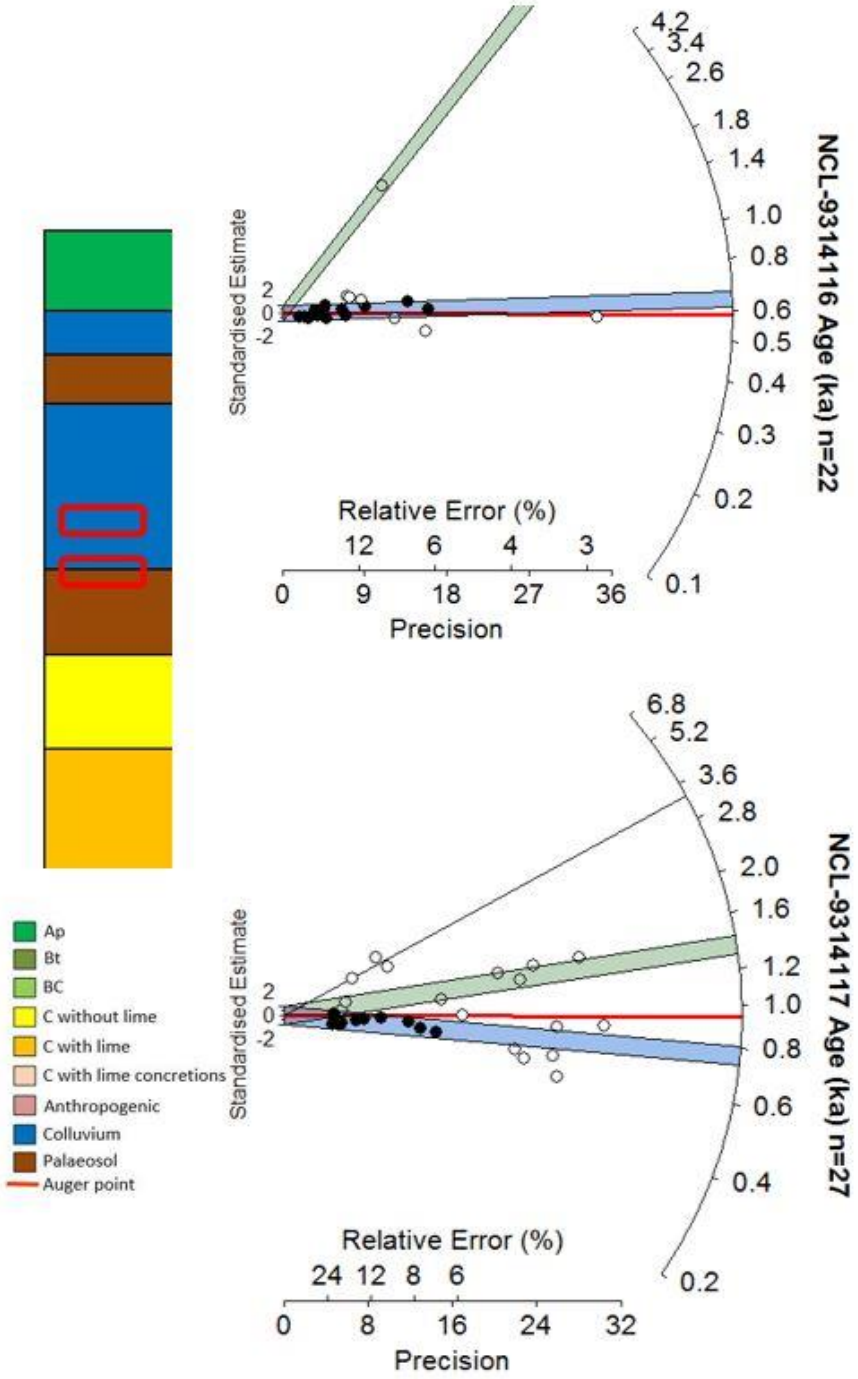

Fig. 36: FMM components of sequential samples are related indicating more or less the same age

5.2 ESTIMATION OF EROSION RATES AT FIELD LEVEL

5.2.1 FROM SOIL PROFILES TO FIELD LEVEL

For Meerssen were the AHN1 and AHN2 compared to estimate erosion by differences in elevation (Heeres, 2014). In this thesis the AHN2 was used again as a base map for erosion simulations. The results of the water accumulation and tillage erosion models were highly dependent on the resolution of the used DEM. For this small slope the DEM with a resolution of 5m gave the clearest picture. Statistically appeared the relationship between the ^{137}Cs concentration and the water accumulation and tillage erosion simulations less bright than visually demonstrated. Scatter plots were made to express the significance of the correlation of the ^{137}Cs distribution and the water and tillage erosion maps in several ways. The R-squared remained though low. As discussed previously seemed that the two forms of soil erosion have also worked against each other at some slope positions.

As in Meerssen resulted the surface ^{137}Cs measurement not in a clear erosive pattern. Wind erosion is completely disregarded while this is a great erosive factor in the Northern provinces of the Netherlands. The land here is flat and the soil often dry. There is, however, assumed that the detachment of soil by wind is in general equal over the whole study location. For both locations was it hard to determine whether the soil erosion occurred during catastrophic events or that the erosion was continuous. With other methods whereby the erosive processes on the surface were measured and modelled, like the amount of sediment captured at several slope positions, might this had been ascertained. It would have been interesting to estimate the amount of soil loss during a year or a shorter period of time as well.

All methods used per soil profile, the concentrations of the fallout isotopes, the anthropogenic Pb and the OSL results, indicated erosion on the two study locations (Fig. 37 and Fig. 38). The total concentrations estimated are lower on the erosive locations and higher at the depositional locations of the fields. Layers directly under the plough zone of these locations are dated older than soil layers at comparable or even deeper soil depth of the depositional locations.

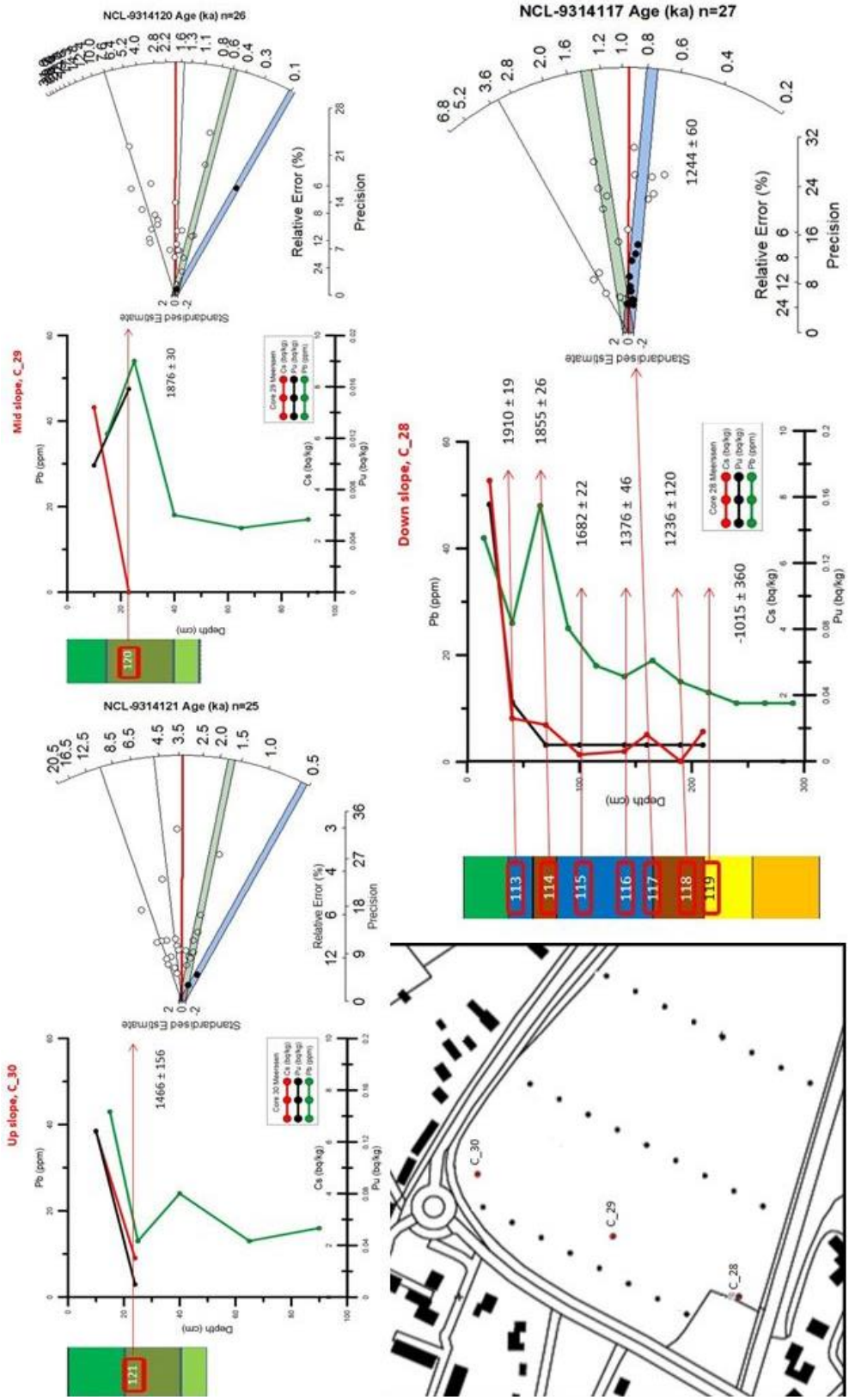

Fig. 37: Concentration profiles of fallout isotopes with age estimate of the youngest component and radial plot of the FMM components

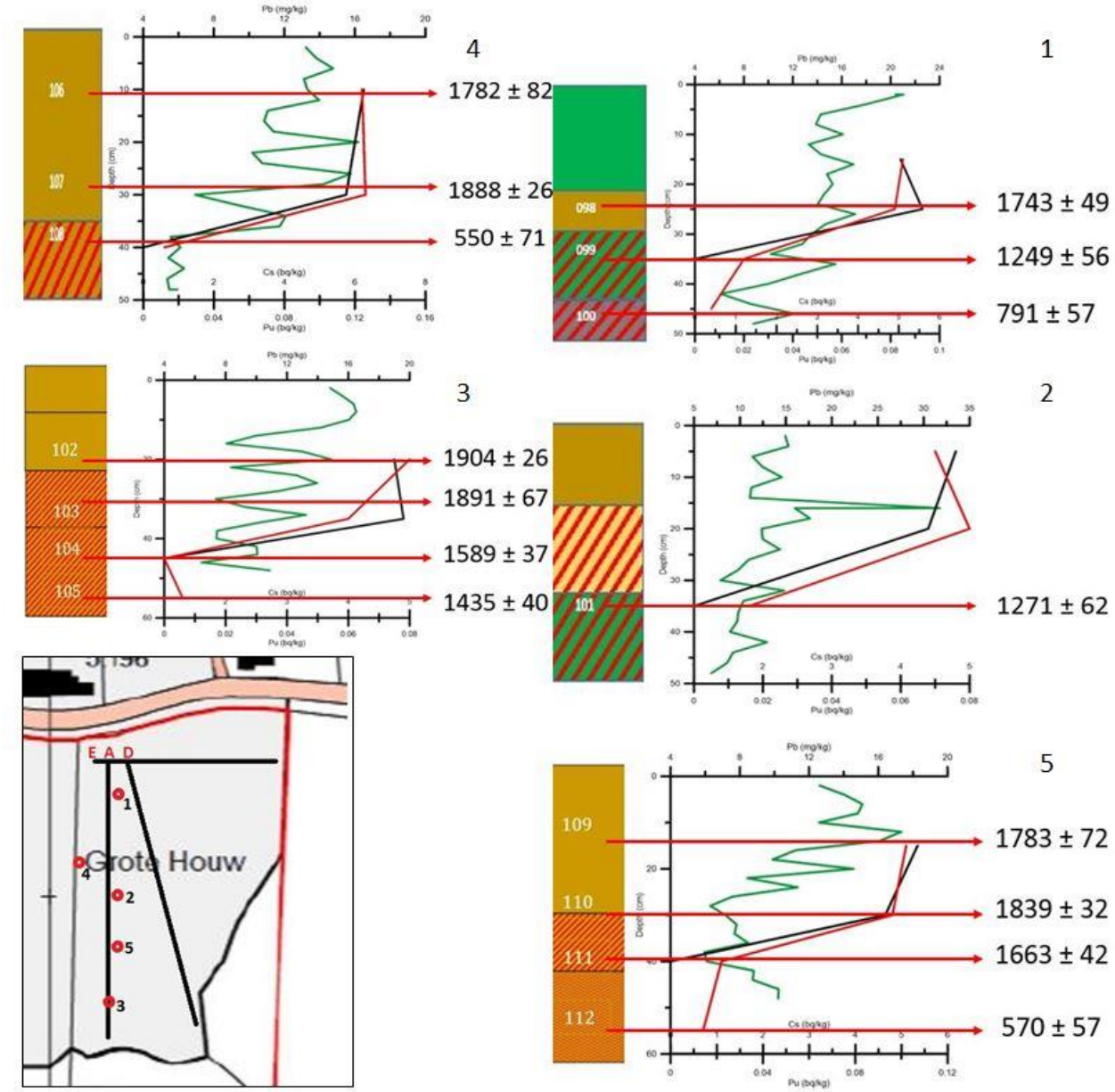

Fig. 38:concentration profiles of fallout isotopes with age estimate of the CAM

5.2.2 MODELS BASED ON FALLOUT ISOTOPES

There are some proportional models available for the calculation of the value of soil loss based on ^{137}Cs. The assumption is however that the ^{137}Cs is completely mixed within the plough layer and that the soil loss is directly proportional to the ^{137}Cs loss from the soil profile. A reference ^{137}Cs inventory on a undisturbed field is needed for the initial ^{137}Cs concentration. The equation can then be written as follows (Walling & Quine, 1990):

$$Y = 10 (BdX/100T)$$

Where:

Y: mean annual soil loss (t $ha^{-1}yr^{-1}$)

B: bulk density of the soil (kg m^{-3})

d: depth of the plough layer (m)

X: percentage reduction in total ^{137}Cs inventory defined as $((A_{ref}-A)/ A_{ref}) \times 100$

Where:

A_{ref}: the local ^{137}Cs reference inventory (Bq m^{-2})

A: the measured ^{137}Cs inventory at the sampling point (Bq m^{-2})

T: the time elapsed since initiation of ^{137}Cs accumulation (yr.)

Comparable models are developed, but al depend strongly on parameter choices (Fig. 39).

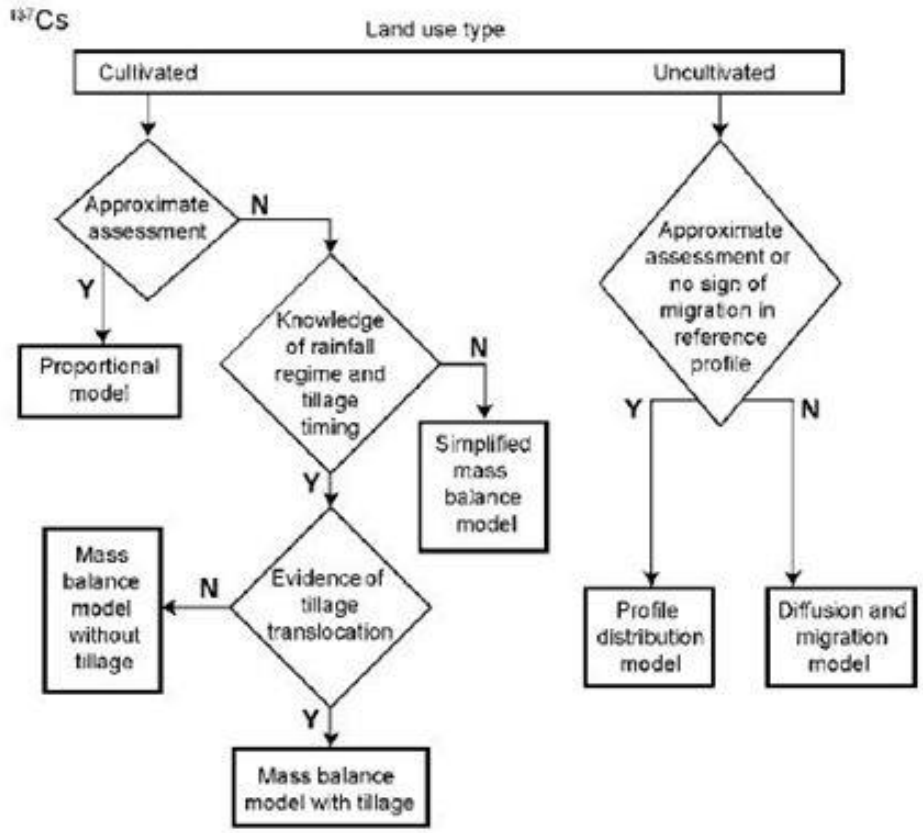

Model type	Parameter and data requirements
Proportional model and Simplified mass balance model	Tillage depth, bulk density, year of tillage commencement
Mass balance model 2	Tillage depth, year of tillage commencement, proportion factor, relaxation depth, record of annual fallout flux [a]
Mass balance model with tillage (Mass balance model 3)	Tillage depth, tillage constant, proportion factor, relaxation depth, slope length and slope gradient for each section of the transect, record of annual fallout flux*
Diffusion and migration model	Diffusion coefficient, relaxation depth, migration coefficient, record of annual fallout flux*
Profile shape model	Profile shape factor

[a] Only required for ^{137}Cs models.

Fig.39: fallout isotope erosion models (Adopted from Walling 2011)

The outcomes of the different models is expected to be different due to the dependency on the amount of parameters and the values chosen. In addition, it is important to know the reference value of the initial ^{137}Cs deposition. It is difficult to find these undisturbed locations in densely populated areas like the Netherlands. The models is also usable with $^{239+240}Pu$, but more than the available information is needed for this fallout isotope as well.

Needed for a proper use of the model:

- Reference inventory
- Particle size correction factors for eroding and depositional sites
- Proportion factor (of the annual radionuclide fallout that is susceptible to mobilization by heavy rainfall, prior to its incorporation into the soil by tillage)
- Tillage constant
- Profile shape factor, migration rate and diffusion coefficient
- Annual deposition flux

2.2.3 APPROXIMATION OF SOIL EROSION RATES

Because information on most of the parameters was not available is an approximation of the soil erosion rate calculated (Fig. 40). From this figure appeared again that the two sample cores on top and mid slope of the location in Meerssen are erosive. 20 to 30 % of the ^{137}Cs and $^{239+240}$Pu concentrations is removed from these locations compared to core 28 downslope. The erosive locations on the Grote Houw are clearly visible as well. Pit 1, 2, and 3 are erosive with rates comparable to Meerssen. ^{137}Cs and Pu indicate some different rate ratios between the pits. It is not clear what could have caused these differences. A small amount of erosion occurred in pit 5 compared to pit 4.

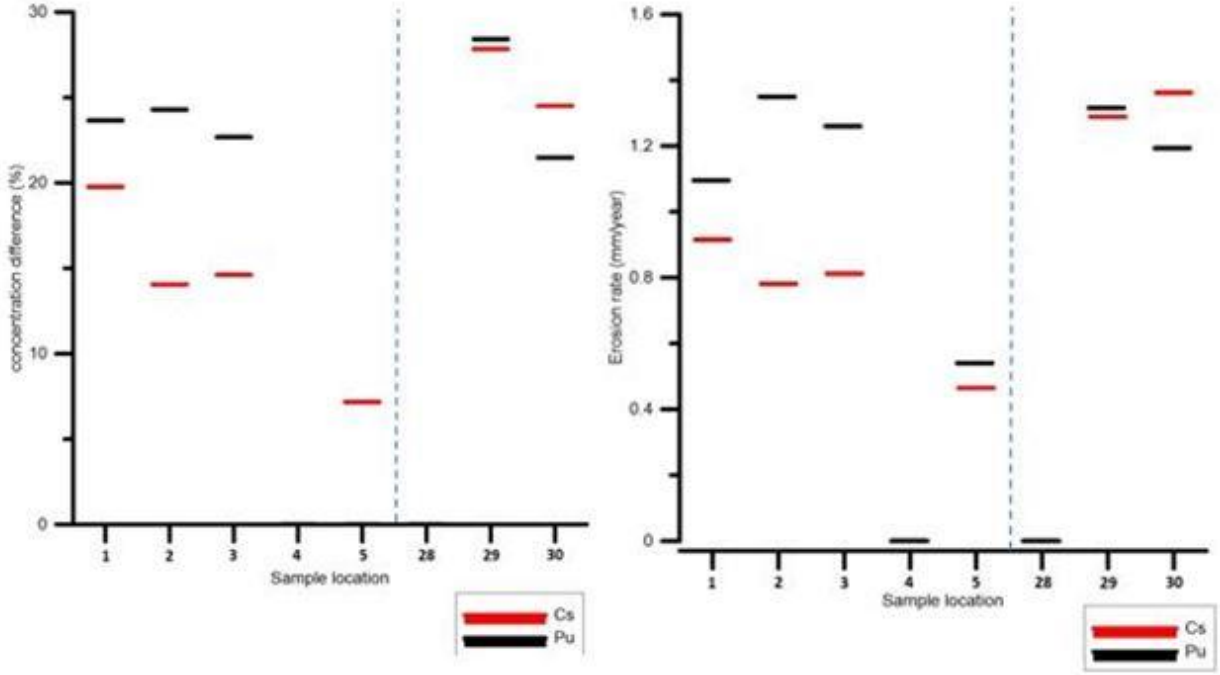

Fig. 40: percentage concentration difference of ^{137}Cs and $^{239+240}$Pu based on the highest concentration and erosion rates in mm/year

These calculations are based on deposition of ^{137}Cs and $^{239+240}$Pu in 1960 (54 years ago). This choice is made because the deposition of Chernobyl seemed to be little at both locations. The only influence of Chernobyl to the calculation is an addition to the concentration, but one can assume that this was the same amount throughout the study location. Mutual relationships between the sample points were therefor not changed. First is the concentration of the fallout isotope calculated in Bq per soil layer with the soil bulk density of 1500 kg/m^3. In addition is the total concentration per profile calculated. The highest total profile concentration is used as a reference value from which a percentage difference is derived with the assumption that all soil material stays on the location. The product of this percentage with the depth of the plough zone gave the amount of soil that is removed from this sample point since 54 years. Then, the erosion rate is calculated in mm/year. ^{137}Cs and $^{239+240}$Pu concentrations indicated erosion in the same order of magnitude especially in

Meerssen. On the Grote Houw are larger differences visible per pit, but are the trends between the pits in ^{137}Cs and $^{239+240}Pu$ concentration similar as well. The method would have been more reliable if it was possible to make use of a reference plot just as in the models introduced by Walling (2011). These are in the densely populated Netherlands, however, hard to find. The quantification of the soil erosion rate was of main interest to this research. Therefore, it was decided to give an approximation of the rates in this way with the available information.

Table 10: Excel spreadsheet of the erosion rate calculations

Meerssen - Cs	cm	cm3	bq/kg	kg soil	bq per layer	total/profile	since 1960	difference	Percentage	cm translocation	cm/year	mm/year
30	30	30	6.40	0.05	0.29	0.31	54	-0.15	-24.51	-7.35	-0.14	-1.36
	10	10	1.50	0.02	0.02							
29	25	25	7.20	0.04	0.27	0.27	54	-0.17	-27.83	-6.96	-0.13	-1.29
	5	5	0.00	0.01	0.00							
28	40	40	8.50	0.06	0.51	0.61	54	0.00				
	20	20	3.30	0.03	0.10							
Meerssen -Pu	cm	cm3	bq/kg	kg soil	bq per layer	total/profile	since 1960	difference	Percentage	cm translocation	cm/year	mm/year
30	30	30	0.13	0.05	0.01	0.01	54	0.00	-21.48	-6.44	-0.12	-1.19
	10	10	0.01	0.02	0.00							
29	25	25	0.12	0.04	0.00	0.00	54	0.00	-28.41	-7.10	-0.13	-1.32
	5	5	0.02	0.01	0.00							
28	40	40	0.16	0.06	0.01	0.01	54	0.01				
	20	20	0.04	0.03	0.00							
GH - Cs	cm	cm3	bq/kg	kg soil	bq per layer	total/profile	since 1960	difference	Percentage	cm translocation	cm/year	mm/year
1	25	25	5.10	0.04	0.38	0.41	54	-0.13	-19.76	-4.94	-0.09	-0.92
			4.90									
	15	15	1.20	0.02	0.03							
	5	5	0.40	0.01	0.00							
2	30	30	4.50	0.05	0.43	0.48	54	-0.09	-14.05	-4.22	-0.08	-0.78
			5.00									
	20	20	1.80	0.03	0.05							
3	30	30	5.00	0.05	0.41	0.47	54	-0.10	-14.61	-4.38	-0.08	-0.81
			4.00									
	20	20	1.00	0.03	0.07							
			1.30									
4	35	35	6.20	0.05	0.66	0.67	54	0.00	0.00	0.00	0.00	0.00
			6.30									
	15	15	0.60	0.02	0.01							
5	35	35	5.10	0.05	0.52	0.57	54	-0.05	-7.17	-2.51	-0.05	-0.46
			4.80									
	20	20	1.10	0.03	0.05							
			0.70									
GH - Pu	cm	cm3	bq/kg	kg soil	bq per layer	total/profile	since 1960	difference	Percentage	cm translocation	cm/year	mm/year
1	25	25	0.08	0.038	0.00	0.01	54	0.00	-23.66	-5.92	-0.11	-1.10
			0.09		0.00							
2	30	30	0.08	0.045	0.00	0.01	54	0.00	-24.29	-7.29	-0.13	-1.35
			0.07		0.00							
3	30	30	0.08	0.045	0.00	0.01	54	0.00	-22.68	-6.80	-0.13	-1.26
			0.08		0.00							
4	35	35	0.13	0.053	0.01	0.01	54	0.00	0.00	0.00	0.00	0.00
			0.12		0.01							
5	35	35	0.11	0.053	0.01	0.01	54	0.00	-8.33	-2.92	-0.05	-0.54
			0.09		0.00							

5.3 RECOMMENDATIONS

To conclude was thought about some implications of this thesis for the RCE and their future research and management plans. The combination of the different methods proved useful to link different processes in one location with anthropogenic influences on the soil structure. Quantification of soil erosion was only possible based on some rough assumptions with the methods used, but that there is the threat of soil erosion is estimated. A sampling design that is suitable for all methods should be carefully considered for next applications. That would have made it easier to compare all results with each other. Soil horizons should have been described more precise and consistent for the purpose of this particular research, because the descriptions of both locations were done now by two different persons. For analysis of the results it would have been easier and probably better when the samples were taken at the same soil depth per location. Although OSL is used to date and the fallout isotopes and anthropogenic lead were used as tracers can be explored in the future whether it had an impact on the results that the first method is based on the sand fraction of the soil and that the others were related to the clay fraction.

For future projects comparable to this thesis is recommended to do first some simple measurements on the estimation of erosion with for example a rainfall simulator. The primary purpose of a rainfall simulator is to determine the water infiltration and erosion characteristics of a given soil. By measuring the amount of soil displacement after application of a simulated rainfall event can be determined in a fast way how vulnerable the soil is to water erosion. Displacement of soil by tillage erosion is more difficult to measure in the field. The simulation model used resulted in plausible patterns. That this pattern did not match the surface analysis of the ^{137}Cs distribution have nothing to do with the value of the tillage simulation. As more detailed information becomes available and it is expected that the models continue to be adjusted using Universal Soil Loss Equations will become increasingly important. Which has received little attention in this study is the difference between event-driven and continuous erosion. For archaeological research this is important because in the latter case, the archaeological objects can be re-buried while in the event-driven erosion they are vulnerable to disappear from the monument. It was, with the current knowledge, not possible to determine this difference on the basis of the methods used. This too would be interesting in the future to investigate.

6. ACKNOWLEDGEMENT

A large group of people was involved in the making of this thesis. First, there was of course Jeroen, my supervisor at the Wageningen University. Tony and Alice were closely involved as well. Certainly the hours in the NCL lab and the help in the analysis by Alice were very valuable for the proceedings of the research process. Secondly, I have had intensive supervision from the RCE by Hans. Also Bertil, Jan-Willem, Menno, Mario and Wim contributed. And then of course, there were the people of Medusa for the ceasium and Michael and Arnaud for the plutonium analysis. But my parents, family and housemates might have had the heaviest recent months ;-) Moreover, I had the great opportunity to be able to present some of this research at the EGU2015.
Thanks everyone!

REFERENCES

Aitken, M. J. (1985). *Thermoluminescence dating* (U.S. edition ed.). London and Orlando and Montreal: Academic press.

Alewell, C., Meusburger, K., Juretzko, G., Mabit, L., & Ketterer, M. E. (2014). Suitability of 239+240Pu and 137Cs as tracers for soil erosion assessment in mountain grasslands. *Chemosphere, 103*, 274-280. doi: 10.1016/j.chemosphere.2013.12.016

An, J., Zheng, F., & Wang, B. (2014). Using 137Cs technique to investigate the spatial distribution of erosion and deposition regimes for a small catchment in the black soil region, Northeast China. *Catena, 123*, 243-251. doi: 10.1016/j.catena.2014.08.009

Arnold, L.J., & Roberts, R.G. (2009). Stochastic modelling of multi-grain equivalent dose (De) distributions: Implications for OSL dating of sediment mixtures. *Quaternary Geochronology,* 4(3), 204-230

Baartman, J. E. M., Temme, A. J. A. M., Schoorl, J. M., Braakhekke, M. H. A., & Veldkamp, T. A. (2012). Did tillage erosion play a role in millennial scale landscape development? *Earth Surface Processes and Landforms, 37*(15), 1615-1626. doi: 10.1002/esp.3262

Cunningham, A.C. and Wallinga, J. (2010) Selection of integration time intervals for quartz OSL decay curves, *Quaternary Geochronology,* 5 (6) pp.657-666

de Groot , T. (2005). De Romeinse villa Meerssen-Onderste Herkenberg. *ROB Rapportage Archeologische Monumentenzorg, 125*.

de Kort, J-W, (2013) Meerssen- Onderste Herkenberg. *Plan van aanpak*. Amersfoort, Rijksdienst voor het cultureel erfgoed.

de Langen, G.J., & Hommes., H.W. (1998) Provincie Fryslân. Metaaldetectie Noord-Westergo 1992-1996. RAAP rapport 298/BOM-rapport 22.

de Langen, G.J. (2007a) De ploeg en het terpencomplex van Dongjum. In: G.J. de Langen & F.A. Veenman (red.), Archeologische Kroniek van Friesland over 2005 en 2006. *De Vrije Fries,* 87, 217-220

Diez-Martín, F. (2010). Evaluating the effect of plowing on the archaeological record: The early middle palaeolithic in the river Duero basin plateaus (north-central Spain). *Quaternary International, 214*(1-2), 30-43. doi: 10.1016/j.quaint.2009.10.024

Duller, G. A. T. (2003). Distinguishing quartz and feldspar in single grain luminescence measurements. *Radiation Measurements, 37*(2), 161-165. doi: 10.1016/s1350-4487(02)00170-1

Fuchs, M., & Lang, A. (2009). Luminescence dating of hillslope deposits—A review. *Geomorphology, 109*(1-2), 17-26. doi: 10.1016/j.geomorph.2008.08.025

Gaspar, L., Navas, A., Walling, D. E., Machín, J., & Gómez Arozamena, J. (2013). Using 137Cs and 210Pbex to assess soil redistribution on slopes at different temporal scales. *Catena, 102*, 46-54. doi: 10.1016/j.catena.2011.01.004

Guérin, G., Mercier, N., & Adamiec, G. (2011). Dose-rate conversion factors: update. *Ancient TL, 29*(1), 5-8.

Heeres, G.C. (2014). Sediment erosion at archeological sites in Limburg, The Netherlands, Master thesis. Soil geography and landscape group Wageningen university

Heimsath, A. M., Chappell, J., Spooner, N. A., & Questiaux, D. G. (2002). Creeping soil. *Geology, 30*(2), 111-114.

Heimsath, A. M., & Jungers, M. C. (2013). 7.13 Processes, Transport, Deposition, and Landforms: Quantifying Creep. 138-151. doi: 10.1016/b978-0-12-374739-6.00158-5

Houk, R. S. (1994). Elemental and Isotopic Analysis by Inductively Coupled Plasma Mass Spectrometry. *Acc. Chem. Res., 27*, 333-339.

Ibrahim, S.A., & Morris, R.C. (1997). Distribution of plutonium among soil phases near a Subsurface Disposal area in Southeastern Idaho, USA. *Journal of Radioanalytical and Nuclear Chemistry, 226*(1-2), 217-220

Jongmans, A.G., van den Berg, M.W., & sonneveld, M.P.W. (2012). Landschappen van Nederland: geologie, bodem en landgebruik. Wageningen Academic Publischers

Ketterer, M. E., Hafer, K. M., Jones, V. J., & Appleby, P. G. (2004). Rapid dating of recent sediments in Loch Ness: inductively coupled plasma mass spectrometric measurements of global fallout plutonium. *Sci Total Environ, 322*(1-3), 221-229. doi: 10.1016/j.scitotenv.2003.09.016

Ketterer, M. E., & Szechenyi, S. C. (2008). Determination of plutonium and other transuranic elements by inductively coupled plasma mass spectrometry: A historical perspective and new frontiers in the environmental sciences. *Spectrochimica Acta Part B: Atomic Spectroscopy, 63*(7), 719-737. doi: 10.1016/j.sab.2008.04.018

Ketterer, M. E., Zheng, J., & Yamada, M. (2012). Applications of transuranics as tracers and chronometers in the environment *Handbook of environmental isotope geochemistry* (pp. 395-417): Springer Berling Heidelberg.

Lair, G. J., Zehetner, F., Hrachowitz, M., Franz, N., Maringer, F.-J., & Gerzabek, M. H. (2009). Dating of soil layers in a young floodplain using iron oxide crystallinity. *Quaternary Geochronology, 4*(3), 260-266. doi: 10.1016/j.quageo.2008.11.003

Madsen, A. T., Murray, A. S., Andersen, T. J., Pejrup, M., & Breuning-Madsen, H. (2005). Optically stimulated luminescence dating of young estuarine sediments: a comparison with 210Pb and 137Cs dating. *Marine Geology, 214*(1-3), 251-268. doi: 10.1016/j.margeo.2004.10.034

Martin-Fernandez, L., & Martinez-Nunez, M. (2011). An empirical approach to estimate soil erosion risk in Spain. *Sci Total Environ, 409*(17), 3114-3123. doi: 10.1016/j.scitotenv.2011.05.010

Murray, A.S. and Wintle, A.G. (2000) Luminescence dating of quartz using an improved single aliquot regenerative-dose protocol, *Radiation measurements*, 32, 57-73

Nicolay, J. A. W. (2010). *Terpbewoning in oostelijk Friesland. Twee opgravingen in het voormalige kweldergebied van Oostergo* (Vol. 12). Groningen: Barkhuis.

Olson, K. R., Gennadiyev, A. N., Zhidkin, A. P., Markelov, M. V., Golosov, V. N., & Lang, J. M. (2013). Use of magnetic tracer and radio-cesium methods to determine past cropland soil erosion amounts and rates. *Catena, 104*, 103-110. doi: 10.1016/j.catena.2012.10.015

Prescott, J. R., & Hutton, J. T. (1994). Cosmic ray contributions to dose rates for luminescence and ESR dating: large depths and long-term time variations. *Radiation Measurements, 23*(2/3), 497-500.

Preusser, F., Degering, D., Fuchs, M., Hilgers, A., Kadereit, A, Klasen, N., Krbetschek, M., Richter, D., & Spencer, J.Q.G. (2008). Luminescence dating: basics, methods and applications. *Quaternary Science Journal*, 57 (1-2), 95-149

Reimann, T., Lindhorst, S., Thomsen, K. J., Murray, A. S., & Frechen, M. (2012). OSL dating of mixed coastal sediment (Sylt, German Bight, North Sea). *Quaternary Geochronology, 11*, 52-67. doi: 10.1016/j.quageo.2012.04.006

Roberts, R. G., Galbraith, R. F., Yoshida, H., Laslett, G. M., & Olley, J. M. (2000). Distinguishing dose populations in sediment mixtures: a test of single-grain optical dating procedures using mixtures of laboratory-dosed quartz. *Radiation Measurements, 32*, 459-465.

Schaub, M., Konz, N., Meusburger, K., & Alewell, C. (2010). Application of in-situ measurement to determine 137Cs in the Swiss Alps. *J Environ Radioact, 101*(5), 369-376. doi: 10.1016/j.jenvrad.2010.02.005

Schoorl, J. M., Boix Fayos, C., de Meijer, R. J., van der Graaf, E. R., & Veldkamp, A. (2004). The 137Cs technique applied to steep Mediterranean slopes (Part II): landscape evolution and model calibration. *Catena, 57*(1), 35-54. doi: 10.1016/j.catena.2003.08.002

Spaan, W.P., Winteraeken, H.J., & Geelen, P. (2010). Adoption of SWC measures in South Limburg (The Netherlands): Experiences of a water manager. *Land Use Policy,* 27(1), 78-85

Stoepker, H. (2005). Het Maaswerkgebied in de Middeleeuwen en de Nieuwe Tijd. *Archeologie in de Maaswerken. Synthese en evaluatie van het nieuwe iventariserend achreologisch onderzoek in de Maaswerken*, 129-148.

Stoutjesdijk, J.F. (1986). De radioactieve besmetting in Nederland ten gevolge van het kernreactor ongeval in Tsjernobyl. *Coordinatie-commissie voor de metingen van radioactiviteit en Xenobiotische stoffen, RIVM.*

Tegen, I., & Dörr, H. (1996). Mobilization of cesium in organic rich soils: correlation with production of dissolved organic carbon. *Water, Air and Soil pollution, 88*, 133-144.

van Egmond, F.M. (2014) Cesium metingen aan monsters en veld. Medusa rapport: 2014-P-495

van der Heiden, M., Huisman, D. J., & van Doesburg, J. (2014). Grote Houw *Programma van Eisen* Amersfoort: Rijksdienst voor het Cultureel Erfgoed.

van Os, B.J.H. & Kosian, M. (2011). RAM 196, Lauwerier, R.G.C.M. et. al. (red.), Vragen over Malta, Onderzoek naar de effectiviteit van de onderzoeksketen, sluipende degradatie en de effecten van vrijstelling, 41-84.

van Rompaey, A. J. J., Verstraeten, G., Van Oost, K., Govers, G., & Poesen, J. (2001). Modelling mean annual sediment yield using a distributed approach. *Earth Surface Processes and Landforms, 26*(11), 1221-1236. doi: 10.1002/esp.275

van Wijngaarden, M., Venema, L. B., de Meijer, R. J., Zwolsman, J. J. G., van Os, B., & Gieske, J. M. J. (2002). Radiometric sand-mud characterisation in the Rhine-Meuse estuary Part A. Fingerprinting. *Geomorphology, 43*, 87-101.

Walling, D.E, Zhang, Y., & He, Q. (2011). Models for deriving estimates of erosion and deposition rates from fallout radionuclide (caesium-137, excess lead-210 and beryllium-7) measurements and the development of user-friendly software for model implementation. *Impact of Soil Conservation Measures on Erosion Control and Soil Quality,* IAEA-TECDOC-1665, pp. 11-33

Walling, D.E, Collins, A.L., & Sichingabula, H.M. (2003). Using unsupported lead-210 measurements to investigate soil erosion and sediment delivery in a small Zambian catchment. *Geomorphology*, 25(3-4), 193-213

Walling, D.E, & Quine, T.A. (1990). Calibration of caesium-137 measurements to provide quantitative erosion rate data. *Land Degradation and Rehabilitation*, 2, 161-175

Walraven, N. (2014). Lead iin rural and urban soils and sediments in the Netherlands: background, pollution, sources and mobility. *Academic Phd report, Vrije universiteit Amsterdam.*

Winteraeken, H. J., & Spaan, W. P. (2010). A new approach to soil erosion and runoff in south Limburg-The Netherlands. *Land Degradation & Development, 21*(4), 346-352. doi: 10.1002/ldr.1009

Yamamoto, M., Yamamori, S., Komura, K., & Sakananoue, M. (1980). Behavior of plutonium and americum in soils. *Journal of radiation research, 21*(3-4), 204-212.

APPENDIX

A: HAND-AUGER DESCRIPTIONS MEERSSEN

boring: MEHE13-2

beschrijver: JWK, datum: 28-7-2014, X: 181.269,10, Y: 321.581,58, precisie locatie: 1 cm, coördinaatsysteem: Rijksdriehoeksmeting, kaartblad: 62A, hoogte: 67,68, precisie hoogte: 1 cm, referentievlak: Normaal Amsterdams Peil, methode hoogtebepaling: GPS, boortype: Edelman-7 cm, doel boring: archeologie - verkenning, landgebruik: braak, vondstzichtbaarheid: slecht, provincie: Limburg, gemeente: Meerssen, plaatsnaam: HERKENBERG, opdrachtgever: RCE, uitvoerder: RCE

0 cm -Mv / 67,68 m +NAP
Algemeen: aard ondergrens: abrupt (<0,3 cm)
Lithologie: leem, zwak zandig, zwak grindig, donkergrijsbruin
Bodemkundig: regelmatig geploegd/bewerkte A-horizont, interpretatie: bouwvoor
Archeologie: fragmenten bouwpuin

30 cm -Mv / 67,38 m +NAP
Algemeen: aard bovengrens: abrupt (<0,3 cm)
Lithologie: leem, zwak zandig, roodbruin, matig stevig
Bodemkundig: B-horizont met ingespoelde klei

40 cm -Mv / 67,28 m +NAP
Algemeen: aard ondergrens: abrupt (<0,3 cm)
Lithologie: leem, zwak zandig, lichtbruin, matig stevig
Archeologie: enkele spikkel houtskool, enkel fragment verbrande klei/leem, enkel fragment bouwpuin
Opmerking: SPOOR?

60 cm -Mv / 67,08 m +NAP
Algemeen: aard bovengrens: abrupt (<0,3 cm), aard ondergrens: abrupt (<0,3 cm)
Lithologie: leem, zwak zandig, lichtbruingeel, matig stevig, kalkloos
Bodemkundig: BC-horizont, enkele Fe- en Mn-vlekken
Opmerking: BC

120 cm -Mv / 66,48 m +NAP
Algemeen: aard bovengrens: abrupt (<0,3 cm), aard ondergrens: abrupt (<0,3 cm)
Lithologie: leem, zwak zandig, lichtbruingeel, matig stevig, kalkloos
Bodemkundig: C-horizont, enkele Fe- en Mn-vlekken

170 cm -Mv / 65,98 m +NAP
Algemeen: aard bovengrens: abrupt (<0,3 cm)
Lithologie: leem, zwak zandig, lichtbruingeel, matig stevig, kalkloos
Bodemkundig: C-horizont, enkele Fe- en Mn-vlekken
Archeologie: fragmenten bouwpuin
Opmerking: PUIN???

175 cm -Mv / 65,93 m +NAP
Lithologie: leem, zwak zandig, lichtbruingeel, matig stevig, kalkloos
Bodemkundig: C-horizont, enkele Fe- en Mn-vlekken
Opmerking: VREEMD GEVLEKT, VERSTOORD?

200 cm -Mv / 65,68 m +NAP
Lithologie: leem, zwak zandig, geel, enkele siltlagen
Bodemkundig: C-horizont, enkele Fe-vlekken

Einde boring op 320 cm -Mv / 64,48 m +NAP

boring: MEHE13-3

beschrijver: JWK, datum: 28-7-2014, X: 181.257,37, Y: 321.559,50, precisie locatie: 1 cm, coördinaatsysteem: Rijksdriehoeksmeting, kaartblad: 62A, hoogte: 67,07, precisie hoogte: 1 cm, referentievlak: Normaal Amsterdams Peil, methode hoogtebepaling: GPS, boortype: Edelman-7 cm, doel boring: archeologie - verkenning, landgebruik: braak, vondstzichtbaarheid: slecht, provincie: Limburg, gemeente: Meerssen, plaatsnaam: HERKENBERG, opdrachtgever: RCE, uitvoerder: RCE

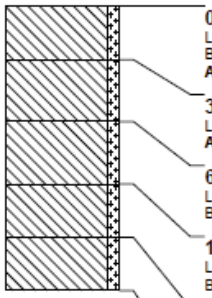

0 cm -Mv / 67,07 m +NAP
Lithologie: leem, zwak zandig, donkergrijsbruin
Bodemkundig: regelmatig geploegd/bewerkte A-horizont, interpretatie: bouwvoor
Archeologie: enkele spikkel houtskool, fragmenten bouwpuin (onbepaald)

30 cm -Mv / 66,77 m +NAP
Lithologie: leem, zwak zandig, bruin
Archeologie: enkel fragment bouwpuin

65 cm -Mv / 66,42 m +NAP
Lithologie: leem, zwak zandig, roodbruin, zeer stevig
Bodemkundig: B-horizont met ingespoelde klei

100 cm -Mv / 66,07 m +NAP
Lithologie: leem, zwak zandig, lichtbruin, zeer stevig, kalkloos
Bodemkundig: BC-horizont

130 cm -Mv / 65,77 m +NAP
Lithologie: leem, zwak zandig, lichtbruingeel, enkele siltlagen, matig stevig, kalkloos
Bodemkundig: C-horizont

Einde boring op 160 cm -Mv / 65,47 m +NAP

boring: MEHE13-4

beschrijver: JWK, datum: 28-7-2014, X: 181.245,69, Y: 321.537,42, precisie locatie: 1 cm, coördinaatsysteem: Rijksdriehoeksmeting, kaartblad: 62A, hoogte: 66,20, precisie hoogte: 1 cm, referentievlak: Normaal Amsterdams Peil, methode hoogtebepaling: GPS, boortype: Edelman-7 cm, doel boring: archeologie - verkenning, landgebruik: braak, vondstzichtbaarheid: slecht, provincie: Limburg, gemeente: Meerssen, plaatsnaam: HERKENBERG, opdrachtgever: RCE, uitvoerder: RCE

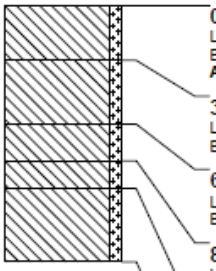

0 cm -Mv / 66,20 m +NAP
Lithologie: leem, zwak zandig, donkergrijsbruin
Bodemkundig: regelmatig geploegd/bewerkte A-horizont, interpretatie: bouwvoor
Archeologie: enkele spikkel houtskool, fragmenten bouwpuin (onbepaald)

30 cm -Mv / 65,90 m +NAP
Lithologie: leem, zwak zandig, roodbruin, zeer stevig
Bodemkundig: B-horizont met ingespoelde klei

65 cm -Mv / 65,55 m +NAP
Lithologie: leem, zwak zandig, bruin, zeer stevig
Bodemkundig: B-horizont met ingespoelde klei, veel Fe- en Mn-vlekken

85 cm -Mv / 65,35 m +NAP
Lithologie: leem, zwak zandig, lichtbruin, zeer stevig, kalkloos
Bodemkundig: BC-horizont

100 cm -Mv / 65,20 m +NAP
Lithologie: leem, zwak zandig, lichtbruingeel, enkele siltlagen, matig stevig, kalkloos
Bodemkundig: C-horizont

Einde boring op 140 cm -Mv / 64,80 m +NAP

boring: MEHE13-5

beschrijver: JWK, datum: 28-7-2014, X: 181.233,98, Y: 321.515,30, precisie locatie: 1 cm, coördinaatsysteem: Rijksdriehoeksmeting, kaartblad: 62A, hoogte: 65,20, precisie hoogte: 1 cm, referentievlak: Normaal Amsterdams Peil, methode hoogtebepaling: GPS, boortype: Edelman-7 cm, doel boring: archeologie - verkenning, landgebruik: braak, vondstzichtbaarheid: slecht, provincie: Limburg, gemeente: Meerssen, plaatsnaam: HERKENBERG, opdrachtgever: RCE, uitvoerder: RCE

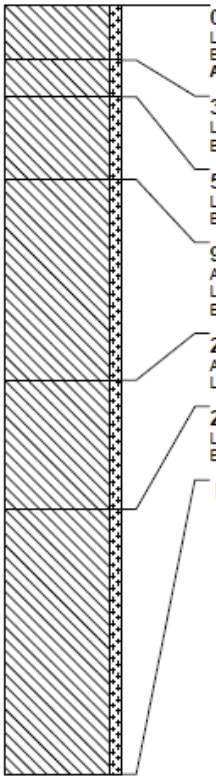

0 cm -Mv / 65,20 m +NAP
Lithologie: leem, zwak zandig, donkergrijsbruin
Bodemkundig: regelmatig geploegd/bewerkte A-horizont, interpretatie: bouwvoor
Archeologie: veel fragmenten bouwpuin

30 cm -Mv / 64,90 m +NAP
Lithologie: leem, zwak zandig, roodbruin, zeer stevig
Bodemkundig: B-horizont met ingespoelde klei

50 cm -Mv / 64,70 m +NAP
Lithologie: leem, zwak zandig, lichtbruin
Bodemkundig: veel Fe- en Mn-vlekken

95 cm -Mv / 64,25 m +NAP
Algemeen: aard ondergrens: abrupt (<0,3 cm)
Lithologie: leem, zwak zandig, lichtbruingeel, enkele siltlagen
Bodemkundig: C-horizont

205 cm -Mv / 63,15 m +NAP
Algemeen: aard bovengrens: abrupt (<0,3 cm)
Lithologie: leem, zwak zandig, lichtgeel, enkele siltlagen, kalkconcreties

275 cm -Mv / 62,45 m +NAP
Lithologie: leem, zwak zandig, lichtgeel
Bodemkundig: enkele Fe-vlekken

Einde boring op 420 cm -Mv / 61,00 m +NAP

boring: MEHE13-6

beschrijver: JWK, datum: 28-7-2014, X: 181.222,29, Y: 321.493,22, precisie locatie: 1 cm, coördinaatsysteem: Rijksdriehoeksmeting, kaartblad: 62A, hoogte: 63,87, precisie hoogte: 1 cm, referentievlak: Normaal Amsterdams Peil, methode hoogtebepaling: GPS, boortype: Edelman-7 cm, doel boring: archeologie - verkenning, landgebruik: braak, vondstzichtbaarheid: slecht, provincie: Limburg, gemeente: Meerssen, plaatsnaam: HERKENBERG, opdrachtgever: RCE, uitvoerder: RCE

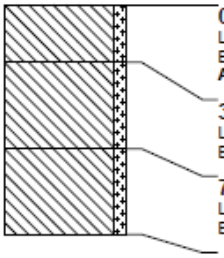

0 cm -Mv / 63,87 m +NAP
Lithologie: leem, zwak zandig, donkergrijsbruin
Bodemkundig: regelmatig geploegd/bewerkte A-horizont, interpretatie: bouwvoor
Archeologie: enkel fragment bouwpuin

30 cm -Mv / 63,57 m +NAP
Lithologie: leem, zwak zandig, lichtbruin, matig stevig
Bodemkundig: BC-horizont, veel Fe-vlekken

75 cm -Mv / 63,12 m +NAP
Lithologie: leem, zwak zandig, lichtbruingeel, enkele siltlagen
Bodemkundig: C-horizont, enkele Fe-vlekken

Einde boring op 120 cm -Mv / 62,67 m +NAP

boring: MEHE13-7

beschrijver: JWK, datum: 28-7-2014, X: 181.210,59, Y: 321.471,13, precisie locatie: 1 cm, coördinaatsysteem: Rijksdriehoeksmeting, kaartblad: 62A, hoogte: 62,25, precisie hoogte: 1 cm, referentievlak: Normaal Amsterdams Peil, methode hoogtebepaling: GPS, boortype: Edelman-7 cm, doel boring: archeologie - verkenning, landgebruik: braak, vondstzichtbaarheid: slecht, provincie: Limburg, gemeente: Meerssen, plaatsnaam: HERKENBERG, opdrachtgever: RCE, uitvoerder: RCE

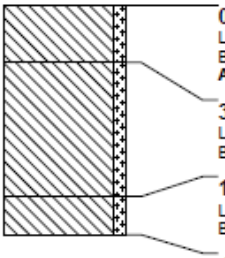

0 cm -Mv / 62,25 m +NAP
Lithologie: leem, zwak zandig, donkergrijsbruin
Bodemkundig: regelmatig geploegd/bewerkte A-horizont, interpretatie: bouwvoor
Archeologie: fragmenten bouwpuin

30 cm -Mv / 61,95 m +NAP
Lithologie: leem, zwak zandig, lichtbruin
Bodemkundig: B-horizont met ingespoelde klei

100 cm -Mv / 61,25 m +NAP
Lithologie: leem, zwak zandig, lichtbruingeel, enkele siltlagen
Bodemkundig: C-horizont

Einde boring op 120 cm -Mv / 61,05 m +NAP

boring: MEHE13-8

beschrijver: JWK, datum: 28-7-2014, X: 181.198,89, Y: 321.449,04, precisie locatie: 1 cm, coördinaatsysteem: Rijksdriehoeksmeting, kaartblad: 62A, hoogte: 60,30, precisie hoogte: 1 cm, referentievlak: Normaal Amsterdams Peil, methode hoogtebepaling: GPS, boortype: Edelman-7 cm, doel boring: archeologie - verkenning, landgebruik: braak, vondstzichtbaarheid: slecht, provincie: Limburg, gemeente: Meerssen, plaatsnaam: HERKENBERG, opdrachtgever: RCE, uitvoerder: RCE

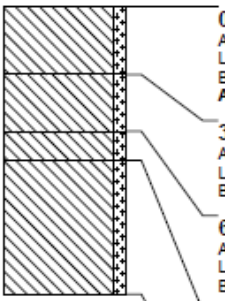

0 cm -Mv / 60,30 m +NAP
Algemeen: aard ondergrens: abrupt (<0,3 cm)
Lithologie: leem, zwak zandig, donkergrijsbruin
Bodemkundig: regelmatig geploegd/bewerkte A-horizont, interpretatie: bouwvoor
Archeologie: fragmenten bouwpuin

35 cm -Mv / 59,95 m +NAP
Algemeen: aard bovengrens: abrupt (<0,3 cm), aard ondergrens: abrupt (<0,3 cm)
Lithologie: leem, zwak zandig, lichtbruin, matig stevig
Bodemkundig: BC-horizont

65 cm -Mv / 59,65 m +NAP
Algemeen: aard bovengrens: abrupt (<0,3 cm), aard ondergrens: abrupt (<0,3 cm)
Lithologie: leem, zwak zandig, lichtbruingeel, matig stevig, kalkloos
Bodemkundig: BC-horizont

80 cm -Mv / 59,50 m +NAP
Algemeen: aard bovengrens: abrupt (<0,3 cm)
Lithologie: leem, zwak zandig, lichtbruingeel, enkele siltlagen, matig stevig, kalkloos
Bodemkundig: C-horizont

Einde boring op 150 cm -Mv / 58,80 m +NAP

boring: MEHE13-9

beschrijver: JWK, datum: 28-7-2014, X: 181.187,18, Y: 321.426,94, precisie locatie: 1 cm, coördinaatsysteem: Rijksdriehoeksmeting, kaartblad: 62A, hoogte: 59,00, precisie hoogte: 1 cm, referentievlak: Normaal Amsterdams Peil, methode hoogtebepaling: GPS, boortype: Edelman-7 cm, doel boring: archeologie - verkenning, landgebruik: braak, vondstzichtbaarheid: slecht, provincie: Limburg, gemeente: Meerssen, plaatsnaam: HERKENBERG, opdrachtgever: RCE, uitvoerder: RCE

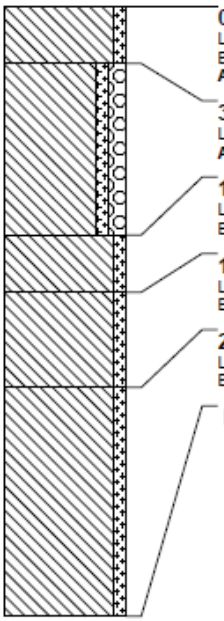

0 cm -Mv / 59,00 m +NAP
Lithologie: leem, zwak zandig, donkergrijsbruin
Bodemkundig: regelmatig geploegd/bewerkte A-horizont, interpretatie: bouwvoor
Archeologie: fragmenten bouwpuin

30 cm -Mv / 58,70 m +NAP
Lithologie: leem, zwak zandig, matig grindig, grijsbruin, interpretatie: colluvium
Archeologie: spikkels houtskool, enkel fragment aardewerk, fragmenten bouwpuin

120 cm -Mv / 57,80 m +NAP
Lithologie: leem, zwak zandig, lichtbruin, matig stevig, kalkloos
Bodemkundig: BC-horizont

150 cm -Mv / 57,50 m +NAP
Lithologie: leem, zwak zandig, lichtbruingeel, enkele siltlagen, matig stevig, kalkloos
Bodemkundig: C-horizont

200 cm -Mv / 57,00 m +NAP
Lithologie: leem, zwak zandig, lichtgeel, enkele siltlagen, matig stevig, kalkloos
Bodemkundig: C-horizont

Einde boring op 320 cm -Mv / 55,80 m +NAP

boring: MEHE13-10

beschrijver: JWK, datum: 28-7-2014, X: 181.200,63, Y: 321.387,31, precisie locatie: 1 cm, coördinaatsysteem: Rijksdriehoeksmeting, kaartblad: 62A, hoogte: 55,07, referentievlak: Normaal Amsterdams Peil, methode hoogtebepaling: GPS, boortype: Edelman-7 cm, doel boring: archeologie - verkenning, landgebruik: braak, vondstzichtbaarheid: slecht, provincie: Limburg, gemeente: Meerssen, opdrachtgever: RCE, uitvoerder: RCE

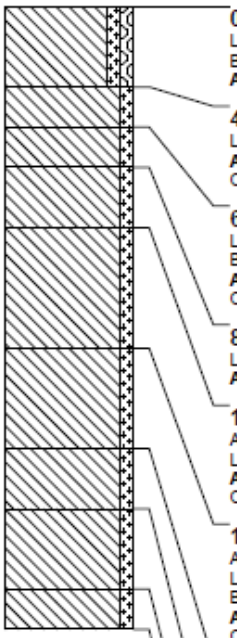

0 cm -Mv / 55,07 m +NAP
Lithologie: leem, zwak zandig, zwak grindig, donkergrijsbruin
Bodemkundig: regelmatig geploegd/bewerkte A-horizont
Archeologie: fragmenten bouwpuin (onbepaald)

40 cm -Mv / 54,67 m +NAP
Lithologie: leem, zwak zandig, lichtgrijsbruin, interpretatie: colluvium
Archeologie: enkel fragment bouwpuin (onbepaald)
Opmerking: STK

60 cm -Mv / 54,47 m +NAP
Lithologie: leem, zwak zandig, grijsbruin, interpretatie: colluvium
Bodemkundig: afgedekt/begraven A-horizont
Archeologie: fragmenten bouwpuin (onbepaald)
Opmerking: STK

80 cm -Mv / 54,27 m +NAP
Lithologie: leem, zwak zandig, lichtgrijsbruin, interpretatie: colluvium
Archeologie: enkel fragment bouwpuin (onbepaald)

110 cm -Mv / 53,97 m +NAP
Algemeen: aard ondergrens: abrupt (<0,3 cm)
Lithologie: leem, zwak zandig, lichtgrijsbruin, interpretatie: colluvium
Archeologie: enkele spikkel houtskool, enkel fragment bouwpuin (onbepaald)
Opmerking: KALKBROKJES, GEEM STKL

170 cm -Mv / 53,37 m +NAP
Algemeen: aard bovengrens: abrupt (<0,3 cm), aard ondergrens: abrupt (<0,3 cm)
Lithologie: leem, zwak zandig, donkergrijsbruin
Bodemkundig: afgedekt/begraven A-horizont
Archeologie: spikkels houtskool, fragmenten bouwpuin (onbepaald)
Opmerking: GEVLEKT, SPOOR

220 cm -Mv / 52,87 m +NAP
Algemeen: aard bovengrens: abrupt (<0,3 cm)
Lithologie: leem, zwak zandig, lichtgrijsbruin, kalkloos
Bodemkundig: veel Fe- en Mn-vlekken

250 cm -Mv / 52,57 m +NAP
Lithologie: leem, zwak zandig, lichtbruingeel, kalkrijk
Bodemkundig: veel Fe- en Mn-vlekken

290 cm -Mv / 52,17 m +NAP
Lithologie: leem, zwak zandig, geel, kalkrijk
Bodemkundig: veel Fe- en Mn-vlekken

Einde boring op 310 cm -Mv / 51,97 m +NAP

boring: MEHE13-11

beschrijver: JWK, datum: 28-7-2014, X: 181.363,31, Y: 321.545,82, precisie locatie: 1 cm, coördinaatsysteem: Rijksdriehoeksmeting, kaartblad: 62A, hoogte: 68,70, precisie hoogte: 1 cm, referentievlak: Normaal Amsterdams Peil, methode hoogtebepaling: GPS, boortype: Edelman-7 cm, doel boring: archeologie - verkenning, landgebruik: braak, vondstzichtbaarheid: slecht, provincie: Limburg, gemeente: Meerssen, opdrachtgever: RCE, uitvoerder: RCE

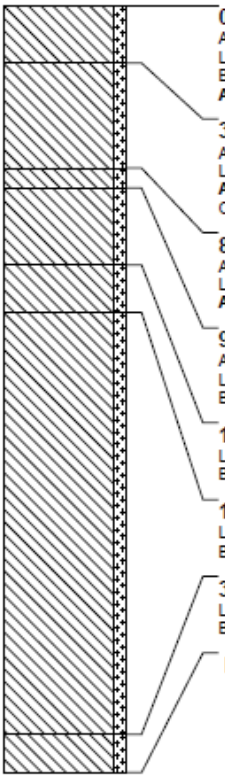

0 cm -Mv / 68,70 m +NAP
Algemeen: aard ondergrens: abrupt (<0,3 cm)
Lithologie: leem, zwak zandig, donkergrijsbruin
Bodemkundig: regelmatig geploegd/bewerkte A-horizont, interpretatie: bouwvoor
Archeologie: enkele spikkel houtskool, veel fragmenten bouwpuin

30 cm -Mv / 68,40 m +NAP
Algemeen: aard bovengrens: abrupt (<0,3 cm), aard ondergrens: geleidelijk (0,3-3 cm)
Lithologie: leem, zwak zandig, bruin
Archeologie: veel fragmenten bouwpuin
Opmerking: SPOOR MERGELBROKKEN/KALKSTEEN

85 cm -Mv / 67,85 m +NAP
Algemeen: aard bovengrens: geleidelijk (0,3-3 cm), aard ondergrens: geleidelijk (0,3-3 cm)
Lithologie: leem, zwak zandig, lichtbruin
Archeologie: enkel fragment bouwpuin

95 cm -Mv / 67,75 m +NAP
Algemeen: aard bovengrens: geleidelijk (0,3-3 cm)
Lithologie: leem, zwak zandig, roodbruin
Bodemkundig: B-horizont met ingespoelde klei

135 cm -Mv / 67,35 m +NAP
Lithologie: leem, zwak zandig, lichtgeelbruin
Bodemkundig: BC-horizont

160 cm -Mv / 67,10 m +NAP
Lithologie: leem, zwak zandig, lichtbruingeel, enkele siltlagen, kalkloos
Bodemkundig: C-horizont

380 cm -Mv / 64,90 m +NAP
Lithologie: leem, zwak zandig, lichtgeel, kalkrijk
Bodemkundig: C-horizont

Einde boring op 400 cm -Mv / 64,70 m +NAP

boring: MEHE13-12

beschrijver: JWK, datum: 28-7-2014, X: 181.351,63, Y: 321.523,73, precisie locatie: 1 cm, coördinaatsysteem: Rijksdriehoeksmeting, kaartblad: 62A, hoogte: 68,04, precisie hoogte: 1 cm, referentievlak: Normaal Amsterdams Peil, methode hoogtebepaling: GPS, boortype: Edelman-7 cm, doel boring: archeologie - verkenning, landgebruik: braak, vondstzichtbaarheid: slecht, provincie: Limburg, gemeente: Meerssen, opdrachtgever: RCE, uitvoerder: RCE

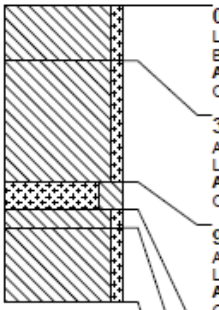

0 cm -Mv / 68,04 m +NAP
Lithologie: leem, zwak zandig, donkergrijsbruin
Bodemkundig: regelmatig geploegd/bewerkte A-horizont, interpretatie: bouwvoor
Archeologie: spikkels houtskool, veel fragmenten bouwpuin
Opmerking: BROKKEN KALK + ROMEINS BETON

30 cm -Mv / 67,74 m +NAP
Algemeen: aard ondergrens: abrupt (<0,3 cm)
Lithologie: leem, zwak zandig, grijsbruin
Archeologie: spikkels houtskool, veel fragmenten bouwpuin
Opmerking: BROKKEN KALK + ROMEINS BETON

95 cm -Mv / 67,09 m +NAP
Algemeen: aard bovengrens: abrupt (<0,3 cm)
Lithologie: zand, sterk siltig, geel, matig grof
Archeologie: enkel fragment bouwpuin
Opmerking: KALKBROKKEN VLOER?

110 cm -Mv / 66,94 m +NAP
Lithologie: leem, zwak zandig, lichtbruin
Bodemkundig: BC-horizont

120 cm -Mv / 66,84 m +NAP
Lithologie: leem, zwak zandig, lichtbruingeel
Bodemkundig: C-horizont

Einde boring op 160 cm -Mv / 66,44 m +NAP

boring: MEHE13-13

beschrijver: JWK, datum: 28-7-2014, X: 181.339,91, Y: 321.501,63, precisie locatie: 1 cm, coördinaatsysteem: Rijksdriehoeksmeting, kaartblad: 62A, hoogte: 67,02, precisie hoogte: 1 cm, referentievlak: Normaal Amsterdams Peil, methode hoogtebepaling: GPS, boortype: Edelman-7 cm, doel boring: archeologie - verkenning, landgebruik: braak, vondstzichtbaarheid: slecht, provincie: Limburg, gemeente: Meerssen, opdrachtgever: RCE, uitvoerder: RCE

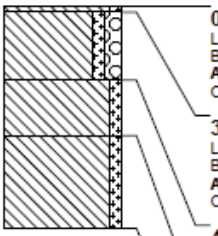

0 cm -Mv / 67,02 m +NAP
Lithologie: leem, zwak zandig, donkergrijsbruin
Bodemkundig: regelmatig geploegd/bewerkte A-horizont, interpretatie: bouwvoor
Archeologie: veel fragmenten bouwpuin
Opmerking: BROKJES MERGEL, MORTEL

3 cm -Mv / 66,99 m +NAP
Lithologie: leem, zwak zandig, matig grindig, donkergrijsbruin
Bodemkundig: regelmatig geploegd/bewerkte A-horizont, interpretatie: bouwvoor
Archeologie: veel fragmenten bouwpuin
Opmerking: BROKJES MERGEL, MORTEL

40 cm -Mv / 66,62 m +NAP
Lithologie: leem, zwak zandig, lichtbruin
Bodemkundig: BC-horizont

70 cm -Mv / 66,32 m +NAP
Lithologie: leem, zwak zandig, lichtbruingeel, enkele siltlagen, matig stevig
Bodemkundig: C-horizont

Einde boring op 120 cm -Mv / 65,82 m +NAP

boring: MEHE13-14

beschrijver: JWK, datum: 28-7-2014, X: 181.328,22, Y: 321.479,56, precisie locatie: 1 cm, coördinaatsysteem: Rijksdriehoeksmeting, kaartblad: 62A, hoogte: 65,71, precisie hoogte: 1 cm, referentievlak: Normaal Amsterdams Peil, methode hoogtebepaling: GPS, boortype: Edelman-7 cm, doel boring: archeologie - verkenning, landgebruik: braak, vondstzichtbaarheid: slecht, provincie: Limburg, gemeente: Meerssen, opdrachtgever: RCE, uitvoerder: RCE

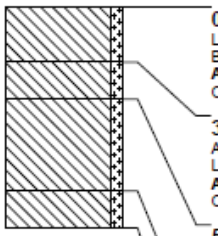

0 cm -Mv / 65,71 m +NAP
Lithologie: leem, zwak zandig, donkergrijsbruin
Bodemkundig: regelmatig geploegd/bewerkte A-horizont, interpretatie: bouwvoor
Archeologie: veel fragmenten bouwpuin
Opmerking: grind en kalksteen

30 cm -Mv / 65,41 m +NAP
Algemeen: aard ondergrens: abrupt (<0,3 cm)
Lithologie: leem, zwak zandig, donkerbruin
Archeologie: enkele spikkel houtskool, fragmenten bouwpuin
Opmerking: KALKSTEENBROKKEN spoor?

50 cm -Mv / 65,21 m +NAP
Algemeen: aard bovengrens: abrupt (<0,3 cm)
Lithologie: leem, zwak zandig, lichtbruin
Bodemkundig: BC-horizont, enkele Fe-vlekken
Opmerking: IETS GEVLEKT

100 cm -Mv / 64,71 m +NAP
Lithologie: leem, zwak zandig, lichtbruingeel, enkele siltlagen
Bodemkundig: C-horizont

Einde boring op 120 cm -Mv / 64,51 m +NAP

boring: MEHE13-15

beschrijver: JWK, datum: 28-7-2014, X: 181.316,50, Y: 321.457,48, precisie locatie: 1 cm, coördinaatsysteem: Rijksdriehoeksmeting, kaartblad: 62A, hoogte: 64,34, precisie hoogte: 1 cm, referentievlak: Normaal Amsterdams Peil, methode hoogtebepaling: GPS, boortype: Edelman-7 cm, doel boring: archeologie - verkenning, landgebruik: braak, vondstzichtbaarheid: slecht, provincie: Limburg, gemeente: Meerssen, opdrachtgever: RCE, uitvoerder: RCE

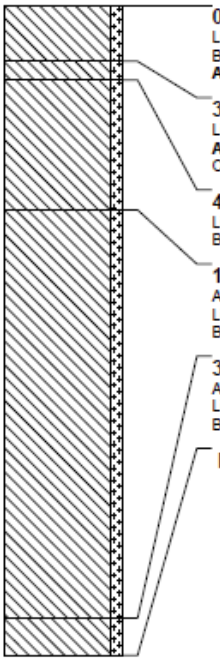

0 cm -Mv / 64,34 m +NAP
Lithologie: leem, zwak zandig, donkergrijsbruin
Bodemkundig: regelmatig geploegd/bewerkte A-horizont, interpretatie: bouwvoor
Archeologie: fragmenten bouwpuin

30 cm -Mv / 64,04 m +NAP
Lithologie: leem, zwak zandig, donkerbruin
Archeologie: fragmenten bouwpuin
Opmerking: VIES, SPOOR?

40 cm -Mv / 63,94 m +NAP
Lithologie: leem, zwak zandig, lichtbruin
Bodemkundig: BC-horizont

110 cm -Mv / 63,24 m +NAP
Algemeen: aard ondergrens: abrupt (<0,3 cm)
Lithologie: leem, zwak zandig, lichtbruingeel, kalkloos
Bodemkundig: C-horizont

330 cm -Mv / 61,04 m +NAP
Algemeen: aard bovengrens: abrupt (<0,3 cm)
Lithologie: leem, zwak zandig, lichtgeel, kalkconcreties
Bodemkundig: C-horizont

Einde boring op 350 cm -Mv / 60,84 m +NAP

boring: MEHE13-16

beschrijver: JWK, datum: 28-7-2014, X: 181.304,78, Y: 321.435,36, precisie locatie: 1 cm, coördinaatsysteem: Rijksdriehoeksmeting, kaartblad: 62A, hoogte: 62,91, precisie hoogte: 1 cm, referentievlak: Normaal Amsterdams Peil, methode hoogtebepaling: GPS, boortype: Edelman-7 cm, doel boring: archeologie - verkenning, landgebruik: braak, vondstzichtbaarheid: slecht, provincie: Limburg, gemeente: Meerssen, opdrachtgever: RCE, uitvoerder: RCE

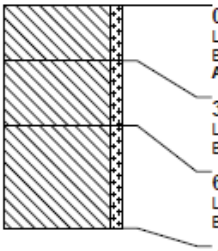

0 cm -Mv / 62,91 m +NAP
Lithologie: leem, zwak zandig, donkergrijsbruin
Bodemkundig: regelmatig geploegd/bewerkte A-horizont, interpretatie: bouwvoor
Archeologie: enkel fragment bouwpuin

30 cm -Mv / 62,61 m +NAP
Lithologie: leem, zwak zandig, lichtbruin, matig stevig
Bodemkundig: BC-horizont

65 cm -Mv / 62,26 m +NAP
Lithologie: leem, zwak zandig, lichtbruingeel, enkele siltlagen
Bodemkundig: C-horizont

Einde boring op 120 cm -Mv / 61,71 m +NAP

boring: MEHE13-17

beschrijver: JWK, datum: 28-7-2014, X: 181.293,10, Y: 321.413,27, precisie locatie: 1 cm, coördinaatsysteem: Rijksdriehoeksmeting, kaartblad: 62A, hoogte: 61,29, precisie hoogte: 1 cm, referentievlak: Normaal Amsterdams Peil, methode hoogtebepaling: GPS, boortype: Edelman-7 cm, doel boring: archeologie - verkenning, landgebruik: braak, vondstzichtbaarheid: slecht, provincie: Limburg, gemeente: Meerssen, opdrachtgever: RCE, uitvoerder: RCE

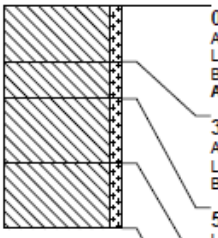

0 cm -Mv / 61,29 m +NAP
Algemeen: aard ondergrens: abrupt (<0,3 cm)
Lithologie: leem, zwak zandig, donkergroenbruin
Bodemkundig: regelmatig geploegd/bewerkte A-horizont, interpretatie: bouwvoor
Archeologie: fragmenten bouwpuin

30 cm -Mv / 60,99 m +NAP
Algemeen: aard bovengrens: abrupt (<0,3 cm)
Lithologie: leem, zwak zandig, bruin
Bodemkundig: B-horizont met ingespoelde klei

50 cm -Mv / 60,79 m +NAP
Lithologie: leem, zwak zandig, lichtbruin

85 cm -Mv / 60,44 m +NAP
Lithologie: leem, zwak zandig, lichtbruingeel
Bodemkundig: C-horizont

Einde boring op 120 cm -Mv / 60,09 m +NAP

boring: MEHE13-18

beschrijver: JWK, datum: 28-7-2014, X: 181.281,39, Y: 321.391,17, precisie locatie: 1 cm, coördinaatsysteem: Rijksdriehoeksmeting, kaartblad: 62A, hoogte: 59,64, precisie hoogte: 1 cm, referentievlak: Normaal Amsterdams Peil, methode hoogtebepaling: GPS, boortype: Edelman-7 cm, doel boring: archeologie - verkenning, landgebruik: braak, vondstzichtbaarheid: slecht, provincie: Limburg, gemeente: Meerssen, opdrachtgever: RCE, uitvoerder: RCE

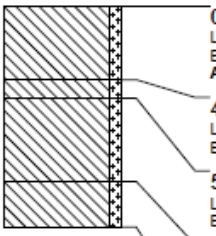

0 cm -Mv / 59,64 m +NAP
Lithologie: leem, zwak zandig, donkergrijsbruin
Bodemkundig: regelmatig geploegd/bewerkte A-horizont, interpretatie: bouwvoor
Archeologie: enkel fragment bouwpuin

40 cm -Mv / 59,24 m +NAP
Lithologie: leem, zwak zandig, bruin, matig stevig
Bodemkundig: B-horizont met ingespoelde klei

50 cm -Mv / 59,14 m +NAP
Lithologie: leem, zwak zandig, lichtbruin, matig stevig
Bodemkundig: BC-horizont

95 cm -Mv / 58,69 m +NAP
Lithologie: leem, zwak zandig, lichtbruingeel, matig stevig, kalkloos
Bodemkundig: C-horizont

Einde boring op 120 cm -Mv / 58,44 m +NAP

boring: MEHE13-19

beschrijver: JWK, datum: 28-7-2014, X: 181.269,68, Y: 321.369,08, precisie locatie: 1 cm, coördinaatsysteem: Rijksdriehoeksmeting, kaartblad: 62A, hoogte: 58,02, precisie hoogte: 1 cm, referentievlak: Normaal Amsterdams Peil, methode hoogtebepaling: GPS, boortype: Edelman-7 cm, doel boring: archeologie - verkenning, landgebruik: braak, vondstzichtbaarheid: slecht, provincie: Limburg, gemeente: Meerssen, opdrachtgever: RCE, uitvoerder: RCE

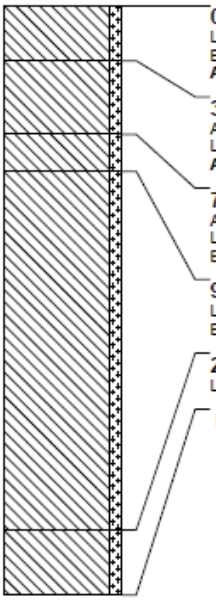

0 cm -Mv / 58,02 m +NAP
Lithologie: leem, zwak zandig, donkergrijsbruin
Bodemkundig: regelmatig geploegd/bewerkte A-horizont, interpretatie: bouwvoor
Archeologie: enkel fragment bouwpuin

30 cm -Mv / 57,72 m +NAP
Algemeen: aard ondergrens: abrupt (<0,3 cm)
Lithologie: leem, zwak zandig, grijsbruin, matig slap, interpretatie: colluvium
Archeologie: enkel fragment bouwpuin

70 cm -Mv / 57,32 m +NAP
Algemeen: aard bovengrens: abrupt (<0,3 cm)
Lithologie: leem, zwak zandig, lichtgeelbruin, matig stevig
Bodemkundig: BC-horizont

90 cm -Mv / 57,12 m +NAP
Lithologie: leem, zwak zandig, lichtbruingeel, enkele siltlagen
Bodemkundig: C-horizont

285 cm -Mv / 55,17 m +NAP
Lithologie: leem, zwak zandig, lichtgeel, kalkrijk

Einde boring op 320 cm -Mv / 54,82 m +NAP

boring: MEHE13-20

beschrijver: JWK, datum: 28-7-2014, X: 181.445,84, Y: 321.487,97, precisie locatie: 1 cm, coördinaatsysteem: Rijksdriehoeksmeting, kaartblad: 62A, hoogte: 68,15, precisie hoogte: 1 cm, referentievlak: Normaal Amsterdams Peil, methode hoogtebepaling: GPS, boortype: Edelman-7 cm, doel boring: archeologie - verkenning, landgebruik: braak, vondstzichtbaarheid: slecht, provincie: Limburg, gemeente: Meerssen, opdrachtgever: RCE, uitvoerder: RCE

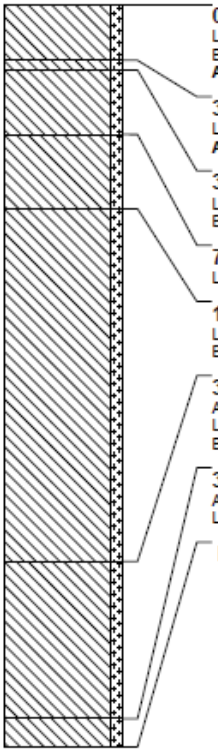

0 cm -Mv / 68,15 m +NAP
Lithologie: leem, zwak zandig, donkerbruingrijs
Bodemkundig: regelmatig geploegd/bewerkte A-horizont, interpretatie: bouwvoor
Archeologie: fragmenten bouwpuin

30 cm -Mv / 67,85 m +NAP
Lithologie: leem, zwak zandig, bruin
Archeologie: veel fragmenten bouwpuin

35 cm -Mv / 67,80 m +NAP
Lithologie: leem, zwak zandig, bruin, matig stevig
Bodemkundig: B-horizont met ingespoelde klei

70 cm -Mv / 67,45 m +NAP
Lithologie: leem, zwak zandig, lichtbruin

110 cm -Mv / 67,05 m +NAP
Lithologie: leem, zwak zandig, lichtbruingeel, enkele siltlagen
Bodemkundig: C-horizont

300 cm -Mv / 65,15 m +NAP
Algemeen: aard ondergrens: abrupt (<0,3 cm)
Lithologie: leem, zwak zandig, lichtbruingeel
Bodemkundig: C-horizont

385 cm -Mv / 64,30 m +NAP
Algemeen: aard bovengrens: abrupt (<0,3 cm)
Lithologie: leem, zwak zandig, lichtgeel, kalkrijk

Einde boring op 400 cm -Mv / 64,15 m +NAP

boring: MEHE13-21

beschrijver: JWK, datum: 28-7-2014, X: 181.434,13, Y: 321.465,87, precisie locatie: 1 cm, coördinaatsysteem: Rijksdriehoeksmeting, kaartblad: 62A, hoogte: 67,46, precisie hoogte: 1 cm, referentievlak: Normaal Amsterdams Peil, methode hoogtebepaling: GPS, boortype: Edelman-7 cm, doel boring: archeologie - verkenning, landgebruik: braak, vondstzichtbaarheid: slecht, provincie: Limburg, gemeente: Meerssen, opdrachtgever: RCE, uitvoerder: RCE

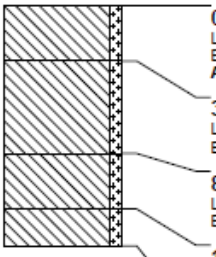

0 cm -Mv / 67,46 m +NAP
Lithologie: leem, zwak zandig, donkergrijsbruin
Bodemkundig: regelmatig geploegd/bewerkte A-horizont, interpretatie: bouwvoor
Archeologie: fragmenten bouwpuin

30 cm -Mv / 67,16 m +NAP
Lithologie: leem, zwak zandig, bruin, zeer stevig
Bodemkundig: B-horizont met ingespoelde klei

80 cm -Mv / 66,66 m +NAP
Lithologie: leem, zwak zandig, lichtgeelbruin, zeer stevig
Bodemkundig: BC-horizont

110 cm -Mv / 66,36 m +NAP
Lithologie: leem, zwak zandig, lichtbruingeel, enkele siltlagen
Bodemkundig: C-horizont

Einde boring op 130 cm -Mv / 66,16 m +NAP

boring: MEHE13-22

beschrijver: JWK, datum: 28-7-2014, X: 181.422,43, Y: 321.443,79, precisie locatie: 1 cm, coördinaatsysteem: Rijksdriehoeksmeting, kaartblad: 62A, hoogte: 66,45, precisie hoogte: 1 cm, referentievlak: Normaal Amsterdams Peil, methode hoogtebepaling: GPS, boortype: Edelman-7 cm, doel boring: archeologie - verkenning, landgebruik: braak, vondstzichtbaarheid: slecht, provincie: Limburg, gemeente: Meerssen, opdrachtgever: RCE, uitvoerder: RCE

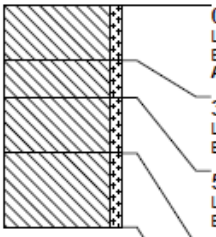

0 cm -Mv / 66,45 m +NAP
Lithologie: leem, zwak zandig, donkergrijsbruin
Bodemkundig: regelmatig geploegd/bewerkte A-horizont, interpretatie: bouwvoor
Archeologie: enkel fragment bouwpuin

30 cm -Mv / 66,15 m +NAP
Lithologie: leem, zwak zandig, roodbruin
Bodemkundig: B-horizont met ingespoelde klei

50 cm -Mv / 65,95 m +NAP
Lithologie: leem, zwak zandig, lichtbruin, matig stevig
Bodemkundig: BC-horizont

80 cm -Mv / 65,65 m +NAP
Lithologie: leem, zwak zandig, lichtbruingeel, enkele siltlagen
Bodemkundig: C-horizont

Einde boring op 120 cm -Mv / 65,25 m +NAP

boring: MEHE13-23

beschrijver: JWK, datum: 28-7-2014, X: 181.410,70, Y: 321.421,70, precisie locatie: 1 cm, coördinaatsysteem: Rijksdriehoeksmeting, kaartblad: 62A, hoogte: 65,14, precisie hoogte: 1 cm, referentievlak: Normaal Amsterdams Peil, methode hoogtebepaling: GPS, boortype: Edelman-7 cm, doel boring: archeologie - verkenning, landgebruik: braak, vondstzichtbaarheid: slecht, provincie: Limburg, gemeente: Meerssen, opdrachtgever: RCE, uitvoerder: RCE

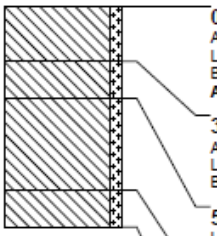

0 cm -Mv / 65,14 m +NAP
Algemeen: aard ondergrens: abrupt (<0,3 cm)
Lithologie: leem, zwak zandig, donkergrijsbruin
Bodemkundig: regelmatig geploegd/bewerkte A-horizont, interpretatie: bouwvoor
Archeologie: enkel fragment bouwpuin

30 cm -Mv / 64,84 m +NAP
Algemeen: aard bovengrens: abrupt (<0,3 cm)
Lithologie: leem, zwak zandig, bruin
Bodemkundig: B-horizont met ingespoelde klei

50 cm -Mv / 64,64 m +NAP
Lithologie: leem, zwak zandig, lichtbruin
Bodemkundig: BC-horizont

100 cm -Mv / 64,14 m +NAP
Lithologie: leem, zwak zandig, lichtgeelbruin
Bodemkundig: C-horizont

Einde boring op 120 cm -Mv / 63,94 m +NAP

boring: MEHE13-24

beschrijver: JWK, datum: 28-7-2014, X: 181.399,02, Y: 321.399,61, precisie locatie: 1 cm, coördinaatsysteem: Rijksdriehoeksmeting, kaartblad: 62A, hoogte: 63,61, precisie hoogte: 1 cm, referentievlak: Normaal Amsterdams Peil, methode hoogtebepaling: GPS, boortype: Edelman-7 cm, doel boring: archeologie - verkenning, landgebruik: braak, provincie: Limburg, gemeente: Meerssen, opdrachtgever: RCE, uitvoerder: RCE

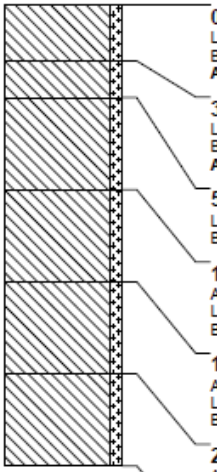

0 cm -Mv / 63,61 m +NAP
Lithologie: leem, zwak zandig, donkergrijsbruin
Bodemkundig: regelmatig geploegd/bewerkte A-horizont, interpretatie: bouwvoor
Archeologie: enkel fragment bouwpuin

30 cm -Mv / 63,31 m +NAP
Lithologie: leem, zwak zandig, donkerbruin
Bodemkundig: B-horizont met ingespoelde klei
Archeologie: fragmenten bouwpuin

50 cm -Mv / 63,11 m +NAP
Lithologie: leem, zwak zandig, lichtbruin
Bodemkundig: BC-horizont

100 cm -Mv / 62,61 m +NAP
Algemeen: aard ondergrens: abrupt (<0,3 cm)
Lithologie: leem, zwak zandig, lichtbruingeel, kalkloos
Bodemkundig: C-horizont

150 cm -Mv / 62,11 m +NAP
Algemeen: aard bovengrens: abrupt (<0,3 cm), aard ondergrens: geleidelijk (0,3-3 cm)
Lithologie: leem, zwak zandig, lichtgeel, kalkrijk
Bodemkundig: C-horizont

200 cm -Mv / 61,61 m +NAP
Algemeen: aard bovengrens: geleidelijk (0,3-3 cm)
Lithologie: leem, zwak zandig, lichtgeel, kalkconcreties
Bodemkundig: C-horizont

Einde boring op 250 cm -Mv / 61,11 m +NAP

boring: MEHE13-25

beschrijver: JWK, datum: 28-7-2014, X: 181.387,32, Y: 321.377,50, precisie locatie: 1 cm, coördinaatsysteem: Rijksdriehoeksmeting, kaartblad: 62A, hoogte: 61,82, precisie hoogte: 1 cm, referentievlak: Normaal Amsterdams Peil, methode hoogtebepaling: GPS, boortype: Edelman-7 cm, doel boring: archeologie - verkenning, landgebruik: braak, provincie: Limburg, gemeente: Meerssen, opdrachtgever: RCE, uitvoerder: RCE

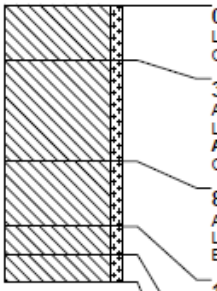

0 cm -Mv / 61,82 m +NAP
Lithologie: leem, zwak zandig, donkerbruingrijs
Opmerking: VIEZE KLEUR

30 cm -Mv / 61,52 m +NAP
Algemeen: aard ondergrens: abrupt (<0,3 cm)
Lithologie: leem, zwak zandig, roodbruin, matig slap
Archeologie: enkele spikkel houtskool, fragmenten bouwpuin
Opmerking: SPOOR?

85 cm -Mv / 60,97 m +NAP
Algemeen: aard bovengrens: abrupt (<0,3 cm)
Lithologie: leem, zwak zandig, lichtbruin, matig stevig, kalkloos
Bodemkundig: BC-horizont

120 cm -Mv / 60,62 m +NAP
Lithologie: leem, zwak zandig, lichtgeel, kalkrijk
Bodemkundig: C-horizont

135 cm -Mv / 60,47 m +NAP
Lithologie: leem, zwak zandig, lichtgeel, kalkconcreties
Bodemkundig: C-horizont

Einde boring op 150 cm -Mv / 60,32 m +NAP

boring: MEHE13-26

beschrijver: JWK, datum: 28-7-2014, X: 181.375,61, Y: 321.355,44, precisie locatie: 1 cm, coördinaatsysteem: Rijksdriehoeksmeting, kaartblad: 62A, hoogte: 60,06, precisie hoogte: 1 cm, referentievlak: Normaal Amsterdams Peil, methode hoogtebepaling: GPS, boortype: Edelman-7 cm, doel boring: archeologie - verkenning, landgebruik: braak, provincie: Limburg, gemeente: Meerssen, opdrachtgever: RCE, uitvoerder: RCE

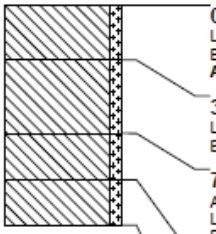

0 cm -Mv / 60,06 m +NAP
Lithologie: leem, zwak zandig, donkergrijsbruin
Bodemkundig: regelmatig geploegd/bewerkte A-horizont, interpretatie: bouwvoor
Archeologie: enkel fragment bouwpuin

30 cm -Mv / 59,76 m +NAP
Lithologie: leem, zwak zandig, lichtbruin
Bodemkundig: BC-horizont

70 cm -Mv / 59,36 m +NAP
Algemeen: aard ondergrens: abrupt (<0,3 cm)
Lithologie: leem, zwak zandig, lichtbruingeel, matig stevig, kalkloos
Bodemkundig: C-horizont

95 cm -Mv / 59,11 m +NAP
Algemeen: aard bovengrens: abrupt (<0,3 cm)
Lithologie: leem, zwak zandig, lichtgeel, matig stevig, kalkconcreties
Bodemkundig: C-horizont

Einde boring op 120 cm -Mv / 58,86 m +NAP

boring: MEHE13-27

beschrijver: JWK, datum: 28-7-2014, X: 181.363,91, Y: 321.333,33, precisie locatie: 1 cm, coördinaatsysteem: Rijksdriehoeksmeting, kaartblad: 62A, hoogte: 58,00, precisie hoogte: 1 cm, referentievlak: Normaal Amsterdams Peil, methode hoogtebepaling: GPS, boortype: Edelman-7 cm, doel boring: archeologie - verkenning, landgebruik: braak, provincie: Limburg, gemeente: Meerssen, opdrachtgever: RCE, uitvoerder: RCE

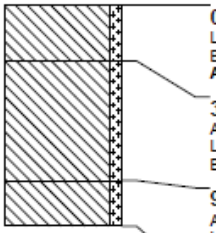

0 cm -Mv / 58,00 m +NAP
Lithologie: leem, zwak zandig, donkergrijsbruin
Bodemkundig: regelmatig geploegd/bewerkte A-horizont, interpretatie: bouwvoor
Archeologie: enkel fragment bouwpuin

30 cm -Mv / 57,70 m +NAP
Algemeen: aard ondergrens: abrupt (<0,3 cm)
Lithologie: leem, zwak zandig, lichtbruin
Bodemkundig: BC-horizont

95 cm -Mv / 57,05 m +NAP
Algemeen: aard bovengrens: abrupt (<0,3 cm)
Lithologie: leem, zwak zandig, lichtgeel, matig stevig, kalkconcreties
Bodemkundig: C-horizont

Einde boring op 120 cm -Mv / 56,80 m +NAP

boring: MEHE13-28

beschrijver: JWK, datum: 28-7-2014, X: 181.200,63, Y: 321.387,31, precisie locatie: 1 cm, coördinaatsysteem: Rijksdriehoeksmeting, kaartblad: 62A, hoogte: 55,07, precisie hoogte: 1 cm, referentievlak: Normaal Amsterdams Peil, methode hoogtebepaling: GPS, boortype: aqualock 10 cm, doel boring: archeologie - verkenning, landgebruik: braak, vondstzichtbaarheid: slecht, provincie: Limburg, gemeente: Meerssen, opdrachtgever: RCE, uitvoerder: RCE, opmerking: MECHANISCHE STEEKBORING THV BORING 10

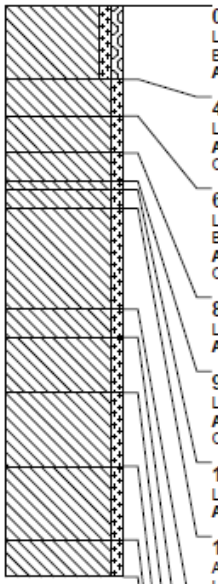

0 cm -Mv / 55,07 m +NAP
Lithologie: leem, zwak zandig, zwak grindig, donkergrijsbruin
Bodemkundig: regelmatig geploegd/bewerkte A-horizont
Archeologie: fragmenten bouwpuin (onbepaald)

40 cm -Mv / 54,67 m +NAP
Lithologie: leem, zwak zandig, lichtgrijsbruin, interpretatie: colluvium
Archeologie: enkel fragment bouwpuin (onbepaald)
Opmerking: STK

60 cm -Mv / 54,47 m +NAP
Lithologie: leem, zwak zandig, grijsbruin, interpretatie: colluvium
Bodemkundig: afgedekt/begraven A-horizont
Archeologie: fragmenten bouwpuin (onbepaald)
Opmerking: STK

80 cm -Mv / 54,27 m +NAP
Lithologie: leem, zwak zandig, lichtgrijsbruin, interpretatie: colluvium
Archeologie: enkel fragment bouwpuin (onbepaald)

95 cm -Mv / 54,12 m +NAP
Lithologie: leem, zwak zandig, lichtgrijsbruin, interpretatie: colluvium
Archeologie: enkel fragment aardewerk, enkel fragment bouwpuin (onbepaald)
Opmerking: KER SPAARZAAM GEGLAZUURD

100 cm -Mv / 54,07 m +NAP
Lithologie: leem, zwak zandig, lichtgrijsbruin, interpretatie: colluvium
Archeologie: enkel fragment bouwpuin (onbepaald)

110 cm -Mv / 53,97 m +NAP
Algemeen: aard ondergrens: abrupt (<0,3 cm)
Lithologie: leem, zwak zandig, lichtgrijsbruin, interpretatie: colluvium
Archeologie: enkele spikkel houtskool, enkel fragment bouwpuin (onbepaald)
Opmerking: KALKBROKJES, GEEN STKL

165 cm -Mv / 53,42 m +NAP
Algemeen: aard bovengrens: abrupt (<0,3 cm), aard ondergrens: abrupt (<0,3 cm)
Lithologie: leem, zwak zandig, grijsbruin
Bodemkundig: afgedekt/begraven A-horizont
Archeologie: spikkels houtskool, fragmenten bouwpuin (onbepaald)
Opmerking: GEVLEKT, SPOOR?

180 cm -Mv / 53,27 m +NAP
Algemeen: aard bovengrens: abrupt (<0,3 cm), aard ondergrens: abrupt (<0,3 cm)
Lithologie: leem, zwak zandig, donkergrijsbruin
Archeologie: spikkels houtskool, fragmenten bouwpuin (onbepaald)
Opmerking: GEVLEKT, SPOOR?

210 cm -Mv / 52,97 m +NAP
Algemeen: aard bovengrens: abrupt (<0,3 cm)
Lithologie: leem, zwak zandig, lichtgrijsbruin, kalkloos
Bodemkundig: veel Fe- en Mn-vlekken

250 cm -Mv / 52,57 m +NAP
Lithologie: leem, zwak zandig, lichtbruingeel, kalkrijk
Bodemkundig: veel Fe- en Mn-vlekken

290 cm -Mv / 52,17 m +NAP
Lithologie: leem, zwak zandig, geel, kalkrijk
Bodemkundig: veel Fe- en Mn-vlekken

Einde boring op 310 cm -Mv / 51,97 m +NAP

boring: MEHE13-29

beschrijver: JWK, datum: 28-7-2014, X: 181.246,73, Y: 321.482,82, precisie locatie: 1 cm, coördinaatsysteem: Rijksdriehoeksmeting, kaartblad: 62A, hoogte: 64,12, precisie hoogte: 1 cm, referentievlak: Normaal Amsterdams Peil, methode hoogtebepaling: GPS, boortype: aqualock 10 cm, doel boring: archeologie - verkenning, landgebruik: braak, provincie: Limburg, gemeente: Meerssen, opdrachtgever: RCE, uitvoerder: RCE, opmerking: STEEKBORING

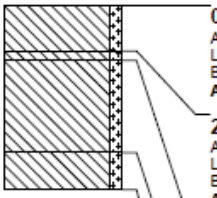

0 cm -Mv / 64,12 m +NAP
Algemeen: aard ondergrens: abrupt (<0,3 cm)
Lithologie: leem, zwak zandig, donkergrijsbruin
Bodemkundig: A-horizont
Archeologie: fragmenten bouwpuin (onbepaald)

25 cm -Mv / 63,87 m +NAP
Algemeen: aard bovengrens: abrupt (<0,3 cm)
Lithologie: leem, zwak zandig, grijsbruin
Bodemkundig: B-horizont met ingespoelde klei
Archeologie: enkel fragment bouwpuin (onbepaald)
Opmerking: BIOTURBATIE

30 cm -Mv / 63,82 m +NAP
Algemeen: aard ondergrens: geleidelijk (0,3-3 cm)
Lithologie: leem, zwak zandig, bruin
Bodemkundig: B-horizont met ingespoelde klei

80 cm -Mv / 63,32 m +NAP
Algemeen: aard bovengrens: geleidelijk (0,3-3 cm)
Lithologie: leem, zwak zandig, lichtgeelbruin
Bodemkundig: BC-horizont

Einde boring op 100 cm -Mv / 63,12 m +NAP

boring: MEHE13-30

beschrijver: JWK, datum: 28-7-2014, X: 181.294,30, Y: 321.585,75, precisie locatie: 1 cm, coördinaatsysteem: Rijksdriehoeksmeting, kaartblad: 62A, hoogte: 68,14, precisie hoogte: 1 cm, referentievlak: Normaal Amsterdams Peil, methode hoogtebepaling: GPS, boortype: aqualock 10 cm, doel boring: archeologie - verkenning, landgebruik: braak, provincie: Limburg, gemeente: Meerssen, opdrachtgever: RCE, uitvoerder: RCE, opmerking: STEEKBORING

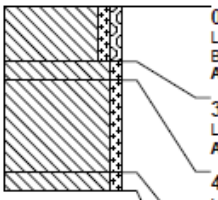

0 cm -Mv / 68,14 m +NAP
Lithologie: leem, zwak zandig, zwak grindig, donkergrijsbruin
Bodemkundig: regelmatig geploegd/bewerkte A-horizont, interpretatie: bouwvoor
Archeologie: fragmenten bouwpuin (onbepaald)

30 cm -Mv / 67,84 m +NAP
Lithologie: leem, zwak zandig, grijsbruin
Archeologie: fragmenten bouwpuin (onbepaald)

40 cm -Mv / 67,74 m +NAP
Lithologie: leem, zwak zandig, bruin
Bodemkundig: B-horizont met ingespoelde klei, veel Fe- en Mn-vlekken

90 cm -Mv / 67,24 m +NAP
Lithologie: leem, zwak zandig, lichtgeelbruin
Bodemkundig: BC-horizont

Einde boring op 100 cm -Mv / 67,14 m +NAP

B: PIT PROFILE DESCRIPTIONS GROTE HOUW

wp1, vlak 104
F17

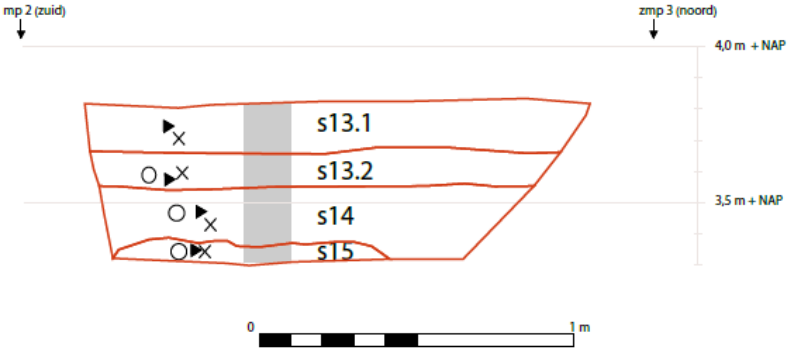

monsters	s13.1	s13.2	s14	s15
○ OSL		v1042	v1043	v1044
× cesium	v1046	v1047	v1048	v1049
▶ plutonium	v1050	v1051	v1052	v1053
loodprofiel		v1045		

vondstmateriaal	
0 - 30 cm	v1006
0 - 60 cm	v1007

wp2, vlak 104
F16

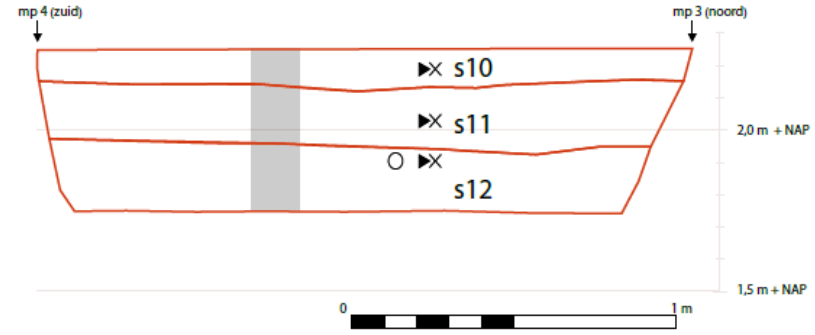

monsters	s10	s11	s12
○ OSL			v1034
× cesium	v1036	v1037	v1038
plutonium	v1039	v1040	v1041
loodprofiel		v1035	

vondstmateriaal	
0 - 30 cm	v1004
0 - 60 cm	v1005

wp3, vlak 104
F12, 14

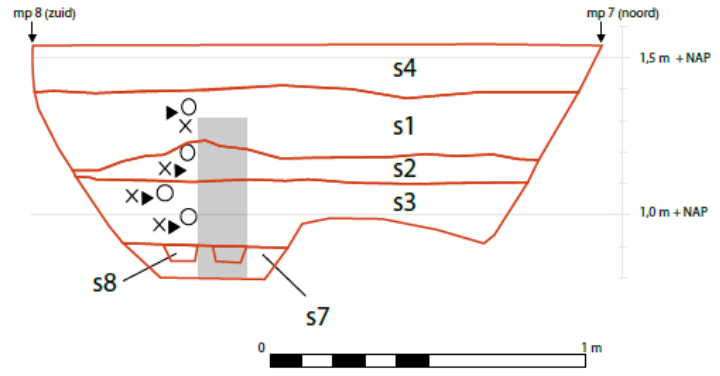

monsters	s1	s2	s3	s3	s7
○ OSL	v1008	v1009	v1010	v1011	
× cesium	v1017	v1018	v1019	v1020	
▶ plutonium	v1013	v1014	v1015	v1016	
loodprofiel			v1012		

vondstmateriaal	
0 - 30 cm	v1000
0 - 60 cm	v1001

wp4 vlak 101
F18

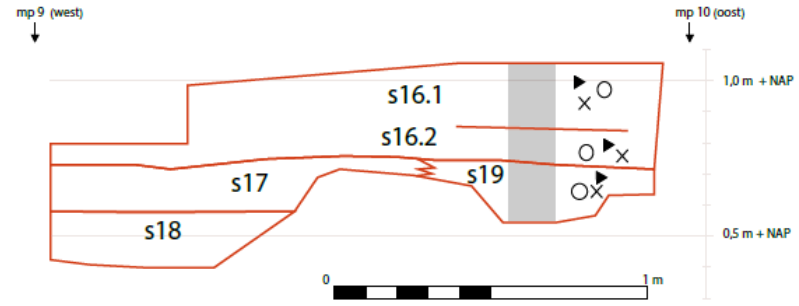

monsters	s16.1	s16.2	s19
○ **OSL**	v1055	v1056	v1057
× **cesium**	v1058	v1059	v1060
▶ **plutonium**	v1061	v1062	v1063
loodprofiel	v1064		

vondstmateriaal	
0 - 40 cm	v1054

wp5, vlak 104
F13, 15

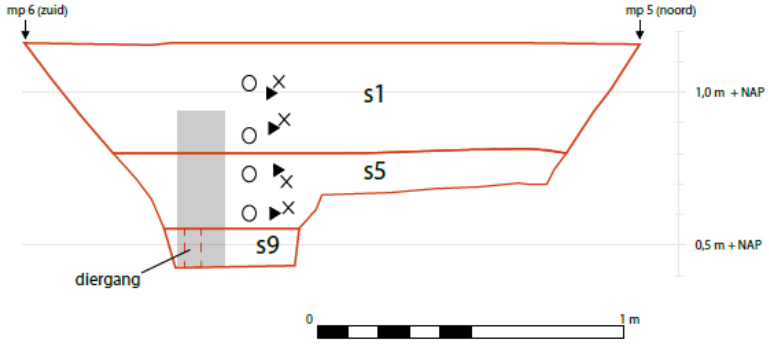

monsters	s1	s1	s5	s9
○ **OSL**	v1021	v1022	v1023	v1024
× **cesium**	v1026	v1027	v1028	v1029
▶ **plutonium**	v1030	v1031	v1032	v1033
loodprofiel	v1025			

vondstmateriaal	
0 - 30 cm	v1002
0 - 60 cm	v1003

C: SURFACE ANALYSIS MEDUSA

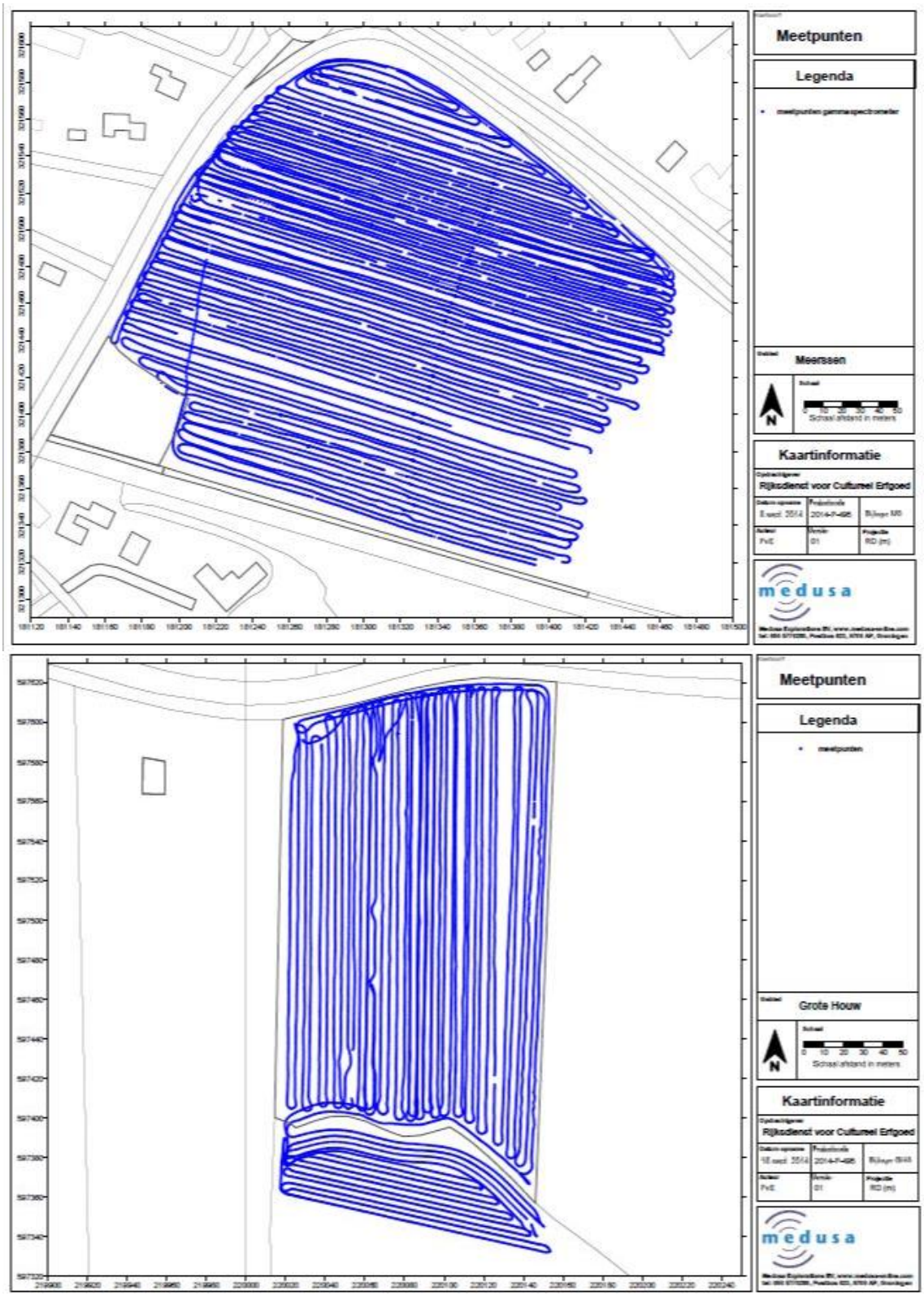

Measurement points surface analysis Meerssen and the Grote Houw